

**(12) STANDARD PATENT  
(19) AUSTRALIAN PATENT OFFICE**

**(11) Application No. AU 2013256044 B2**

(54) Title  
**System and methods for coping with Doppler effects in distributed-input distributed-output wireless systems**

(51) International Patent Classification(s)  
**G08B 13/18** (2006.01)

(21) Application No: **2013256044** (22) Date of Filing: **2013.05.03**

(87) WIPO No: **WO13/166464**

(30) Priority Data

(31) Number **13/464,648** (32) Date **2012.05.04** (33) Country **US**

(43) Publication Date: **2013.11.07**  
(44) Accepted Journal Date: **2017.05.25**

(71) Applicant(s)  
**Rearden, LLC**

(72) Inventor(s)  
**Forenza, Antonio;Perlman, Stephen G.**

(74) Agent / Attorney  
**Ellis Terry, C/- Spruson Ferguson GPO Box 3898, SYDNEY, NSW, 2001, AU**

(56) Related Art  
**US 20120093078 A1**  
**US 20090195355 A1**

(12) INTERNATIONAL APPLICATION PUBLISHED UNDER THE PATENT COOPERATION TREATY (PCT)

(19) World Intellectual Property Organization

International Bureau



(10) International Publication Number

WO 2013/166464 A1

(43) International Publication Date  
7 November 2013 (07.11.2013)

WIPO | PCT

(51) International Patent Classification:  
*G08B 13/18 (2006.01)*

(21) International Application Number:  
PCT/US2013/039580

(22) International Filing Date:  
3 May 2013 (03.05.2013)

(25) Filing Language:  
English

(26) Publication Language:  
English

(30) Priority Data:  
13/464,648 4 May 2012 (04.05.2012) US

(71) Applicant: REARDEN, LLC [US/US]; 355 Bryant Street, Suite 110, San Francisco, California 94107 (US).

(72) Inventors: FORENZA, Antonio; 355 Bryant Street, Suite 110, San Francisco, California 94107 (US). PERLMAN, Stephen G.; 355 Bryant Street, Suite 110, San Francisco, California 94107 (US).

(74) Agents: VINCENT, Lester J. et al.; Blakely, Sokoloff, Taylor & Zafman LLP, 1279 Oakmead Parkway, Sunnyvale, California 94085 (US).

(81) Designated States (unless otherwise indicated, for every kind of national protection available): AE, AG, AL, AM, AO, AT, AU, AZ, BA, BB, BG, BH, BN, BR, BW, BY, BZ, CA, CH, CL, CN, CO, CR, CU, CZ, DE, DK, DM, DO, DZ, EC, EE, EG, ES, FI, GB, GD, GE, GH, GM, GT, HN, HR, HU, ID, IL, IN, IS, JP, KE, KG, KM, KN, KP, KR, KZ, LA, LC, LK, LR, LS, LT, LU, LY, MA, MD, ME, MG, MK, MN, MW, MX, MY, MZ, NA, NG, NI, NO, NZ, OM, PA, PE, PG, PH, PL, PT, QA, RO, RS, RU, RW, SC, SD, SE, SG, SK, SL, SM, ST, SV, SY, TH, TJ, TM, TN, TR, TT, TZ, UA, UG, US, UZ, VC, VN, ZA, ZM, ZW.

(84) Designated States (unless otherwise indicated, for every kind of regional protection available): ARIPO (BW, GH, GM, KE, LR, LS, MW, MZ, NA, RW, SD, SL, SZ, TZ, UG, ZM, ZW), Eurasian (AM, AZ, BY, KG, KZ, RU, TJ, TM), European (AL, AT, BE, BG, CH, CY, CZ, DE, DK, EE, ES, FI, FR, GB, GR, HR, HU, IE, IS, IT, LT, LU, LV, MC, MK, MT, NL, NO, PL, PT, RO, RS, SE, SI, SK, SM, TR), OAPI (BF, BJ, CF, CG, CI, CM, GA, GN, GQ, GW, ML, MR, NE, SN, TD, TG).

Published:

— with international search report (Art. 21(3))

(54) Title: SYSTEM AND METHODS FOR COPING WITH DOPPLER EFFECTS IN DISTRIBUTED-INPUT DISTRIBUTED-OUTPUT WIRELESS SYSTEMS

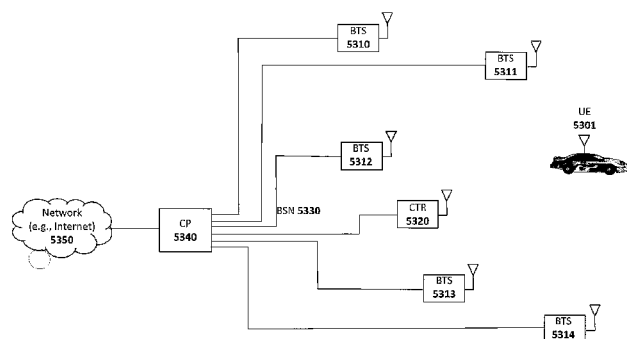


Fig. 53

(57) Abstract: A system and methods are described which compensate for the adverse effect of Doppler on the performance of DIDO systems. One embodiment of such a system employs different selection algorithms to adaptively adjust the active BTSs to different UEs based by tracking the changing channel conditions. Another embodiment utilizes channel prediction to estimate the future CSI or DIDO precoding weights, thereby eliminating errors due to outdated CSI.

WO 2013/166464 A1

**SYSTEM AND METHODS FOR COPING WITH DOPPLER EFFECTS IN  
DISTRIBUTED-INPUT DISTRIBUTED-OUTPUT WIRELESS SYSTEMS****RELATED APPLICATIONS**

**[0001]** This application is a continuation-in-part of the following co-pending U.S. Patent Applications:

**[0002]** U.S. Application Serial No. 12/917,257, filed November 1, 2010, entitled “Systems And Methods To Coordinate Transmissions In Distributed Wireless Systems Via User Clustering”; U.S. Application Serial No. 12/802,988, filed June 16, 2010, entitled “Interference Management, Handoff, Power Control And Link Adaptation In Distributed-Input Distributed-Output (DIDO) Communication Systems”; U.S. Application Serial No. 12/802,976, filed June 16, 2010, entitled “System And Method For Adjusting DIDO Interference Cancellation Based On Signal Strength Measurements”, now U.S. Issued Patent 8,170,081, Issued on May 1, 2012; U.S. Application Serial No. 12/802,974, filed June 16, 2010, entitled “System And Method For Managing Inter-Cluster Handoff Of Clients Which Traverse Multiple DIDO Clusters”; U.S. Application Serial No. 12/802,989, filed June 16, 2010, entitled “System And Method For Managing Handoff Of A Client Between Different Distributed-Input-Distributed-Output (DIDO) Networks Based On Detected Velocity Of The Client”; U.S. Application Serial No. 12/802,958, filed June 16, 2010, entitled “System And Method For Power Control And Antenna Grouping In A Distributed-Input-Distributed-Output (DIDO) Network”; U.S. Application Serial No. 12/802,975, filed June 16, 2010, entitled “System And Method For Link adaptation In DIDO Multicarrier Systems”; U.S. Application Serial No. 12/802,938, filed June 16, 2010, entitled “System And Method For DIDO Precoding Interpolation In Multicarrier Systems”; U.S. Application Serial No. 12/630,627, filed December 3, 2009, entitled ”System and Method For Distributed Antenna Wireless Communications”; U.S. Application Serial No. 12/143,503, filed June 20, 2008 entitled ”System and Method For Distributed Input-Distributed Output Wireless Communications”, now U.S. Issued Patent 8,160,121, Issued on April 17, 2009; U.S. Application Serial No. 11/894,394, filed August 20, 2007 entitled, ”System and Method for Distributed Input Distributed Output Wireless Communications”, now U.S. Issued Patent 7,599,420, Issued on October 6, 2009; U.S. Application Serial No. 11/894,362, filed August 20, 2007 entitled, ”System and method for Distributed Input-Distributed Wireless Communications”, now U.S. Issued Patent, 7,633,994, Issued on December 15, 2009; U.S. Application Serial No. 11/894,540, filed August 20, 2007 entitled ”System and Method For Distributed Input-Distributed Output Wireless Communications”, now U.S. Issued Patent No. 7,636,381, Issued on December 22, 2009; U.S. Application Serial No. 11/256,478, filed October 21, 2005 entitled ”System and Method For Spatial-Multiplexed Tropospheric Scatter Communications”, now U.S.

6181P526XPCT

Issued Patent 7,711,030, Issued on May 4, 2010; U.S. Application Serial No. 10/817,731, filed April 2, 2004 entitled “System and Method For Enhancing Near Vertical Incidence Skywave (“NVIS”) Communication Using Space-Time Coding”, now U.S. Issued Patent No. 7,885,354, Issued on February 28, 2011.

## **BACKGROUND**

**[0003]** Prior art multi-user wireless systems may include only a single base station or several base stations.

**[0004]** A single WiFi base station (e.g., utilizing 2.4 GHz 802.11b, g or n protocols) attached to a broadband wired Internet connection in an area where there are no other WiFi access points (e.g. a WiFi access point attached to DSL within a rural home) is an example of a relatively simple multi-user wireless system that is a single base station that is shared by one or more users that are within its transmission range. If a user is in the same room as the wireless access point, the user will typically experience a high-speed link with few transmission disruptions (e.g. there may be packet loss from 2.4GHz interferers, like microwave ovens, but not from spectrum sharing with other WiFi devices). If a user is a medium distance away or with a few obstructions in the path between the user and WiFi access point, the user will likely experience a medium-speed link. If a user is approaching the edge of the range of the WiFi access point, the user will likely experience a low-speed link, and may be subject to periodic drop-outs if changes to the channel result in the signal SNR dropping below usable levels. And, finally, if the user is beyond the range of the WiFi base station, the user will have no link at all.

**[0005]** When multiple users access the WiFi base station simultaneously, then the available data throughput is shared among them. Different users will typically place different throughput demands on a WiFi base station at a given time, but at times when the aggregate throughput demands exceed the available throughput from the WiFi base station to the users, then some or all users will receive less data throughput than they are seeking. In an extreme situation where a WiFi access point is shared among a very large number of users, throughput to each user can slow down to a crawl, and worse, data throughput to each user may arrive in short bursts separated by long periods of no data throughput at all, during which time other users are served. This “choppy” data delivery may impair certain applications, like media streaming.

**[0006]** Adding additional WiFi base stations in situations with a large number of users will only help up to a point. Within the 2.4GHz ISM band in the U.S., there are 3 non-interfering channels that can be used for WiFi, and if 3 WiFi base stations in the same coverage area are configured to each use a different non-interfering channel, then the aggregate throughput of the coverage area among multiple users will be increased up to a factor of 3. But, beyond that,

## 6181P526XPCT

adding more WiFi base stations in the same coverage area will not increase aggregate throughput, since they will start sharing the same available spectrum among them, effectively utilizing time-division multiplexed access (TDMA) by “taking turns” using the spectrum. This situation is often seen in coverage areas with high population density, such as within multi-dwelling units. For example, a user in a large apartment building with a WiFi adapter may well experience very poor throughput due to dozens of other interfering WiFi networks (e.g. in other apartments) serving other users that are in the same coverage area, even if the user’s access point is in the same room as the client device accessing the base station. Although the link quality is likely good in that situation, the user would be receiving interference from neighbor WiFi adapters operating in the same frequency band, reducing the effective throughput to the user.

**[0007]** Current multiuser wireless systems, including both unlicensed spectrum, such as WiFi, and licensed spectrum, suffer from several limitations. These include coverage area, downlink (DL) data rate and uplink (UL) data rate. Key goals of next generation wireless systems, such as WiMAX and LTE, are to improve coverage area and DL and UL data rate via multiple-input multiple-output (MIMO) technology. MIMO employs multiple antennas at transmit and receive sides of wireless links to improve link quality (resulting in wider coverage) or data rate (by creating multiple non-interfering spatial channels to every user). If enough data rate is available for every user (note, the terms “user” and “client” are used herein interchangeably), however, it may be desirable to exploit channel spatial diversity to create non-interfering channels to multiple users (rather than single user), according to multiuser MIMO (MU-MIMO) techniques. *See, e.g.*, the following references:

**[0008]** G. Caire and S. Shamai, “On the achievable throughput of a multiantenna Gaussian broadcast channel,” *IEEE Trans. Info.Th.*, vol. 49, pp. 1691–1706, July 2003.

**[0009]** P. Viswanath and D. Tse, “Sum capacity of the vector Gaussian broadcast channel and uplink-downlink duality,” *IEEE Trans. Info. Th.*, vol. 49, pp. 1912–1921, Aug. 2003.

**[0010]** S. Vishwanath, N. Jindal, and A. Goldsmith, “Duality, achievable rates, and sum-rate capacity of Gaussian MIMO broadcast channels,” *IEEE Trans. Info. Th.*, vol. 49, pp. 2658–2668, Oct. 2003.

**[0011]** W. Yu and J. Cioffi, “Sum capacity of Gaussian vector broadcast channels,” *IEEE Trans. Info. Th.*, vol. 50, pp. 1875–1892, Sep. 2004.

**[0012]** M. Costa, “Writing on dirty paper,” *IEEE Transactions on Information Theory*, vol. 29, pp. 439–441, May 1983.

**[0013]** M. Bengtsson, “A pragmatic approach to multi-user spatial multiplexing,” *Proc. of Sensor Array and Multichannel Sign. Proc. Workshop*, pp. 130–134, Aug. 2002.

[0014] K.-K. Wong, R. D. Murch, and K. B. Letaief, “Performance enhancement of multiuser MIMO wireless communication systems,” IEEE Trans. Comm., vol. 50, pp. 1960–1970, Dec. 2002.

[0015] M. Sharif and B. Hassibi, “On the capacity of MIMO broadcast channel with partial side information,” IEEE Trans. Info.Th., vol. 51, pp. 506–522, Feb. 2005.

[0016] For example, in MIMO 4x4 systems (i.e., four transmit and four receive antennas), 10MHz bandwidth, 16-QAM modulation and forward error correction (FEC) coding with rate 3/4 (yielding spectral efficiency of 3bps/Hz), the ideal peak data rate achievable at the physical layer for every user is  $4 \times 30\text{Mbps} = 120\text{Mbps}$ , which is much higher than required to deliver high definition video content (which may only require  $\sim 10\text{Mbps}$ ). In MU-MIMO systems with four transmit antennas, four users and single antenna per user, in ideal scenarios (i.e., independent identically distributed, i.i.d., channels) downlink data rate may be shared across the four users and channel spatial diversity may be exploited to create four parallel 30Mbps data links to the users.

Different MU-MIMO schemes have been proposed as part of the LTE standard as described, for example, in 3GPP, “Multiple Input Multiple Output in UTRA”, 3GPP TR 25.876 V7.0.0, Mar. 2007; 3GPP, “Base Physical channels and modulation”, TS 36.211, V8.7.0, May 2009; and 3GPP, “Multiplexing and channel coding”, TS 36.212, V8.7.0, May 2009. However, these schemes can provide only up to 2X improvement in DL data rate with four transmit antennas. Practical implementations of MU-MIMO techniques in standard and proprietary cellular systems by companies like ArrayComm (*see, e.g.*, ArrayComm, “Field-proven results”, <http://www.arraycomm.com/serve.php?page=proof>) have yielded up to a  $\sim 3X$  increase (with four transmit antennas) in DL data rate via space division multiple access (SDMA). A key limitation of MU-MIMO schemes in cellular networks is lack of spatial diversity at the transmit side.

Spatial diversity is a function of antenna spacing and multipath angular spread in the wireless links. In cellular systems employing MU-MIMO techniques, transmit antennas at a base station are typically clustered together and placed only one or two wavelengths apart due to limited real estate on antenna support structures (referred to herein as “towers,” whether physically tall or not) and due to limitations on where towers may be located. Moreover, multipath angular spread is low since cell towers are typically placed high up (10 meters or more) above obstacles to yield wider coverage.

[0017] Other practical issues with cellular system deployment include excessive cost and limited availability of locations for cellular antenna locations (e.g. due to municipal restrictions on antenna placement, cost of real-estate, physical obstructions, etc.) and the cost and/or availability of network connectivity to the transmitters (referred to herein as “backhaul”).

## 6181P526XPCT

Further, cellular systems often have difficulty reaching clients located deeply in buildings due to losses from walls, ceilings, floors, furniture and other impediments.

**[0018]** Indeed, the entire concept of a cellular structure for wide-area network wireless presupposes a rather rigid placement of cellular towers, an alternation of frequencies between adjacent cells, and frequently sectorization, so as to avoid interference among transmitters (either base stations or users) that are using the same frequency. As a result, a given sector of a given cell ends up being a shared block of DL and UL spectrum among all of the users in the cell sector, which is then shared among these users primarily in only the time domain. For example, cellular systems based on Time Division Multiple Access (TDMA) and Code Division Multiple Access (CDMA) both share spectrum among users in the time domain. By overlaying such cellular systems with sectorization, perhaps a 2-3X spatial domain benefit can be achieved. And, then by overlaying such cellular systems with a MU-MIMO system, such as those described previously, perhaps another 2-3X space-time domain benefit can be achieved. But, given that the cells and sectors of the cellular system are typically in fixed locations, often dictated by where towers can be placed, even such limited benefits are difficult to exploit if user density (or data rate demands) at a given time does not match up well with tower/sector placement. A cellular smart phone user often experiences the consequence of this today where the user may be talking on the phone or downloading a web page without any trouble at all, and then after driving (or even walking) to a new location will suddenly see the voice quality drop or the web page slow to a crawl, or even lose the connection entirely. But, on a different day, the user may have the exact opposite occur in each location. What the user is probably experiencing, assuming the environmental conditions are the same, is the fact that user density (or data rate demands) is highly variable, but the available total spectrum (and thereby total data rate, using prior art techniques) to be shared among users at a given location is largely fixed.

**[0019]** Further, prior art cellular systems rely upon using different frequencies in different adjacent cells, typically 3 different frequencies. For a given amount of spectrum, this reduces the available data rate by 3X.

**[0020]** So, in summary, prior art cellular systems may lose perhaps 3X in spectrum utilization due to cellularization, and may improve spectrum utilization by perhaps 3X through sectorization and perhaps 3X more through MU-MIMO techniques, resulting in a net  $3*3/3 = 3X$  potential spectrum utilization. Then, that bandwidth is typically divided up among users in the time domain, based upon what sector of what cell the users fall into at a given time. There are even further inefficiencies that result due to the fact that a given user's data rate demands are typically independent of the user's location, but the available data rate varies depending on the link quality between the user and the base station. For example, a user further from a cellular

base station will typically have less available data rate than a user closer to a base station. Since the data rate is typically shared among all of the users in a given cellular sector, the result of this is that all users are impacted by high data rate demands from distant users with poor link quality (e.g. on the edge of a cell) since such users will still demand the same amount of data rate, yet they will be consuming more of the shared spectrum to get it.

**[0021]** Other proposed spectrum sharing systems, such as that used by WiFi (e.g., 802.11b, g, and n) and those proposed by the White Spaces Coalition, share spectrum very inefficiently since simultaneous transmissions by base stations within range of a user result in interference, and as such, the systems utilize collision avoidance and sharing protocols. These spectrum sharing protocols are within the time domain, and so, when there are a large number of interfering base stations and users, no matter how efficient each base station itself is in spectrum utilization, collectively the base stations are limited to time domain sharing of the spectrum among each other. Other prior art spectrum sharing systems similarly rely upon similar methods to mitigate interference among base stations (be they cellular base stations with antennas on towers or small scale base stations, such as WiFi Access Points (APs)). These methods include limiting transmission power from the base station so as to limit the range of interference, beamforming (via synthetic or physical means) to narrow the area of interference, time-domain multiplexing of spectrum and/or MU-MIMO techniques with multiple clustered antennas on the user device, the base station or both. And, in the case of advanced cellular networks in place or planned today, frequently many of these techniques are used at once.

**[0022]** But, what is apparent by the fact that even advanced cellular systems can achieve only about a 3X increase in spectrum utilization compared to a single user utilizing the spectrum is that all of these techniques have done little to increase the aggregate data rate among shared users for a given area of coverage. In particular, as a given coverage area scales in terms of users, it becomes increasingly difficult to scale the available data rate within a given amount of spectrum to keep pace with the growth of users. For example, with cellular systems, to increase the aggregate data rate within a given area, typically the cells are subdivided into smaller cells (often called nano-cells or femto-cells). Such small cells can become extremely expensive given the limitations on where towers can be placed, and the requirement that towers must be placed in a fairly structured pattern so as to provide coverage with a minimum of “dead zones”, yet avoid interference between nearby cells using the same frequencies. Essentially, the coverage area must be mapped out, the available locations for placing towers or base stations must be identified, and then given these constraints, the designers of the cellular system must make do with the best they can. And, of course, if user data rate demands grow over time, then the designers of the cellular system must yet again remap the coverage area, try to find locations for

6181P526XPCT

towers or base stations, and once again work within the constraints of the circumstances. And, very often, there simply is no good solution, resulting in dead zones or inadequate aggregate data rate capacity in a coverage area. In other words, the rigid physical placement requirements of a cellular system to avoid interference among towers or base stations utilizing the same frequency results in significant difficulties and constraints in cellular system design, and often is unable to meet user data rate and coverage requirements.

**[0023]** So-called prior art “cooperative” and “cognitive” radio systems seek to increase the spectral utilization in a given area by using intelligent algorithms within radios such that they can minimize interference among each other and/or such that they can potentially “listen” for other spectrum use so as to wait until the channel is clear. Such systems are proposed for use particularly in unlicensed spectrum in an effort to increase the spectrum utilization of such spectrum.

**[0024]** A mobile ad hoc network (MANET) (see [http://en.wikipedia.org/wiki/Mobile\\_ad\\_hoc\\_network](http://en.wikipedia.org/wiki/Mobile_ad_hoc_network)) is an example of a cooperative self-configuring network intended to provide peer-to-peer communications, and could be used to establish communication among radios without cellular infrastructure, and with sufficiently low-power communications, can potentially mitigate interference among simultaneous transmissions that are out of range of each other. A vast number of routing protocols have been proposed and implemented for MANET systems (see [http://en.wikipedia.org/wiki/List\\_of\\_ad-hoc\\_routing\\_protocols](http://en.wikipedia.org/wiki/List_of_ad-hoc_routing_protocols) for a list of dozens of routing protocols in a wide range of classes), but a common theme among them is they are all techniques for routing (e.g. repeating) transmissions in such a way to minimize transmitter interference within the available spectrum, towards the goal of particular efficiency or reliability paradigms.

**[0025]** All of the prior art multi-user wireless systems seek to improve spectrum utilization within a given coverage area by utilizing techniques to allow for simultaneous spectrum utilization among base stations and multiple users. Notably, in all of these cases, the techniques utilized for simultaneous spectrum utilization among base stations and multiple users achieve the simultaneous spectrum use by multiple users by mitigating interference among the waveforms to the multiple users. For example, in the case of 3 base stations each using a different frequency to transmit to one of 3 users, there interference is mitigated because the 3 transmissions are at 3 different frequencies. In the case of sectorization from a base station to 3 different users, each 180 degrees apart relative to the base station, interference is mitigated because the beamforming prevents the 3 transmissions from overlapping at any user.

**[0026]** When such techniques are augmented with MU-MIMO, and, for example, each base station has 4 antennas, then this has the potential to increase downlink throughput by a factor of

4, by creating four non-interfering spatial channels to the users in given coverage area. But it is still the case that some technique must be utilized to mitigate the interference among multiple simultaneous transmissions to multiple users in different coverage areas.

**[0027]** And, as previously discussed, such prior art techniques (e.g. cellularization, sectorization) not only typically suffer from increasing the cost of the multi-user wireless system and/or the flexibility of deployment, but they typically run into physical or practical limitations of aggregate throughput in a given coverage area. For example, in a cellular system, there may not be enough available locations to install more base stations to create smaller cells. And, in an MU-MIMO system, given the clustered antenna spacing at each base station location, the limited spatial diversity results in asymptotically diminishing returns in throughput as more antennas are added to the base station.

**[0028]** And further, in the case of multi-user wireless systems where the user location and density is unpredictable, it results in unpredictable (with frequently abrupt changes) in throughput, which is inconvenient to the user and renders some applications (e.g. the delivery of services requiring predictable throughput) impractical or of low quality. Thus, prior art multi-user wireless systems still leave much to be desired in terms of their ability to provide predictable and/or high-quality services to users.

**[0029]** Despite the extraordinary sophistication and complexity that has been developed for prior art multi-user wireless systems over time, there exist common themes: transmissions are distributed among different base stations (or ad hoc transceivers) and are structured and/or controlled so as to avoid the RF waveform transmissions from the different base stations and/or different ad hoc transceivers from interfering with each other at the receiver of a given user.

**[0030]** Or, to put it another way, it is taken as a given that if a user happens to receive transmissions from more than one base station or ad hoc transceiver at the same time, the interference from the multiple simultaneous transmissions will result in a reduction of the SNR and/or bandwidth of the signal to the user which, if severe enough, will result in loss of all or some of the potential data (or analog information) that would otherwise have been received by the user.

**[0031]** Thus, in a multiuser wireless system, it is necessary to utilize one or more spectrum sharing approaches or another to avoid or mitigate such interference to users from multiple base stations or ad hoc transceivers transmitting at the same frequency at the same time. There are a vast number of prior art approaches to avoiding such interference, including controlling base stations' physical locations (e.g. cellularization), limiting power output of base stations and/or ad hoc transceivers (e.g. limiting transmit range), beamforming/sectorization, and time domain multiplexing. In short, all of these spectrum sharing systems seek to address the limitation of

6181P526XPCT

multiuser wireless systems that when multiple base stations and/or ad hoc transceivers transmitting simultaneously at the same frequency are received by the same user, the resulting interference reduces or destroys the data throughput to the affected user. If a large percentage, or all, of the users in the multi-user wireless system are subject to interference from multiple base stations and/or ad hoc transceivers (e.g. in the event of the malfunction of a component of a multi-user wireless system), then it can result in a situation where the aggregate throughput of the multi-user wireless system is dramatically reduced, or even rendered non-functional..

**[0032]** Prior art multi-user wireless systems add complexity and introduce limitations to wireless networks and frequently result in a situation where a given user's experience (e.g. available bandwidth, latency, predictability, reliability) is impacted by the utilization of the spectrum by other users in the area. Given the increasing demands for aggregate bandwidth within wireless spectrum shared by multiple users, and the increasing growth of applications that can rely upon multi-user wireless network reliability, predictability and low latency for a given user, it is apparent that prior art multi-user wireless technology suffers from many limitations. Indeed, with the limited availability of spectrum suitable for particular types of wireless communications (e.g. at wavelengths that are efficient in penetrating building walls), it may be the case that prior art wireless techniques will be insufficient to meet the increasing demands for bandwidth that is reliable, predictable and low-latency.

**[0033]** Prior art related to the current invention describes beamforming systems and methods for null-steering in multiuser scenarios. Beamforming was originally conceived to maximize received signal-to-noise ratio (SNR) by dynamically adjusting phase and/or amplitude of the signals (i.e., beamforming weights) fed to the antennas of the array, thereby focusing energy toward the user's direction. In multiuser scenarios, beamforming can be used to suppress interfering sources and maximize signal-to-interference-plus-noise ratio (SINR). For example, when beamforming is used at the receiver of a wireless link, the weights are computed to create nulls in the direction of the interfering sources. When beamforming is used at the transmitter in multiuser downlink scenarios, the weights are calculated to pre-cancel inter-user interference and maximize the SINR to every user. Alternative techniques for multiuser systems, such as BD precoding, compute the precoding weights to maximize throughput in the downlink broadcast channel. The co-pending applications, which are incorporated herein by reference, describe the foregoing techniques (see co-pending applications for specific citations).

**[0034]** Reference to any prior art in this specification does not constitute an admission that such prior art forms part of the common general knowledge.

**[0035]** It is an object of the present invention to provide a multiuser multiple antenna system and method which overcome at least some of the problems of the prior art or which at least provide the public with a useful choice.

**[0036]** According to a first aspect of the invention there is provided a multiuser (MU) multiple antenna system (MAS) comprising: one or more centralized units communicatively coupled to multiple distributed transceiver stations or antennas via a network; the network consisting of wireline or wireless links or a combination of both, employed as a backhaul communication channel; the MU-MAS adaptively reconfiguring to compensate for Doppler effects due to user mobility or changes in the propagation environment.

**[0037]** According to a further aspect there is provided a method implemented within a multiuser (MU) multiple antenna system (MAS) to compensate for Doppler effects comprising: measuring Doppler velocity of a first mobile user relative to a plurality of base transceiver stations (BTSs); and dynamically assigning the first mobile user to a first BTS or to a first set of BTSs of the plurality of BTSs based on the measured Doppler velocity for the first BTS relative to other BTSs.

**[0038]** According to a yet further aspect there is provided multiuser (MU) multiple antenna system (MAS) to compensate for Doppler effects comprising: a plurality of base transceiver stations (BTSs); a first mobile user establishing a communication link with each of the BTSs; a centralized processor (CP) measuring Doppler velocity of a first mobile user relative to each of the BTSs and dynamically assigning the first mobile user to a first BTS of the plurality of BTSs based on the measured Doppler velocity for the first BTS relative to other BTSs.

**[0039]** It is acknowledged that the terms "comprise", "comprises" and "comprising" may, under varying jurisdictions, be attributed with either an exclusive or an inclusive meaning. For the purpose of this specification, and unless otherwise noted, these terms are intended to have an inclusive meaning - i.e. they will be taken to mean an inclusion of the listed components that the use directly references, but optionally also the inclusion of other non-specified components or elements.

#### **BRIEF DESCRIPTION OF THE DRAWINGS**

**[0040]** A better understanding of the present invention can be obtained from the following detailed description given by way of example with reference to the drawings, in which:

**[0041]** **FIG. 1** illustrates a main DIDO cluster surrounded by neighboring DIDO clusters in one embodiment of the invention.

**[0042]** **FIG. 2** illustrates frequency division multiple access (FDMA) techniques employed in one embodiment of the invention.

[0043] **FIG. 3** illustrates time division multiple access (TDMA) techniques employed in one embodiment of the invention.

[0044] **FIG. 4** illustrates different types of interfering zones addressed in one embodiment of the invention.

[0045] **FIG. 5** illustrates a framework employed in one embodiment of the invention.

[0046] **FIG. 6** illustrates a graph showing SER as a function of the SNR, assuming SIR=10dB for the target client in the interfering zone.

[0047] **FIG. 7** illustrates a graph showing SER derived from two IDCI-precoding techniques.

[0048] **FIG. 8** illustrates an exemplary scenario in which a target client moves from a main DIDO cluster to an interfering cluster.

[0049] **FIG. 9** illustrates the signal-to-interference-plus-noise ratio (SINR) as a function of distance (D).

[0050] **FIG. 10** illustrates the symbol error rate (SER) performance of the three scenarios for 4-QAM modulation in flat-fading narrowband channels.

[0051] **FIG. 11** illustrates a method for IDCI precoding according to one embodiment of the invention.

[0052] **FIG. 12** illustrates the SINR variation in one embodiment as a function of the client's distance from the center of main DIDO clusters.

[0053] **FIG. 13** illustrates one embodiment in which the SER is derived for 4-QAM modulation.

[0054] **FIG. 14** illustrates one embodiment of the invention in which a finite state machine implements a handoff algorithm.

[0055] **FIG. 15** illustrates depicts one embodiment of a handoff strategy in the presence of shadowing.

[0056] **FIG. 16** illustrates a hysteresis loop mechanism when switching between any two states in Fig. 93.

[0057] **FIG. 17** illustrates one embodiment of a DIDO system with power control.

[0058] **FIG. 18** illustrates the SER versus SNR assuming four DIDO transmit antennas and four clients in different scenarios.

[0059] **FIG. 19** illustrates MPE power density as a function of distance from the source of RF radiation for different values of transmit power according to one embodiment of the invention.

[0060] **FIGS. 20a-b** illustrate different distributions of low-power and high-power DIDO distributed antennas.

[0061] **FIGS. 21a-b** illustrate two power distributions corresponding to the configurations in Figs. 20a and 20b, respectively.

[0062] **FIG. 22a-b** illustrate the rate distribution for the two scenarios shown in Figs. 99a and 99b, respectively.

[0063] **FIG. 23** illustrates one embodiment of a DIDO system with power control.

[0064] **FIG. 24** illustrates one embodiment of a method which iterates across all antenna groups according to Round-Robin scheduling policy for transmitting data.

[0065] **FIG. 25** illustrates a comparison of the uncoded SER performance of power control with antenna grouping against conventional eigenmode selection in U.S. Patent No. 7,636,381.

[0066] **FIGS. 26a-c** illustrate three scenarios in which BD precoding dynamically adjusts the precoding weights to account for different power levels over the wireless links between DIDO antennas and clients.

[0067] **FIG. 27** illustrates the amplitude of low frequency selective channels (assuming  $\beta = 1$ ) over delay domain or instantaneous PDP (upper plot) and frequency domain (lower plot) for DIDO 2x2 systems

[0068] **FIG. 28** illustrates one embodiment of a channel matrix frequency response for DIDO 2x2, with a single antenna per client.

[0069] **FIG. 29** illustrates one embodiment of a channel matrix frequency response for DIDO 2x2, with a single antenna per client for channels characterized by high frequency selectivity (e.g., with  $\beta = 0.1$ ).

[0070] **FIG. 30** illustrates exemplary SER for different QAM schemes (i.e., 4-QAM, 16-QAM, 64-QAM).

[0071] **FIG. 31** illustrates one embodiment of a method for implementing link adaptation (LA) techniques.

[0072] **FIG. 32** illustrates SER performance of one embodiment of the link adaptation (LA) techniques.

[0073] **FIG. 33** illustrates the entries of the matrix in equation (28) as a function of the OFDM tone index for DIDO 2x2 systems with  $N_{FFT} = 64$  and  $L_0 = 8$ .

[0074] **FIG. 34** illustrates the SER versus SNR for  $L_0 = 8$ ,  $M=N_t=2$  transmit antennas and a variable number of P.

[0075] **FIG. 35** illustrates the SER performance of one embodiment of an interpolation method for different DIDO orders and  $L_0 = 16$ .

[0076] **FIG. 36** illustrates one embodiment of a system which employs super-clusters, DIDO-clusters and user-clusters.

6181P526XPCT

[0077] **FIG. 37** illustrates a system with user clusters according to one embodiment of the invention.

[0078] **FIGS. 38a-b** illustrate link quality metric thresholds employed in one embodiment of the invention.

[0079] **FIGS. 39-41** illustrate examples of link-quality matrices for establishing user clusters.

[0080] **FIG. 42** illustrates an embodiment in which a client moves across different different DIDO clusters.

[0081] **FIGS. 43-46** illustrate relationships between the resolution of spherical arrays and their area  $A$  in one embodiment of the invention.

[0082] **FIG. 47** illustrates the degrees of freedom of MIMO systems in practical indoor and outdoor propagation scenarios.

[0083] **FIG. 48** illustrates the degrees of freedom in DIDO systems as a function of the array diameter.

[0084] **FIG. 49** illustrates one embodiment which includes multiple centralized processors (CP) and distributed nodes (DN) that communicate via wireline or wireless connections.

[0085] **FIG. 50** illustrates one embodiment in which CPs exchange control information with the unlicensed DNs and reconfigure them to shut down the frequency bands for licensed use.

[0086] **FIG. 51** illustrates one embodiment in which an entire spectrum is allocated to the new service and control information is used by the CPs to shut down all unlicensed DNs to avoid interference with the licensed DNs.

[0087] **FIG. 52** illustrates one embodiment of a cloud wireless system including multiple CPs, distributed nodes and a network interconnecting the CPs to the DNs.

[0088] **FIGS. 53-59** illustrate embodiments of a multiuser (MU) multiple antenna system (MAS) that adaptively reconfigures parameters to compensate for Doppler effects due to user mobility or changes in the propagation environment.

[0089] **FIG. 60** illustrates a plurality of BTSs, some of which have good SNR and some of which have low Doppler with respect to a UE.

[0090] **FIG. 61** illustrates one embodiment of a matrix containing values of SNR and Doppler recorded by a CP for a plurality of BTS-UE links.

[0091] **FIG. 62** illustrates the channel gain (or CSI) at different times in accordance with one embodiment of the invention.

### **DETAILED DESCRIPTION**

[0092] One solution to overcome many of the above prior art limitations is an embodiment of Distributed-Input Distributed-Output (DIDO) technology. DIDO technology is described in

6181P526XPCT

the following patents and patent applications, all of which are assigned the assignee of the present patent and are incorporated by reference. The present application is a continuation in part (CIP) to these patent applications. These patents and applications are sometimes referred to collectively herein as the “related patents and applications”:

[0093] U.S. Application Serial No. 13/232,996, filed September 14, 2011, entitled “Systems And Methods To Exploit Areas of Coherence in Wireless Systems”

[0094] U.S. Application Serial No. 13/233,006, filed September 14, 2011, entitled “Systems and Methods for Planned Evolution and Obsolescence of Multiuser Spectrum.”

[0095] U.S. Application Serial No. 12/917,257, filed November 1, 2010, entitled “Systems And Methods To Coordinate Transmissions In Distributed Wireless Systems Via User Clustering”

[0096] U.S. Application Serial No. 12/802,988, filed June 16, 2010, entitled “Interference Management, Handoff, Power Control And Link Adaptation In Distributed-Input Distributed-Output (DIDO) Communication Systems”

[0097] U.S. Application Serial No. 12/802,976, filed June 16, 2010, entitled “System And Method For Adjusting DIDO Interference Cancellation Based On Signal Strength Measurements”

[0098] U.S. Application Serial No. 12/802,974, filed June 16, 2010, entitled “System And Method For Managing Inter-Cluster Handoff Of Clients Which Traverse Multiple DIDO Clusters”

[0099] U.S. Application Serial No. 12/802,989, filed June 16, 2010, entitled “System And Method For Managing Handoff Of A Client Between Different Distributed-Input-Distributed-Output (DIDO) Networks Based On Detected Velocity Of The Client”

[00100] U.S. Application Serial No. 12/802,958, filed June 16, 2010, entitled “System And Method For Power Control And Antenna Grouping In A Distributed-Input-Distributed-Output (DIDO) Network”

[00101] U.S. Application Serial No. 12/802,975, filed June 16, 2010, entitled “System And Method For Link adaptation In DIDO Multicarrier Systems”

[00102] U.S. Application Serial No. 12/802,938, filed June 16, 2010, entitled “System And Method For DIDO Precoding Interpolation In Multicarrier Systems”

[00103] U.S. Application Serial No. 12/630,627, filed December 2, 2009, entitled ”System and Method For Distributed Antenna Wireless Communications”

[00104] U.S. Patent No. 7,599,420, filed August 20, 2007, issued Oct. 6, 2009, entitled “System and Method for Distributed Input Distributed Output Wireless Communication”;

12 Mar 2015  
2013256044

6181P526XPCT

**[00105]** U.S. Patent No. 7,633,994, filed August 20, 2007, issued Dec. 15, 2009, entitled “System and Method for Distributed Input Distributed Output Wireless Communication”;

**[00106]** U.S. Patent No. 7,636,381, filed August 20, 2007, issued Dec. 22, 2009, entitled “System and Method for Distributed Input Distributed Output Wireless Communication”;

**[00107]** U.S. Application Serial No. 12/143,503, filed June 20, 2008 entitled, ”System and Method For Distributed Input-Distributed Output Wireless Communications”;

**[00108]** U.S. Application Serial No. 11/256,478, filed October 21, 2005 entitled “System and Method For Spatial-Multiplexed Tropospheric Scatter Communications”;

**[00109]** U.S. Patent No. 7,418,053, filed July 30, 2004, issued August 26, 2008, entitled “System and Method for Distributed Input Distributed Output Wireless Communication”;

**[00110]** U.S. Application Serial No. 10/817,731, filed April 2, 2004 entitled “System and Method For Enhancing Near Vertical Incidence Skywave (“NVIS”) Communication Using Space-Time Coding.

**[00111]** To reduce the size and complexity of the present patent application, the disclosure of some of the related patents and applications is not explicitly set forth below. Please see the related patents and applications for a full detailed description of the disclosure.

**[00112]** Note that section I below (Disclosure From Related Application Serial No. 12/802,988) utilizes its own set of endnotes which refer to prior art references and prior applications assigned to the assignee of the present application. The endnote citations are listed at the end of section I (just prior to the heading for Section II). Citations in Section II uses may have numerical designations for its citations which overlap with those used in Section I even though these numerical designations identify different references (listed at the end of Section II). Thus, references identified by a particular numerical designation may be identified within the section in which the numerical designation is used.

## **I. Disclosure From Related Application Serial No. 12/802,988**

### **1. Methods to Remove Inter-cluster Interference**

**[00113]** Described below are wireless radio frequency (RF) communication systems and methods employing a plurality of distributed transmitting antennas to create locations in space with zero RF energy. When  $M$  transmit antennas are employed, it is possible to create up to  $(M-1)$  points of zero RF energy in predefined locations. In one embodiment of the invention, the points of zero RF energy are wireless devices and the transmit antennas are aware of the channel state information (CSI) between the transmitters and the receivers. In one embodiment, the CSI is computed at the receivers and fed back to the transmitters. In another embodiment, the CSI is computed at the transmitter via training from the receivers, assuming channel reciprocity is exploited. The transmitters may utilize the CSI to determine the interfering signals to be

6181P526XPCT

simultaneously transmitted. In one embodiment, block diagonalization (BD) precoding is employed at the transmit antennas to generate points of zero RF energy.

**[00114]** The system and methods described herein differ from the conventional receive/transmit beamforming techniques described above. In fact, receive beamforming computes the weights to suppress interference at the receive side (via null-steering), whereas some embodiments of the invention described herein apply weights at the transmit side to create interference patterns that result in one or multiple locations in space with “zero RF energy.” Unlike conventional transmit beamforming or BD precoding designed to maximize signal quality (or SINR) to every user or downlink throughput, respectively, the systems and methods described herein minimize signal quality under certain conditions and/or from certain transmitters, thereby creating points of zero RF energy at the client devices (sometimes referred to herein as “users”). Moreover, in the context of distributed-input distributed-output (DIDO) systems (described in our related patents and applications), transmit antennas distributed in space provide higher degrees of freedom (i.e., higher channel spatial diversity) that can be exploited to create multiple points of zero RF energy and/or maximum SINR to different users. For example, with  $M$  transmit antennas it is possible to create up to  $(M-1)$  points of RF energy. By contrast, practical beamforming or BD multiuser systems are typically designed with closely spaced antennas at the transmit side that limit the number of simultaneous users that can be serviced over the wireless link, for any number of transmit antennas  $M$ .

**[00115]** Consider a system with  $M$  transmit antennas and  $K$  users, with  $K < M$ . We assume the transmitter is aware of the CSI ( $\mathbf{H} \in \mathbb{C}^{K \times M}$ ) between the  $M$  transmit antennas and  $K$  users. For simplicity, every user is assumed to be equipped with single antenna, but the same method can be extended to multiple receive antennas per user. The precoding weights ( $\mathbf{w} \in \mathbb{C}^{M \times 1}$ ) that create zero RF energy at the  $K$  users’ locations are computed to satisfy the following condition

$$\mathbf{H}\mathbf{w} = \mathbf{0}^{K \times 1}$$

where  $\mathbf{0}^{K \times 1}$  is the vector with all zero entries and  $\mathbf{H}$  is the channel matrix obtained by combining the channel vectors ( $\mathbf{h}_k \in \mathbb{C}^{1 \times M}$ ) from the  $M$  transmit antennas to the  $K$  users as

$$\mathbf{H} = \begin{bmatrix} \mathbf{h}_1 \\ \vdots \\ \mathbf{h}_k \\ \vdots \\ \mathbf{h}_K \end{bmatrix}.$$

In one embodiment, singular value decomposition (SVD) of the channel matrix  $\mathbf{H}$  is computed and the precoding weight  $\mathbf{w}$  is defined as the right singular vector corresponding to the null subspace (identified by zero singular value) of  $\mathbf{H}$ .

The transmit antennas employ the weight vector defined above to transmit RF energy, while creating K points of zero RF energy at the locations of the K users such that the signal received at the k<sup>th</sup> user is given by

$$r_k = \mathbf{h}_k \mathbf{w} s_k + n_k = 0 + n_k$$

where  $n_k \in \mathbb{C}^{1 \times 1}$  is the additive white Gaussian noise (AWGN) at the k<sup>th</sup> user.

In one embodiment, singular value decomposition (SVD) of the channel matrix  $\mathbf{H}$  is computed and the precoding weight  $\mathbf{w}$  is defined as the right singular vector corresponding to the null subspace (identified by zero singular value) of  $\mathbf{H}$ .

**[00116]** In another embodiment, the wireless system is a DIDO system and points of zero RF energy are created to pre-cancel interference to the clients between different DIDO coverage areas. In U.S. Application Serial No. 12/630,627, a DIDO system is described which includes:

- DIDO clients
- DIDO distributed antennas
- DIDO base transceiver stations (BTS)
- DIDO base station network (BSN)

Every BTS is connected via the BSN to multiple distributed antennas that provide service to given coverage area called *DIDO cluster*. In the present patent application we describe a system and method for removing interference between adjacent DIDO clusters. As illustrated in **Figure 1**, we assume the *main* DIDO cluster hosts the client (i.e. a user device served by the multi-user DIDO system) affected by interference (or *target client*) from the *neighbor* clusters.

**[00117]** In one embodiment, neighboring clusters operate at different frequencies according to frequency division multiple access (FDMA) techniques similar to conventional cellular systems. For example, with frequency reuse factor of 3, the same carrier frequency is reused every third DIDO cluster as illustrated in **Figure 2**. In **Figure 2**, the different carrier frequencies are identified as F<sub>1</sub>, F<sub>2</sub> and F<sub>3</sub>. While this embodiment may be used in some implementations, this solution yields loss in spectral efficiency since the available spectrum is divided in multiple subbands and only a subset of DIDO clusters operate in the same subband. Moreover, it requires complex cell planning to associate different DIDO clusters to different frequencies, thereby preventing interference. Like prior art cellular systems, such cellular planning requires specific placement of antennas and limiting of transmit power to as to avoid interference between clusters using the same frequency.

**[00118]** In another embodiment, neighbor clusters operate in the same frequency band, but at different time slots according to time division multiple access (TDMA) technique. For example, as illustrated in **Figure 3** DIDO transmission is allowed only in time slots T<sub>1</sub>, T<sub>2</sub>, and T<sub>3</sub> for certain clusters, as illustrated. Time slots can be assigned equally to different clusters, such that

## 6181P526XPCT

different clusters are scheduled according to a Round-Robin policy. If different clusters are characterized by different data rate requirements (i.e., clusters in crowded urban environments as opposed to clusters in rural areas with fewer number of clients per area of coverage), different priorities are assigned to different clusters such that more time slots are assigned to the clusters with larger data rate requirements. While TDMA as described above may be employed in one embodiment of the invention, a TDMA approach may require time synchronization across different clusters and may result in lower spectral efficiency since interfering clusters cannot use the same frequency at the same time.

**[00119]** In one embodiment, all neighboring clusters transmit at the same time in the same frequency band and use spatial processing across clusters to avoid interference. In this embodiment, the multi-cluster DIDO system: (i) uses conventional DIDO precoding within the main cluster to transmit simultaneous non-interfering data streams within the same frequency band to multiple clients (such as described in the related patents and applications, including 7,599,420; 7,633,994; 7,636,381; and Application Serial No. 12/143,503); (ii) uses DIDO precoding with interference cancellation in the neighbor clusters to avoid interference to the clients lying in the *interfering zones* 8010 in **Figure 4**, by creating points of zero radio frequency (RF) energy at the locations of the target clients. If a target client is in an interfering zone 410, it will receive the sum of the RF containing the data stream from the main cluster 411 and the zero RF energy from the interfering cluster 412-413, which will simply be the RF containing the data stream from the main cluster. Thus, adjacent clusters can utilize the same frequency simultaneously without target clients in the interfering zone suffering from interference.

**[00120]** In practical systems, the performance of DIDO precoding may be affected by different factors such as: channel estimation error or Doppler effects (yielding obsolete channel state information at the DIDO distributed antennas); intermodulation distortion (IMD) in multicarrier DIDO systems; time or frequency offsets. As a result of these effects, it may be impractical to achieve points of zero RF energy. However, as long as the RF energy at the target client from the interfering clusters is negligible compared to the RF energy from the main cluster, the link performance at the target client is unaffected by the interference. For example, let us assume the client requires 20dB signal-to-noise ratio (SNR) to demodulate 4-QAM constellations using forward error correction (FEC) coding to achieve target bit error rate (BER) of  $10^{-6}$ . If the RF energy at the target client received from the interfering cluster is 20dB below the RF energy received from the main cluster, the interference is negligible and the client can demodulate data successfully within the predefined BER target. Thus, the term “zero RF energy” as used herein does not necessarily mean that the RF energy from interfering RF signals is zero. Rather, it means that the RF energy is sufficiently low relative to the RF energy of the desired

6181P526XPCT

RF signal such that the desired RF signal may be received at the receiver. Moreover, while certain desirable thresholds for interfering RF energy relative to desired RF energy are described, the underlying principles of the invention are not limited to any particular threshold values.

**[00121]** There are different types of interfering zones 8010 as shown in **Figure 4**. For example, “type A” zones (as indicated by the letter “A” in Figure 80) are affected by interference from only one neighbor cluster, whereas “type B” zones (as indicated by the letter “B”) account for interference from two or multiple neighbor clusters.

**[00122]** **Figure 5** depicts a framework employed in one embodiment of the invention. The dots denote DIDO distributed antennas, the crosses refer to the DIDO clients and the arrows indicate the directions of propagation of RF energy. The DIDO antennas in the main cluster transmit precoded data signals to the clients MC 501 in that cluster. Likewise, the DIDO antennas in the interfering cluster serve the clients IC 502 within that cluster via conventional DIDO precoding. The green cross 503 denotes the target client TC 503 in the interfering zone. The DIDO antennas in the main cluster 511 transmit precoded data signals to the target client (black arrows) via conventional DIDO precoding. The DIDO antennas in the interfering cluster 512 use precoding to create zero RF energy towards the directions of the target client 503 (green arrows).

**[00123]** The received signal at target client  $k$  in any interfering zone 410A, B in **Figure 4** is given by

$$\mathbf{r}_k = \mathbf{H}_k \mathbf{W}_k \mathbf{s}_k + \mathbf{H}_k \sum_{u=1, u \neq k}^U \mathbf{W}_u \mathbf{s}_u + \sum_{c=1}^C \mathbf{H}_{c,k} \sum_{i=1}^{I_c} \mathbf{W}_{c,i} \mathbf{s}_{c,i} + \mathbf{n}_k \quad (1)$$

where  $k=1, \dots, K$ , with  $K$  being the number of clients in the interfering zone 8010A, B,  $U$  is the number of clients in the main DIDO cluster,  $C$  is the number of interfering DIDO clusters 412-413 and  $I_c$  is the number of clients in the interfering cluster  $c$ . Moreover,  $\mathbf{r}_k \in \mathbb{C}^{N \times M}$  is the vector containing the receive data streams at client  $k$ , assuming  $M$  transmit DIDO antennas and  $N$  receive antennas at the client devices;  $\mathbf{s}_k \in \mathbb{C}^{N \times 1}$  is the vector of transmit data streams to client  $k$  in the main DIDO cluster;  $\mathbf{s}_u \in \mathbb{C}^{N \times 1}$  is the vector of transmit data streams to client  $u$  in the main DIDO cluster;  $\mathbf{s}_{c,i} \in \mathbb{C}^{N \times 1}$  is the vector of transmit data streams to client  $i$  in the  $c^{\text{th}}$  interfering DIDO cluster;  $\mathbf{n}_k \in \mathbb{C}^{N \times 1}$  is the vector of additive white Gaussian noise (AWGN) at the  $N$  receive antennas of client  $k$ ;  $\mathbf{H}_k \in \mathbb{C}^{N \times M}$  is the DIDO channel matrix from the  $M$  transmit DIDO antennas to the  $N$  receive antennas at client  $k$  in the main DIDO cluster;  $\mathbf{H}_{c,k} \in \mathbb{C}^{N \times M}$  is the DIDO channel matrix from the  $M$  transmit DIDO antennas to the  $N$  receive antennas at client  $k$  in the  $c^{\text{th}}$  interfering DIDO cluster;  $\mathbf{W}_k \in \mathbb{C}^{M \times N}$  is the matrix of DIDO precoding weights to client  $k$  in the main DIDO cluster;  $\mathbf{W}_u \in \mathbb{C}^{M \times N}$  is the matrix of DIDO precoding weights to client  $u$  in the

main DIDO cluster;  $\mathbf{W}_{c,i} \in \mathbb{C}^{M \times N}$  is the matrix of DIDO precoding weights to client  $i$  in the  $c^{\text{th}}$  interfering DIDO cluster.

**[00124]** To simplify the notation and without loss of generality, we assume all clients are equipped with  $N$  receive antennas and there are  $M$  DIDO distributed antennas in every DIDO cluster, with  $M \geq (N \cdot U)$  and  $M \geq (N \cdot I_c)$ ,  $\forall c = 1, \dots, C$ . If  $M$  is larger than the total number of receive antennas in the cluster, the extra transmit antennas are used to pre-cancel interference to the target clients in the interfering zone or to improve link robustness to the clients within the same cluster via diversity schemes described in the related patents and applications, including 7,599,420; 7,633,994; 7,636,381; and Application Serial No. 12/143,503.

**[00125]** The DIDO precoding weights are computed to pre-cancel inter-client interference within the same DIDO cluster. For example, block diagonalization (BD) precoding described in the related patents and applications, including 7,599,420; 7,633,994; 7,636,381; and Application Serial No. 12/143,503 and [7] can be used to remove inter-client interference, such that the following condition is satisfied in the main cluster

$$\mathbf{H}_k \mathbf{W}_u = \mathbf{0}^{N \times N}; \quad \forall u = 1, \dots, U; \text{ with } u \neq k. \quad (2)$$

The precoding weight matrices in the neighbor DIDO clusters are designed such that the following condition is satisfied

$$\mathbf{H}_{c,k} \mathbf{W}_{c,i} = \mathbf{0}^{N \times N}; \quad \forall c = 1, \dots, C \text{ and } \forall i = 1, \dots, I_c. \quad (3)$$

To compute the precoding matrices  $\mathbf{W}_{c,i}$ , the downlink channel from the  $M$  transmit antennas to the  $I_c$  clients in the interfering cluster as well as to client  $k$  in the interfering zone is estimated and the precoding matrix is computed by the DIDO BTS in the interfering cluster. If BD method is used to compute the precoding matrices in the interfering clusters, the following effective channel matrix is built to compute the weights to the  $i^{\text{th}}$  client in the neighbor clusters

$$\bar{\mathbf{H}}_{c,i} = \begin{bmatrix} \mathbf{H}_{c,k} \\ \tilde{\mathbf{H}}_{c,i} \end{bmatrix} \quad (4)$$

where  $\tilde{\mathbf{H}}_{c,i}$  is the matrix obtained from the channel matrix  $\mathbf{H}_c \in \mathbb{C}^{(N \cdot I_c) \times M}$  for the interfering cluster  $c$ , where the rows corresponding to the  $i^{\text{th}}$  client are removed.

Substituting conditions (2) and (3) into (1), we obtain the received data streams for target client  $k$ , where intra-cluster and inter-cluster interference is removed

$$\mathbf{r}_k = \mathbf{H}_k \mathbf{W}_k \mathbf{s}_k + \mathbf{n}_k. \quad (5)$$

The precoding weights  $\mathbf{W}_{c,i}$  in (1) computed in the neighbor clusters are designed to transmit precoded data streams to all clients in those clusters, while pre-cancelling interference to the target client in the interfering zone. The target client receives precoded data only from its main cluster. In a different embodiment, the same data stream is sent to the target client from both

main and neighbor clusters to obtain diversity gain. In this case, the signal model in (5) is expressed as

$$\mathbf{r}_k = (\mathbf{H}_k \mathbf{W}_k + \sum_{c=1}^C \mathbf{H}_{c,k} \mathbf{W}_{c,k}) \mathbf{s}_k + \mathbf{n}_k \quad (6)$$

where  $\mathbf{W}_{c,k}$  is the DIDO precoding matrix from the DIDO transmitters in the  $c^{\text{th}}$  cluster to the target client  $k$  in the interfering zone. Note that the method in (6) requires time synchronization across neighboring clusters, which may be complex to achieve in large systems, but nonetheless, is quite feasible if the diversity gain benefit justifies the cost of implementation.

**[00126]** We begin by evaluating the performance of the proposed method in terms of symbol error rate (SER) as a function of the signal-to-noise ratio (SNR). Without loss of generality, we define the following signal model assuming single antenna per client and reformulate (1) as

$$r_k = \sqrt{\text{SNR}} \mathbf{h}_k \mathbf{w}_k s_k + \sqrt{\text{INR}} \mathbf{h}_{c,k} \sum_{i=1}^I \mathbf{w}_{c,i} s_{c,i} + n_k \quad (7)$$

where INR is the interference-to-noise ratio defined as  $\text{INR} = \text{SNR}/\text{SIR}$  and SIR is the signal-to-interference ratio.

**[00127]** **Figure 6** shows the SER as a function of the SNR, assuming  $\text{SIR} = 10\text{dB}$  for the target client in the interfering zone. Without loss of generality, we measured the SER for 4-QAM and 16-QAM without forwards error correction (FEC) coding. We fix the target SER to 1% for uncoded systems. This target corresponds to different values of SNR depending on the modulation order (i.e.,  $\text{SNR} = 20\text{dB}$  for 4-QAM and  $\text{SNR} = 28\text{dB}$  for 16-QAM). Lower SER targets can be satisfied for the same values of SNR when using FEC coding due to coding gain. We consider the scenario of two clusters (one main cluster and one interfering cluster) with two DIDO antennas and two clients (equipped with single antenna each) per cluster. One of the clients in the main cluster lies in the interfering zone. We assume flat-fading narrowband channels, but the following results can be extended to frequency selective multicarrier (OFDM) systems, where each subcarrier undergoes flat-fading. We consider two scenarios: (i) one with *inter-DIDO-cluster interference* (IDCI) where the precoding weights  $\mathbf{w}_{c,i}$  are computed without accounting for the target client in the interfering zone; and (ii) the other where the IDCI is removed by computing the weights  $\mathbf{w}_{c,i}$  to cancel IDCI to the target client. We observe that in presence of IDCI the SER is high and above the predefined target. With IDCI-precoding at the neighbor cluster the interference to the target client is removed and the SER targets are reached for  $\text{SNR} > 20\text{dB}$ .

**[00128]** The results in **Figure 6** assumes IDCI-precoding as in (5). If IDCI-precoding at the neighbor clusters is also used to precode data streams to the target client in the interfering zone as in (6), additional diversity gain is obtained. **Figure 7** compares the SER derived from two techniques: (i) “Method 1” using the IDCI-precoding in (5); (ii) “Method 2” employing IDCI-precoding in (6) where the neighbor clusters also transmit precoded data stream to the target

client. Method 2 yields  $\sim 3$ dB gain compared to conventional IDCI-precoding due to additional array gain provided by the DIDO antennas in the neighbor cluster used to transmit precoded data stream to the target client. More generally, the array gain of Method 2 over Method 1 is proportional to  $10^*\log_{10}(C+1)$ , where  $C$  is the number of neighbor clusters and the factor “1” refers to the main cluster.

**[00129]** Next, we evaluate the performance of the above method as a function of the target client’s location with respect to the interfering zone. We consider one simple scenario where a target client 8401 moves from the main DIDO cluster 802 to the interfering cluster 803, as depicted in **Figure 8**. We assume all DIDO antennas 812 within the main cluster 802 employ BD precoding to cancel intra-cluster interference to satisfy condition (2). We assume single interfering DIDO cluster, single receiver antenna at the client device 801 and equal pathloss from all DIDO antennas in the main or interfering cluster to the client (i.e., DIDO antennas placed in circle around the client). We use one simplified pathloss model with pathloss exponent 4 (as in typical urban environments) [11].

The analysis hereafter is based on the following simplified signal model that extends (7) to account for pathloss

$$r_k = \sqrt{\frac{\text{SNR} \cdot D_o^4}{D^4}} \mathbf{h}_k \mathbf{w}_k s_k + \sqrt{\frac{\text{SNR} \cdot D_o^4}{(1-D)^4}} \mathbf{h}_{c,k} \sum_{i=1}^I \mathbf{w}_{c,i} s_{c,i} + n_k \quad (8)$$

where the signal-to-interference (SIR) is derived as  $\text{SIR} = ((1-D)/D)^4$ . In modeling the IDCI, we consider three scenarios: i) ideal case with no IDCI; ii) IDCI pre-cancelled via BD precoding in the interfering cluster to satisfy condition (3); iii) with IDCI, not pre-cancelled by the neighbor cluster.

**[00130]** **Figure 9** shows the signal-to-interference-plus-noise ratio (SINR) as a function of  $D$  (i.e., as the target client moves from the main cluster 802 towards the DIDO antennas 813 in the interfering cluster 8403). The SINR is derived as the ratio of signal power and interference plus noise power using the signal model in (8). We assume that  $D_o=0.1$  and  $\text{SNR}=50$ dB for  $D=D_o$ . In absence of IDCI the wireless link performance is only affected by noise and the SINR decreases due to pathloss. In presence of IDCI (i.e., without IDCI-precoding) the interference from the DIDO antennas in the neighbor cluster contributes to reduce the SINR.

**[00131]** **Figure 10** shows the symbol error rate (SER) performance of the three scenarios above for 4-QAM modulation in flat-fading narrowband channels. These SER results correspond to the SINR in **Figure 9**. We assume SER threshold of 1% for uncoded systems (i.e., without FEC) corresponding to SINR threshold  $\text{SINR}_T=20$ dB in **Figure 9**. The SINR threshold depends on the modulation order used for data transmission. Higher modulation orders are typically characterized by higher  $\text{SINR}_T$  to achieve the same target error rate. With FEC, lower target

SER can be achieved for the same SINR value due to coding gain. In case of IDCI without precoding, the target SER is achieved only within the range  $D < 0.25$ . With IDCI-precoding at the neighbor cluster the range that satisfies the target SER is extended up to  $D < 0.6$ . Beyond that range, the SINR increases due to pathloss and the SER target is not satisfied.

**[00132]** One embodiment of a method for IDCI precoding is shown in **Figure 11** and consists of the following steps:

- **SIR estimate 1101:** Clients estimate the signal power from the main DIDO cluster (i.e., based on received precoded data) and the interference-plus-noise signal power from the neighbor DIDO clusters. In single-carrier DIDO systems, the frame structure can be designed with short periods of silence. For example, periods of silence can be defined between training for channel estimation and precoded data transmissions during channel state information (CSI) feedback. In one embodiment, the interference-plus-noise signal power from neighbor clusters is measured during the periods of silence from the DIDO antennas in the main cluster. In practical DIDO multicarrier (OFDM) systems, null tones are typically used to prevent direct current (DC) offset and attenuation at the edge of the band due to filtering at transmit and receive sides. In another embodiment employing multicarrier systems, the interference-plus-noise signal power is estimated from the null tones. Correction factors can be used to compensate for transmit/receive filter attenuation at the edge of the band. Once the signal-plus-interference-and-noise power ( $P_S$ ) from the main cluster and the interference-plus-noise power from neighbor clusters ( $P_{IN}$ ) are estimated, the client computes the SINR as

$$\text{SINR} = \frac{P_S - P_{IN}}{P_{IN}}. \quad (9)$$

Alternatively, the SINR estimate is derived from the received signal strength indication (RSSI) used in typical wireless communication systems to measure the radio signal power.

We observe the metric in (9) cannot discriminate between noise and interference power level. For example, clients affected by shadowing (i.e., behind obstacles that attenuate the signal power from all DIDO distributed antennas in the main cluster) in interference-free environments may estimate low SINR even though they are not affected by inter-cluster interference.

A more reliable metric for the proposed method is the SIR computed as

$$\text{SIR} = \frac{P_S - P_{IN}}{P_{IN} - P_N} \quad (10)$$

where  $P_N$  is the noise power. In practical multicarrier OFDM systems, the noise power  $P_N$  in (10) is estimated from the null tones, assuming all DIDO antennas from main and neighbor clusters use the same set of null tones. The interference-plus-noise power ( $P_{IN}$ ), is estimated from the period of silence as mentioned above. Finally, the signal-plus-interference-and-noise power ( $P_S$ ) is derived from the data tones. From these estimates, the client computes the SIR in (10).

- **Channel estimation at neighbor clusters 1102-1103:** If the estimated SIR in (10) is below predefined threshold ( $SIR_T$ ), determined at 8702 in **Figure 11**, the client starts listening to training signals from neighbor clusters. Note that  $SIR_T$  depends on the modulation and FEC coding scheme (MCS) used for data transmission. Different SIR targets are defined depending on the client's MCS. When DIDO distributed antennas from different clusters are time-synchronized (i.e., locked to the same pulse-per-second, PPS, time reference), the client exploits the training sequence to deliver its channel estimates to the DIDO antennas in the neighbor clusters at 8703. The training sequence for channel estimation in the neighbor clusters are designed to be orthogonal to the training from the main cluster. Alternatively, when DIDO antennas in different clusters are not time-synchronized, orthogonal sequences (with good cross-correlation properties) are used for time synchronization in different DIDO clusters. Once the client locks to the time/frequency reference of the neighbor clusters, channel estimation is carried out at 1103.
- **IDCI Precoding 1104:** Once the channel estimates are available at the DIDO BTS in the neighbor clusters, IDCI-precoding is computed to satisfy the condition in (3). The DIDO antennas in the neighbor clusters transmit precoded data streams only to the clients in their cluster, while pre-cancelling interference to the clients in the interfering zone 410 in **Figure 4**. We observe that if the client lies in the type B interfering zone 410 in **Figure 4**, interference to the client is generated by multiple clusters and IDCI-precoding is carried out by all neighbor clusters at the same time.

## Methods for Handoff

**[00133]** Hereafter, we describe different handoff methods for clients that move across DIDO clusters populated by distributed antennas that are located in separate areas or that provide different kinds of services (i.e., low- or high-mobility services).

### a. Handoff Between Adjacent DIDO Clusters

**[00134]** In one embodiment, the IDCI-precoder to remove inter-cluster interference described above is used as a baseline for handoff methods in DIDO systems. Conventional handoff in cellular systems is conceived for clients to switch seamlessly across cells served by different base stations. In DIDO systems, handoff allows clients to move from one cluster to another without loss of connection.

**[00135]** To illustrate one embodiment of a handoff strategy for DIDO systems, we consider again the example in **Figure 8** with only two clusters 802 and 803. As the client 801 moves from the main cluster (C1) 802 to the neighbor cluster (C2) 803, one embodiment of a handoff method dynamically calculates the signal quality in different clusters and selects the cluster that yields the lowest error rate performance to the client.

**[00136]** **Figure 12** shows the SINR variation as a function of the client's distance from the center of clusters C1. For 4-QAM modulation without FEC coding, we consider target SINR=20dB. The line identified by circles represents the SINR for the target client being served by the DIDO antennas in C1, when both C1 and C2 use DIDO precoding without interference cancellation. The SINR decreases as a function of D due to pathloss and interference from the neighboring cluster. When IDCI-precoding is implemented at the neighboring cluster, the SINR loss is only due to pathloss (as shown by the line with triangles), since interference is completely removed. Symmetric behavior is experienced when the client is served from the neighboring cluster. One embodiment of the handoff strategy is defined such that, as the client moves from C1 to C2, the algorithm switches between different DIDO schemes to maintain the SINR above predefined target.

**[00137]** From the plots in **Figure 12**, we derive the SER for 4-QAM modulation in **Figure 13**. We observe that, by switching between different precoding strategies, the SER is maintained within predefined target.

**[00138]** One embodiment of the handoff strategy is as follows.

- **C1-DIDO and C2-DIDO precoding:** When the client lies within C1, away from the interfering zone, both clusters C1 and C2 operate with conventional DIDO precoding independently.
- **C1-DIDO and C2-IDCI precoding:** As the client moves towards the interfering zone, its SIR or SINR degrades. When the target  $\text{SINR}_{T1}$  is reached, the target client starts estimating the channel from all DIDO antennas in C2 and provides the CSI to the BTS of C2. The BTS in C2 computes IDCI-precoding and transmits to all clients in C2 while preventing interference to the target client. For as long as the target client is within the interfering zone, it will continue to provide its CSI to both C1 and C2.

- **C1-IDCI and C2-DIDO precoding:** As the client moves towards C2, its SIR or SINR keeps decreasing until it again reaches a target. At this point the client decides to switch to the neighbor cluster. In this case, C1 starts using the CSI from the target client to create zero interference towards its direction with IDCI-precoding, whereas the neighbor cluster uses the CSI for conventional DIDO-precoding. In one embodiment, as the SIR estimate approaches the target, the clusters C1 and C2 try both DIDO- and IDCI-precoding schemes alternatively, to allow the client to estimate the SIR in both cases. Then the client selects the best scheme, to maximize certain error rate performance metric. When this method is applied, the cross-over point for the handoff strategy occurs at the intersection of the curves with triangles and rhombus in **Figure 12**. One embodiment uses the modified IDCI-precoding method described in (6) where the neighbor cluster also transmits precoded data stream to the target client to provide array gain. With this approach the handoff strategy is simplified, since the client does not need to estimate the SINR for both strategies at the cross-over point.
- **C1-DIDO and C2-DIDO precoding:** As the client moves out of the interference zone towards C2, the main cluster C1 stops pre-cancelling interference towards that target client via IDCI-precoding and switches back to conventional DIDO-precoding to all clients remaining in C1. This final cross-over point in our handoff strategy is useful to avoid unnecessary CSI feedback from the target client to C1, thereby reducing the overhead over the feedback channel. In one embodiment a second target  $SINR_{T2}$  is defined. When the SINR (or SIR) increases above this target, the strategy is switched to C1-DIDO and C2-DIDO. In one embodiment, the cluster C1 keeps alternating between DIDO- and IDCI-precoding to allow the client to estimate the SINR. Then the client selects the method for C1 that more closely approaches the target  $SINR_{T1}$  from above.

**[00139]** The method described above computes the SINR or SIR estimates for different schemes in real time and uses them to select the optimal scheme. In one embodiment, the handoff algorithm is designed based on the finite-state machine illustrated in **Figure 14**. The client keeps track of its current state and switches to the next state when the SINR or SIR drops below or above the predefined thresholds illustrated in **Figure 12**. As discussed above, in state 1201, both clusters C1 and C2 operate with conventional DIDO precoding independently and the client is served by cluster C1; in state 1202, the client is served by cluster C1, the BTS in C2 computes IDCI-precoding and cluster C1 operates using conventional DIDO precoding; in state 1203, the client is served by cluster C2, the BTS in C1 computes IDCI-precoding and cluster C2

6181P526XPCT

operates using conventional DIDO precoding; and in state 1204, the client is served by cluster C2, and both clusters C1 and C2 operate with conventional DIDO precoding independently.

**[00140]** In presence of shadowing effects, the signal quality or SIR may fluctuate around the thresholds as shown in **Figure 15**, causing repetitive switching between consecutive states in **Figure 14**. Changing states repetitively is an undesired effect, since it results in significant overhead on the control channels between clients and BTSs to enable switching between transmission schemes. **Figure 15** depicts one example of a handoff strategy in the presence of shadowing. In one embodiment, the shadowing coefficient is simulated according to log-normal distribution with variance 3 [3]. Hereafter, we define some methods to prevent repetitive switching effect during DIDO handoff.

**[00141]** One embodiment of the invention employs a *hysteresis loop* to cope with state switching effects. For example, when switching between “C1-DIDO,C2-IDCI” 9302 and “C1-IDCI,C2-DIDO” 9303 states in **Figure 14** (or vice versa) the threshold  $\text{SINR}_{T1}$  can be adjusted within the range  $A_1$ . This method avoids repetitive switches between states as the signal quality oscillates around  $\text{SINR}_{T1}$ . For example, **Figure 16** shows the hysteresis loop mechanism when switching between any two states in **Figure 14**. To switch from state B to A the SIR must be larger than  $(\text{SIR}_{T1}+A_1/2)$ , but to switch back from A to B the SIR must drop below  $(\text{SIR}_{T1}-A_1/2)$ .

**[00142]** In a different embodiment, the threshold  $\text{SINR}_{T2}$  is adjusted to avoid repetitive switching between the first and second (or third and fourth) states of the finite-state machine in **Figure 14**. For example, a range of values  $A_2$  may be defined such that the threshold  $\text{SINR}_{T2}$  is chosen within that range depending on channel condition and shadowing effects.

**[00143]** In one embodiment, depending on the variance of shadowing expected over the wireless link, the SINR threshold is dynamically adjusted within the range  $[\text{SINR}_{T2}, \text{SINR}_{T2}+A_2]$ . The variance of the log-normal distribution can be estimated from the variance of the received signal strength (or RSSI) as the client moves from its current cluster to the neighbor cluster.

**[00144]** The methods above assume the client triggers the handoff strategy. In one embodiment, the handoff decision is deferred to the DIDO BTSs, assuming communication across multiple BTSs is enabled.

**[00145]** For simplicity, the methods above are derived assuming no FEC coding and 4-QAM. More generally, the SINR or SIR thresholds are derived for different modulation coding schemes (MCSs) and the handoff strategy is designed in combination with link adaptation (*see, e.g.*, U.S. Patent No. 7,636,381) to optimize downlink data rate to each client in the interfering zone.

### b. Handoff Between Low- and High-Doppler DIDO Networks

**[00146]** DIDO systems employ closed-loop transmission schemes to precode data streams over the downlink channel. Closed-loop schemes are inherently constrained by latency over the feedback channel. In practical DIDO systems, computational time can be reduced by transceivers with high processing power and it is expected that most of the latency is introduced by the DIDO BSN, when delivering CSI and baseband precoded data from the BTS to the distributed antennas. The BSN can be comprised of various network technologies including, but not limited to, digital subscriber lines (DSL), cable modems, fiber rings, T1 lines, hybrid fiber coaxial (HFC) networks, and/or fixed wireless (e.g., WiFi). Dedicated fiber typically has very large bandwidth and low latency, potentially less than a millisecond in local region, but it is less widely deployed than DSL and cable modems. Today, DSL and cable modem connections typically have between 10-25ms in last-mile latency in the United States, but they are very widely deployed.

**[00147]** The maximum latency over the BSN determines the maximum Doppler frequency that can be tolerated over the DIDO wireless link without performance degradation of DIDO precoding. For example, in [1] we showed that at the carrier frequency of 400MHz, networks with latency of about 10msec (i.e., DSL) can tolerate clients' velocity up to 8mph (running speed), whereas networks with 1msec latency (i.e., fiber ring) can support speed up to 70mph (i.e., freeway traffic).

**[00148]** We define two or multiple DIDO sub-networks depending on the maximum Doppler frequency that can be tolerated over the BSN. For example, a BSN with high-latency DSL connections between the DIDO BTS and distributed antennas can only deliver low mobility or fixed-wireless services (i.e., *low-Doppler network*), whereas a low-latency BSN over a low-latency fiber ring can tolerate high mobility (i.e., *high-Doppler network*). We observe that the majority of broadband users are not moving when they use broadband, and further, most are unlikely to be located near areas with many high speed objects moving by (e.g., next to a highway) since such locations are typically less desirable places to live or operate an office. However, there are broadband users who will be using broadband at high speeds (e.g., while in a car driving on the highway) or will be near high speed objects (e.g., in a store located near a highway). To address these two differing user Doppler scenarios, in one embodiment, a low-Doppler DIDO network consists of a typically larger number of DIDO antennas with relatively low power (i.e., 1W to 100W, for indoor or rooftop installation) spread across a wide area, whereas a high-Doppler network consists of a typically lower number of DIDO antennas with high power transmission (i.e., 100W for rooftop or tower installation). The low-Doppler DIDO network serves the typically larger number of low-Doppler users and can do so at typically lower

6181P526XPCT

connectivity cost using inexpensive high-latency broadband connections, such as DSL and cable modems. The high-Doppler Dido network serves the typically fewer number of high-Doppler users and can do so at typically higher connectivity cost using more expensive low-latency broadband connections, such as fiber.

**[00149]** To avoid interference across different types of Dido networks (e.g. low-Doppler and high-Doppler), different multiple access techniques can be employed such as: time division multiple access (TDMA), frequency division multiple access (FDMA), or code division multiple access (CDMA).

**[00150]** Hereafter, we propose methods to assign clients to different types of Dido networks and enable handoff between them. The network selection is based on the type of mobility of each client. The client's velocity ( $v$ ) is proportional to the maximum Doppler shift according to the following equation [6]

$$f_d = \frac{v}{\lambda} \sin \theta \quad (11)$$

where  $f_d$  is the maximum Doppler shift,  $\lambda$  is the wavelength corresponding to the carrier frequency and  $\theta$  is the angle between the vector indicating the direction transmitter-client and the velocity vector.

**[00151]** In one embodiment, the Doppler shift of every client is calculated via blind estimation techniques. For example, the Doppler shift can be estimated by sending RF energy to the client and analyzing the reflected signal, similar to Doppler radar systems.

**[00152]** In another embodiment, one or multiple Dido antennas send training signals to the client. Based on those training signals, the client estimates the Doppler shift using techniques such as counting the zero-crossing rate of the channel gain, or performing spectrum analysis. We observe that for fixed velocity  $v$  and client's trajectory, the angular velocity  $v \sin \theta$  in (11) may depend on the relative distance of the client from every Dido antenna. For example, Dido antennas in the proximity of a moving client yield larger angular velocity and Doppler shift than faraway antennas. In one embodiment, the Doppler velocity is estimated from multiple Dido antennas at different distances from the client and the average, weighted average or standard deviation is used as an indicator for the client's mobility. Based on the estimated Doppler indicator, the Dido BTS decides whether to assign the client to low- or high-Doppler networks.

**[00153]** The Doppler indicator is periodically monitored for all clients and sent back to the BTS. When one or multiple clients change their Doppler velocity (i.e., client riding in the bus versus client walking or sitting), those clients are dynamically re-assigned to different Dido network that can tolerate their level of mobility.

**[00154]** Although the Doppler of low-velocity clients can be affected by being in the vicinity of high-velocity objects (e.g. near a highway), the Doppler is typically far less than the Doppler

of clients that are in motion themselves. As such, in one embodiment, the velocity of the client is estimated (e.g. by using a means such as monitoring the clients position using GPS), and if the velocity is low, the client is assigned to a low-Doppler network, and if the velocity if high, the client is assigned to a high-Doppler network.

### Methods for Power Control and Antenna Grouping

**[00155]** The block diagram of DIDO systems with power control is depicted in **Figure 17**. One or multiple data streams ( $s_k$ ) for every client ( $1, \dots, U$ ) are first multiplied by the weights generated by the DIDO precoding unit. Precoded data streams are multiplied by power scaling factor computed by the power control unit, based on the input channel quality information (CQI). The CQI is either fed back from the clients to DIDO BTS or derived from the uplink channel assuming uplink-downlink channel reciprocity. The  $U$  precoded streams for different clients are then combined and multiplexed into  $M$  data streams ( $t_m$ ), one for each of the  $M$  transmit antennas. Finally, the streams  $t_m$  are sent to the digital-to-analog converter (DAC) unit, the radio frequency (RF) unit, power amplifier (PA) unit and finally to the antennas.

**[00156]** The power control unit measures the CQI for all clients. In one embodiment, the CQI is the average SNR or RSSI. The CQI varies for different clients depending on pathloss or shadowing. Our power control method adjusts the transmit power scaling factors  $P_k$  for different clients and multiplies them by the precoded data streams generated for different clients. Note that one or multiple data streams may be generated for every client, depending on the number of clients' receive antennas.

**[00157]** To evaluate the performance of the proposed method, we defined the following signal model based on (5), including pathloss and power control parameters

$$\mathbf{r}_k = \sqrt{\text{SNR} P_k \alpha_k} \mathbf{H}_k \mathbf{W}_k \mathbf{s}_k + \mathbf{n}_k \quad (12)$$

where  $k=1, \dots, U$ ,  $U$  is the number of clients,  $\text{SNR} = P_o/N_o$ , with  $P_o$  being the average transmit power,  $N_o$  the noise power and  $\alpha_k$  the pathloss/shadowing coefficient. To model pathloss/shadowing, we use the following simplified model

$$\alpha_k = e^{-a \frac{k-1}{U}} \quad (13)$$

where  $a=4$  is the pathloss exponent and we assume the pathloss increases with the clients' index (i.e., clients are located at increasing distance from the DIDO antennas).

**[00158]** **Figure 18** shows the SER versus SNR assuming four DIDO transmit antennas and four clients in different scenarios. The ideal case assumes all clients have the same pathloss (i.e.,  $a=0$ ), yielding  $P_k=1$  for all clients. The plot with squares refers to the case where clients have different pathloss coefficients and no power control. The curve with dots is derived from the same scenario (with pathloss) where the power control coefficients are chosen such that  $P_k =$

$1/\alpha_k$ . With the power control method, more power is assigned to the data streams intended to the clients that undergo higher pathloss/shadowing, resulting in 9dB SNR gain (for this particular scenario) compared to the case with no power control.

**[00159]** The Federal Communications Commission (FCC) (and other international regulatory agencies) defines constraints on the maximum power that can be transmitted from wireless devices to limit the exposure of human body to electromagnetic (EM) radiation. There are two types of limits [2]: i) “occupational/controlled” limit, where people are made fully aware of the radio frequency (RF) source via fences, warnings or labels; ii) “general population/uncontrolled” limit where there is no control over the exposure.

**[00160]** Different emission levels are defined for different types of wireless devices. In general, DIDO distributed antennas used for indoor/outdoor applications qualify for the FCC category of “mobile” devices, defined as [2]:

“transmitting devices designed to be used in other than fixed locations that would normally be used with radiating structures maintained 20 cm or more from the body of the user or nearby persons.”

**[00161]** The EM emission of “mobile” devices is measured in terms of maximum permissible exposure (MPE), expressed in  $\text{mW/cm}^2$ . **Figure 19** shows the MPE power density as a function of distance from the source of RF radiation for different values of transmit power at 700MHz carrier frequency. The maximum allowed transmit power to meet the FCC “uncontrolled” limit for devices that typically operate beyond 20cm from the human body is 1W.

**[00162]** Less restrictive power emission constraints are defined for transmitters installed on rooftops or buildings, away from the “general population”. For these “rooftop transmitters” the FCC defines a looser emission limit of 1000W, measured in terms of effective radiated power (ERP).

**[00163]** Based on the above FCC constraints, in one embodiment we define two types of DIDO distributed antennas for practical systems:

- **Low-power (LP)** transmitters: located anywhere (i.e., indoor or outdoor) at any height, with maximum transmit power of **1W** and 5Mbps consumer-grade broadband (e.g. DSL, cable modem, Fibe To The Home (FTTH)) backhaul connectivity.
- **High-power (HP)** transmitters: rooftop or building mounted antennas at height of approximately 10 meters, with transmit power of **100W** and a commercial-grade broadband (e.g. optical fiber ring) backhaul (with effectively “unlimited” data rate compared to the throughput available over the DIDO wireless links).

**[00164]** Note that LP transmitters with DSL or cable modem connectivity are good candidates for low-Doppler DIDO networks (as described in the previous section), since their

clients are mostly fixed or have low mobility. HP transmitters with commercial fiber connectivity can tolerate higher client's mobility and can be used in high-Doppler DIDO networks.

**[00165]** To gain practical intuition on the performance of DIDO systems with different types of LP/HP transmitters, we consider the practical case of DIDO antenna installation in downtown Palo Alto, CA. **Figure 20a** shows a random distribution of  $N_{LP}=100$  low-power DIDO distributed antennas in Palo Alto. In **Figure 20b**, 50 LP antennas are substituted with  $N_{HP}=50$  high-power transmitters.

**[00166]** Based on the DIDO antenna distributions in **Figures 20a-b**, we derive the coverage maps in Palo Alto for systems using DIDO technology. **Figures 21a** and **21b** show two power distributions corresponding to the configurations in **Figure 20a** and **Figure 20b**, respectively. The received power distribution (expressed in dBm) is derived assuming the pathloss/shadowing model for urban environments defined by the 3GPP standard [3] at the carrier frequency of 700MHz. We observe that using 50% of HP transmitters yields better coverage over the selected area.

**[00167]** **Figures 22a-b** depict the rate distribution for the two scenarios above. The throughput (expressed in Mbps) is derived based on power thresholds for different modulation coding schemes defined in the 3GPP long-term evolution (LTE) standard in [4,5]. The total available bandwidth is fixed to 10MHz at 700MHz carrier frequency. Two different frequency allocation plans are considered: i) 5MHz spectrum allocated only to the LP stations; ii) 9MHz to HP transmitters and 1MHz to LP transmitters. Note that lower bandwidth is typically allocated to LP stations due to their DSL backhaul connectivity with limited throughput. **Figures 22a-b** shows that when using 50% of HP transmitters it is possible to increase significantly the rate distribution, raising the average per-client data rate from 2.4Mbps in **Figure 22a** to 38Mbps in **Figure 22b**.

**[00168]** Next, we defined algorithms to control power transmission of LP stations such that higher power is allowed at any given time, thereby increasing the throughput over the downlink channel of DIDO systems in **Figure 22b**. We observe that the FCC limits on the power density is defined based on average over time as [2]

$$S = \frac{\sum_{n=1}^N S_n t_n}{T_{MPE}} \quad (14)$$

where  $T_{MPE} = \sum_{n=1}^N t_n$  is the MPE averaging time,  $t_n$  is the period of time of exposure to radiation with power density  $S_n$ . For “controlled” exposure the average time is 6 minutes, whereas for “uncontrolled” exposure it is increased up to 30 minutes. Then, any power source is

allowed to transmit at larger power levels than the MPE limits, as long as the average power density in (14) satisfies the FCC limit over 30 minute average for “uncontrolled” exposure.

**[00169]** Based on this analysis, we define adaptive power control methods to increase instantaneous per-antenna transmit power, while maintaining average power per DIDO antenna below MPE limits. We consider DIDO systems with more transmit antennas than active clients. This is a reasonable assumption given that DIDO antennas can be conceived as inexpensive wireless devices (similar to WiFi access points) and can be placed anywhere there is DSL, cable modem, optical fiber, or other Internet connectivity.

**[00170]** The framework of DIDO systems with adaptive per-antenna power control is depicted in **Figure 23**. The amplitude of the digital signal coming out of the multiplexer 234 is dynamically adjusted with power scaling factors  $S_1, \dots, S_M$ , before being sent to the DAC units 235. The power scaling factors are computed by the power control unit 232 based on the CQI 233.

**[00171]** In one embodiment,  $N_g$  DIDO antenna groups are defined. Every group contains at least as many DIDO antennas as the number of active clients ( $K$ ). At any given time, only one group has  $N_a > K$  active DIDO antennas transmitting to the clients at larger power level ( $S_o$ ) than MPE limit ( $\overline{MPE}$ ). One method iterates across all antenna groups according to Round-Robin scheduling policy depicted in **Figure 24**. In another embodiment, different scheduling techniques (i.e., proportional-fair scheduling [8]) are employed for cluster selection to optimize error rate or throughput performance.

**[00172]** Assuming Round-Robin power allocation, from (14) we derive the average transmit power for every DIDO antenna as

$$S = S_o \frac{t_o}{T_{MPE}} \leq \overline{MPE} \quad (15)$$

where  $t_o$  is the period of time over which the antenna group is active and  $T_{MPE}=30\text{min}$  is the average time defined by the FCC guidelines [2]. The ratio in (15) is the *duty factor* (DF) of the groups, defined such that the average transmit power from every DIDO antenna satisfies the MPE limit ( $\overline{MPE}$ ). The duty factor depends on the number of active clients, the number of groups and active antennas per-group, according to the following definition

$$DF \triangleq \frac{K}{N_g N_a} = \frac{t_o}{T_{MPE}}. \quad (16)$$

The SNR gain (in dB) obtained in DIDO systems with power control and antenna grouping is expressed as a function of the duty factor as

$$G_{dB} = 10 \log_{10} \left( \frac{1}{DF} \right). \quad (17)$$

We observe the gain in (17) is achieved at the expense of  $G_{dB}$  additional transmit power across all DIDO antennas.

In general, the total transmit power from all  $N_a$  of all  $N_g$  groups is defined as

$$\bar{P} = \sum_{j=1}^{N_g} \sum_{i=1}^{N_a} P_{ij} \quad (18)$$

where the  $P_{ij}$  is the average per-antenna transmit power given by

$$P_{ij} = \frac{1}{T_{MPE}} \int_0^{T_{MPE}} S_{ij}(t) dt \leq \overline{MPE} \quad (19)$$

and  $S_{ij}(t)$  is the power spectral density for the  $i^{\text{th}}$  transmit antenna within the  $j^{\text{th}}$  group. In one embodiment, the power spectral density in (19) is designed for every antenna to optimize error rate or throughput performance.

**[00173]** To gain some intuition on the performance of the proposed method, consider 400 DIDO distributed antennas in a given coverage area and 400 clients subscribing to a wireless Internet service offered over DIDO systems. It is unlikely that every Internet connection will be fully utilized all the time. Let us assume that 10% of the clients will be actively using the wireless Internet connection at any given time. Then, 400 DIDO antennas can be divided in  $N_g=10$  groups of  $N_a=40$  antennas each, every group serving  $K=40$  active clients at any given time with duty factor  $DF=0.1$ . The SNR gain resulting from this transmission scheme is  $G_{dB}=10\log_{10}(1/DF)=10$ dB, provided by 10dB additional transmit power from all DIDO antennas. We observe, however, that the average per-antenna transmit power is constant and is within the MPE limit.

**[00174]** **Figure 25** compares the (uncoded) SER performance of the above power control with antenna grouping against conventional eigenmode selection in U.S. Patent No. 7,636,381. All schemes use BD precoding with four clients, each client equipped with single antenna. The SNR refers to the ratio of per-transmit-antenna power over noise power (i.e., per-antenna transmit SNR). The curve denoted with DIDO 4x4 assumes four transmit antenna and BD precoding. The curve with squares denotes the SER performance with two extra transmit antennas and BD with eigenmode selection, yielding 10dB SNR gain (at 1% SER target) over conventional BD precoding. Power control with antenna grouping and  $DF=1/10$  yields 10dB gain at the same SER target as well. We observe that eigenmode selection changes the slope of the SER curve due to diversity gain, whereas our power control method shifts the SER curve to the left (maintaining the same slope) due to increased average transmit power. For comparison, the SER with larger duty factor  $DF=1/50$  is shown to provide additional 7dB gain compared to  $DF=1/10$ .

**[00175]** Note that our power control may have lower complexity than conventional eigenmode selection methods. In fact, the antenna ID of every group can be pre-computed and shared among DIDO antennas and clients via lookup tables, such that only  $K$  channel estimates are required at any given time. For eigenmode selection,  $(K+2)$  channel estimates are computed and additional computational processing is required to select the eigenmode that minimizes the SER at any given time for all clients.

**[00176]** Next, we describe another method involving DIDO antenna grouping to reduce CSI feedback overhead in some special scenarios. **Figure 26a** shows one scenario where clients (dots) are spread randomly in one area covered by multiple DIDO distributed antennas (crosses). The average power over every transmit-receive wireless link can be computed as

$$\mathbf{A} = \{|\mathbf{H}|^2\}. \quad (20)$$

where  $\mathbf{H}$  is the channel estimation matrix available at the DIDO BTS.

**[00177]** The matrices  $\mathbf{A}$  in **Figures 26a-c** are obtained numerically by averaging the channel matrices over 1000 instances. Two alternative scenarios are depicted in **Figure 26b** and **Figure 26c**, respectively, where clients are grouped together around a subset of DIDO antennas and receive negligible power from DIDO antennas located far away. For example, **Figure 26b** shows two groups of antennas yielding block diagonal matrix  $\mathbf{A}$ . One extreme scenario is when every client is very close to only one transmitter and the transmitters are far away from one another, such that the power from all other DIDO antennas is negligible. In this case, the DIDO link degenerates in multiple SISO links and  $\mathbf{A}$  is a diagonal matrix as in **Figure 26c**.

**[00178]** In all three scenarios above, the BD precoding dynamically adjusts the precoding weights to account for different power levels over the wireless links between DIDO antennas and clients. It is convenient, however, to identify multiple *groups* within the DIDO cluster and operate DIDO precoding only within each group. Our proposed grouping method yields the following advantages:

- **Computational gain:** DIDO precoding is computed only within every group in the cluster. For example, if BD precoding is used, singular value decomposition (SVD) has complexity  $O(n^3)$ , where  $n$  is the minimum dimension of the channel matrix  $\mathbf{H}$ . If  $\mathbf{H}$  can be reduced to a block diagonal matrix, the SVD is computed for every block with reduced complexity. In fact, if the channel matrix is divided into two block matrices with dimensions  $n_1$  and  $n_2$  such that  $n=n_1+n_2$ , the complexity of the SVD is only  $O(n_1^3)+O(n_2^3)<O(n^3)$ . In the extreme case, if  $\mathbf{H}$  is diagonal matrix, the DIDO link reduce to multiple SISO links and no SVD calculation is required.
- **Reduced CSI feedback overhead:** When DIDO antennas and clients are divided into groups, in one embodiment, the CSI is computed from the clients to the antennas only

within the same group. In TDD systems, assuming channel reciprocity, antenna grouping reduces the number of channel estimates to compute the channel matrix  $\mathbf{H}$ .

In FDD systems where the CSI is fed back over the wireless link, antenna grouping further yields reduction of CSI feedback overhead over the wireless links between DIDO antennas and clients.

### Multiple Access Techniques for the DIDO Uplink Channel

**[00179]** In one embodiment of the invention, different multiple access techniques are defined for the DIDO uplink channel. These techniques can be used to feedback the CSI or transmit data streams from the clients to the DIDO antennas over the uplink. Hereafter, we refer to feedback CSI and data streams as *uplink streams*.

- **Multiple-input multiple-output (MIMO):** the uplink streams are transmitted from the client to the DIDO antennas via open-loop MIMO multiplexing schemes. This method assumes all clients are time/frequency synchronized. In one embodiment, synchronization among clients is achieved via training from the downlink and all DIDO antennas are assumed to be locked to the same time/frequency reference clock. Note that variations in delay spread at different clients may generate jitter between the clocks of different clients that may affect the performance of MIMO uplink scheme. After the clients send uplink streams via MIMO multiplexing schemes, the receive DIDO antennas may use non-linear (i.e., maximum likelihood, ML) or linear (i.e., zeros-forcing, minimum mean squared error) receivers to cancel co-channel interference and demodulate the uplink streams individually.
- **Time division multiple access (TDMA):** Different clients are assigned to different time slots. Every client sends its uplink stream when its time slot is available.
- **Frequency division multiple access (FDMA):** Different clients are assigned to different carrier frequencies. In multicarrier (OFDM) systems, subsets of tones are assigned to different clients that transmit the uplink streams simultaneously, thereby reducing latency.
- **Code division multiple access (CDMA):** Every client is assigned to a different pseudo-random sequence and orthogonality across clients is achieved in the code domain.

**[00180]** In one embodiment of the invention, the clients are wireless devices that transmit at much lower power than the DIDO antennas. In this case, the DIDO BTS defines client sub-groups based on the uplink SNR information, such that interference across sub-groups is minimized. Within every sub-group, the above multiple access techniques are employed to create

orthogonal channels in time, frequency, space or code domains thereby avoiding uplink interference across different clients.

**[00181]** In another embodiment, the uplink multiple access techniques described above are used in combination with antenna grouping methods presented in the previous section to define different client groups within the DIDO cluster.

### System and Method for Link Adaptation in DIDO Multicarrier Systems

**[00182]** Link adaptation methods for DIDO systems exploiting time, frequency and space selectivity of wireless channels were defined in U.S. Patent No. 7,636,381. Described below are embodiments of the invention for link adaptation in multicarrier (OFDM) DIDO systems that exploit time/frequency selectivity of wireless channels.

**[00183]** We simulate Rayleigh fading channels according to the exponentially decaying power delay profile (PDP) or Saleh-Valenzuela model in [9]. For simplicity, we assume single-cluster channel with multipath PDP defined as

$$P_n = e^{-\beta n} \quad (21)$$

where  $n=0, \dots, L-1$ , is the index of the channel tap,  $L$  is the number of channel taps and  $\beta = 1/\sigma_{DS}$  is the PDP exponent that is an indicator of the channel coherence bandwidth, inverse proportional to the channel delay spread ( $\sigma_{DS}$ ). Low values of  $\beta$  yield frequency-flat channels, whereas high values of  $\beta$  produce frequency selective channels. The PDP in (21) is normalized such that the total average power for all  $L$  channel taps is unitary

$$\bar{P}_n = \frac{P_n}{\sum_{i=0}^{L-1} P_i}. \quad (22)$$

**Figure 27** depicts the amplitude of low frequency selective channels (assuming  $\beta = 1$ ) over delay domain or instantaneous PDP (upper plot) and frequency domain (lower plot) for DIDO 2x2 systems. The first subscript indicates the client, the second subscript the transmit antenna. High frequency selective channels (with  $\beta = 0.1$ ) are shown in **Figure 28**.

**[00184]** Next, we study the performance of DIDO precoding in frequency selective channels. We compute the DIDO precoding weights via BD, assuming the signal model in (1) that satisfies the condition in (2). We reformulate the DIDO receive signal model in (5), with the condition in (2), as

$$\mathbf{r}_k = \mathbf{H}_{ek} \mathbf{s}_k + \mathbf{n}_k. \quad (23)$$

**[00185]** where  $\mathbf{H}_{ek} = \mathbf{H}_k \mathbf{W}_k$  is the *effective channel matrix* for user  $k$ . For DIDO 2x2, with a single antenna per client, the effective channel matrix reduces to one value with a frequency response shown in **Figure 29** and for channels characterized by high frequency selectivity (e.g., with  $\beta = 0.1$ ) in **Figure 28**. The continuous line in **Figure 29** refers to client 1, whereas the line with dots refers to client 2. Based on the channel quality metric in **Figure 29** we define

time/frequency domain link adaptation (LA) methods that dynamically adjust MCSs, depending on the changing channel conditions.

**[00186]** We begin by evaluating the performance of different MCSs in AWGN and Rayleigh fading SISO channels. For simplicity, we assume no FEC coding, but the following LA methods can be extended to systems that include FEC.

**[00187]** **Figure 30** shows the SER for different QAM schemes (i.e., 4-QAM, 16-QAM, 64-QAM). Without loss of generality, we assume target SER of 1% for uncoded systems. The SNR thresholds to meet that target SER in AWGN channels are 8dB, 15.5dB and 22dB for the three modulation schemes, respectively. In Rayleigh fading channels, it is well known the SER performance of the above modulation schemes is worse than AWGN [13] and the SNR thresholds are: 18.6dB, 27.3dB and 34.1dB, respectively. We observe that DIDO precoding transforms the multi-user downlink channel into a set of parallel SISO links. Hence, the same SNR thresholds as in **Figure 30** for SISO systems hold for DIDO systems on a client-by-client basis. Moreover, if instantaneous LA is carried out, the thresholds in AWGN channels are used.

**[00188]** The key idea of the proposed LA method for DIDO systems is to use low MCS orders when the channel undergoes deep fades in the time domain or frequency domain (depicted in **Figure 28**) to provide link-robustness. Contrarily, when the channel is characterized by large gain, the LA method switches to higher MCS orders to increase spectral efficiency. One contribution of the present application compared to U.S. Patent No. 7,636,381 is to use the effective channel matrix in (23) and in **Figure 29** as a metric to enable adaptation.

**[00189]** The general framework of the LA methods is depicted in **Figure 31** and defined as follows:

- **CSI estimation:** At 3171 the DIDO BTS computes the CSI from all users. Users may be equipped with single or multiple receive antennas.
- **DIDO precoding:** At 3172, the BTS computes the DIDO precoding weights for all users. In one embodiment, BD is used to compute these weights. The precoding weights are calculated on a tone-by-tone basis.
- **Link-quality metric calculation:** At 3173 the BTS computes the frequency-domain link quality metrics. In OFDM systems, the metrics are calculated from the CSI and DIDO precoding weights for every tone. In one embodiment of the invention, the link-quality metric is the average SNR over all OFDM tones. We define this method as **LA1** (based on average SNR performance). In another embodiment, the link quality metric is the frequency response of the effective channel in (23). We define this method as **LA2** (based on tone-by-tone performance to exploit frequency diversity). If every client has single antenna, the frequency-domain effective channel is depicted in **Figure 29**. If the

clients have multiple receive antennas, the link-quality metric is defined as the Frobenius norm of the effective channel matrix for every tone. Alternatively, multiple link-quality metrics are defined for every client as the singular values of the effective channel matrix in (23).

- **Bit-loading algorithm:** At 3174, based on the link-quality metrics, the BTS determines the MCSs for different clients and different OFDM tones. For LA1 method, the same MCS is used for all clients and all OFDM tones based on the SNR thresholds for Rayleigh fading channels in **Figure 30**. For LA2, different MCSs are assigned to different OFDM tones to exploit channel frequency diversity.
- **Precoded data transmission:** At 3175, the BTS transmits precoded data streams from the DIDO distributed antennas to the clients using the MCSs derived from the bit-loading algorithm. One header is attached to the precoded data to communicate the MCSs for different tones to the clients. For example, if eight MCSs are available and the OFDM symbols are defined with  $N=64$  tone,  $\log_2(8)*N=192$  bits are required to communicate the current MCS to every client. Assuming 4-QAM (2 bits/symbol spectral efficiency) is used to map those bits into symbols, only  $192/2/N=1.5$  OFDM symbols are required to map the MCS information. In another embodiment, multiple subcarriers (or OFDM tones) are grouped into subbands and the same MCS is assigned to all tones in the same subband to reduce the overhead due to control information. Moreover, the MCS are adjusted based on temporal variations of the channel gain (proportional to the coherence time). In fixed-wireless channel (characterized by low Doppler effect) the MCS are recalculated every fraction of the channel coherence time, thereby reducing the overhead required for control information.

**[00190]** **Figure 32** shows the SER performance of the LA methods described above. For comparison, the SER performance in Rayleigh fading channels is plotted for each of the three QAM schemes used. The LA2 method adapts the MCSs to the fluctuation of the effective channel in the frequency domain, thereby providing 1.8bps/Hz gain in spectral efficiency for low SNR (i.e., SNR=20dB) and 15dB gain in SNR (for SNR>35dB) compared to LA1.

### System and Method for DIDO Precoding Interpolation in Multicarrier Systems

**[00191]** The computational complexity of DIDO systems is mostly localized at the centralized processor or BTS. The most computationally expensive operation is the calculation of the precoding weights for all clients from their CSI. When BD precoding is employed, the BTS has to carry out as many singular value decomposition (SVD) operations as the number of

## 6181P526XPCT

clients in the system. One way to reduce complexity is through parallelized processing, where the SVD is computed on a separate processor for every client.

**[00192]** In multicarrier DIDO systems, each subcarrier undergoes flat-fading channel and the SVD is carried out for every client over every subcarrier. Clearly the complexity of the system increases linearly with the number of subcarriers. For example, in OFDM systems with 1MHz signal bandwidth, the cyclic prefix ( $L_0$ ) must have at least eight channel taps (i.e., duration of 8 microseconds) to avoid intersymbol interference in outdoor urban macrocell environments with large delay spread [3]. The size ( $N_{FFT}$ ) of the fast Fourier transform (FFT) used to generate the OFDM symbols is typically set to multiple of  $L_0$  to reduce loss of data rate. If  $N_{FFT}=64$ , the effective spectral efficiency of the system is limited by a factor  $N_{FFT}/(N_{FFT}+L_0)=89\%$ . Larger values of  $N_{FFT}$  yield higher spectral efficiency at the expense of higher computational complexity at the DIDO precoder.

**[00193]** One way to reduce computational complexity at the DIDO precoder is to carry out the SVD operation over a subset of tones (that we call *pilot tones*) and derive the precoding weights for the remaining tones via interpolation. Weight interpolation is one source of error that results in inter-client interference. In one embodiment, optimal weight interpolation techniques are employed to reduce inter-client interference, yielding improved error rate performance and lower computational complexity in multicarrier systems. In DIDO systems with  $M$  transmit antennas,  $U$  clients and  $N$  receive antennas per clients, the condition for the precoding weights of the  $k^{\text{th}}$  client ( $\mathbf{W}_k$ ) that guarantees zero interference to the other clients  $u$  is derived from (2) as

$$\mathbf{H}_u \mathbf{W}_k = \mathbf{0}^{N \times N}; \quad \forall u = 1, \dots, U; \text{ with } u \neq k \quad (24)$$

where  $\mathbf{H}_u$  are the channel matrices corresponding to the other DIDO clients in the system.

**[00194]** In one embodiment of the invention, the objective function of the weight interpolation method is defined as

$$f(\boldsymbol{\Theta}_k) = \sum_{\substack{u=1 \\ u \neq k}}^U \|\mathbf{H}_u \widehat{\mathbf{W}}_k(\boldsymbol{\Theta}_k)\|_F \quad (25)$$

where  $\boldsymbol{\Theta}_k$  is the set of parameters to be optimized for user  $k$ ,  $\widehat{\mathbf{W}}_k(\boldsymbol{\Theta}_k)$  is the *weight interpolation matrix* and  $\|\cdot\|_F$  denotes the Frobenius norm of a matrix. The optimization problem is formulated as

$$\boldsymbol{\Theta}_{k,\text{opt}} = \arg \min_{\boldsymbol{\Theta}_k \in \Theta_k} f(\boldsymbol{\Theta}_k) \quad (26)$$

where  $\Theta_k$  is the feasible set of the optimization problem and  $\boldsymbol{\Theta}_{k,\text{opt}}$  is the optimal solution.

**[00195]** The objective function in (25) is defined for one OFDM tone. In another embodiment of the invention, the objective function is defined as linear combination of the Frobenius norm in (25) of the matrices for all the OFDM tones to be interpolated. In another

embodiment, the OFDM spectrum is divided into subsets of tones and the optimal solution is given by

$$\boldsymbol{\theta}_{k,\text{opt}} = \arg \min_{\boldsymbol{\theta}_k \in \Theta_k} \max_{n \in A} f(n, \boldsymbol{\theta}_k) \quad (27)$$

where  $n$  is the OFDM tone index and  $A$  is the subset of tones.

**[00196]** The weight interpolation matrix  $\mathbf{W}_k(\boldsymbol{\theta}_k)$  in (25) is expressed as a function of a set of parameters  $\boldsymbol{\theta}_k$ . Once the optimal set is determined according to (26) or (27), the optimal weight matrix is computed. In one embodiment of the invention, the weight interpolation matrix of given OFDM tone  $n$  is defined as linear combination of the weight matrices of the pilot tones. One example of weight interpolation function for beamforming systems with single client was defined in [11]. In DIDO multi-client systems we write the weight interpolation matrix as

$$\widehat{\mathbf{W}}_k(lN_0 + n, \theta_k) = (1 - c_n) \cdot \mathbf{W}(l) + c_n e^{j\theta_k} \cdot \mathbf{W}(l + 1) \quad (28)$$

where  $0 \leq l \leq (L_0-1)$ ,  $L_0$  is the number of pilot tones and  $c_n = (n - 1)/N_0$ , with  $N_0 = N_{FFT}/L_0$ . The weight matrix in (28) is then normalized such that  $\|\widehat{\mathbf{W}}_k\|_F = \sqrt{NM}$  to guarantee unitary power transmission from every antenna. If  $N=1$  (single receive antenna per client), the matrix in (28) becomes a vector that is normalized with respect to its norm. In one embodiment of the invention, the pilot tones are chosen uniformly within the range of the OFDM tones. In another embodiment, the pilot tones are adaptively chosen based on the CSI to minimize the interpolation error.

**[00197]** We observe that one key difference of the system and method in [11] against the one proposed in this patent application is the objective function. In particular, the systems in [11] assumes multiple transmit antennas and single client, so the related method is designed to maximize the product of the precoding weight by the channel to maximize the receive SNR for the client. This method, however, does not work in multi-client scenarios, since it yields inter-client interference due to interpolation error. By contrast, our method is designed to minimize inter-client interference thereby improving error rate performance to all clients.

**[00198]** **Figure 33** shows the entries of the matrix in (28) as a function of the OFDM tone index for DIDO 2x2 systems with  $N_{FFT} = 64$  and  $L_0 = 8$ . The channel PDP is generated according to the model in (21) with  $\beta = 1$  and the channel consists of only eight channel taps. We observe that  $L_0$  must be chosen to be larger than the number of channel taps. The solid lines in **Figure 33** represent the ideal functions, whereas the dotted lines are the interpolated ones. The interpolated weights match the ideal ones for the pilot tones, according to the definition in (28). The weights computed over the remaining tones only approximate the ideal case due to estimation error.

**[00199]** One way to implement the weight interpolation method is via exhaustive search over the feasible set  $\Theta_k$  in (26). To reduce the complexity of the search, we quantize the feasible set

into  $P$  values uniformly in the range  $[0, 2\pi]$ . **Figure 34** shows the SER versus SNR for  $L_0 = 8$ ,  $M=N_t=2$  transmit antennas and variable number of  $P$ . As the number of quantization levels increases, the SER performance improves. We observe the case  $P=10$  approaches the performance of  $P=100$  for much lower computational complexity, due to reduced number of searches.

**[00200]** **Figure 35** shows the SER performance of the interpolation method for different DIDO orders and  $L_0 = 16$ . We assume the number of clients is the same as the number of transmit antennas and every client is equipped with single antenna. As the number of clients increases the SER performance degrades due to increase inter-client interference produced by weight interpolation errors.

**[00201]** In another embodiment of the invention, weight interpolation functions other than those in (28) are used. For example, linear prediction autoregressive models [12] can be used to interpolate the weights across different OFDM tones, based on estimates of the channel frequency correlation.

## References

- [00202]** [1] A. Forenza and S. G. Perlman, "System and method for distributed antenna wireless communications", U.S. Application Serial No. 12/630,627, filed December 2, 2009, entitled "System and Method For Distributed Antenna Wireless Communications"
- [00203]** [2] FCC, "Evaluating compliance with FCC guidelines for human exposure to radiofrequency electromagnetic fields," OET Bulletin 65, Ed. 97-01, Aug. 1997
- [00204]** [3] 3GPP, "Spatial Channel Model AHG (Combined ad-hoc from 3GPP & 3GPP2)", SCM Text V6.0, April 22, 2003
- [00205]** [4] 3GPP TR 25.912, "Feasibility Study for Evolved UTRA and UTRAN", V9.0.0 (2009-10)
- [00206]** [5] 3GPP TR 25.913, "Requirements for Evolved UTRA (E-UTRA) and Evolved UTRAN (E-UTRAN)", V8.0.0 (2009-01)
- [00207]** [6] W. C. Jakes, *Microwave Mobile Communications*, IEEE Press, 1974
- [00208]** [7] K. K. Wong, et al., "A joint channel diagonalization for multiuser MIMO antenna systems," IEEE Trans. Wireless Comm., vol. 2, pp. 773-786, July 2003;
- [00209]** [8] P. Viswanath, et al., "Opportunistic beamforming using dump antennas," IEEE Trans. On Inform. Theory, vol. 48, pp. 1277-1294, June 2002.
- [00210]** [9] A. A. M. Saleh, et al., "A statistical model for indoor multipath propagation," IEEE Jour. Select. Areas in Comm., vol. 195 SAC-5, no. 2, pp. 128-137, Feb. 1987.
- [00211]** [10] A. Paulraj, et al., *Introduction to Space-Time Wireless Communications*, Cambridge University Press, 40 West 20th Street, New York, NY, USA, 2003.

[00212] [11] J. Choi, et al., "Interpolation Based Transmit Beamforming for MIMO-OFDM with Limited Feedback," *IEEE Trans. on Signal Processing*, vol. 53, no. 11, pp. 4125-4135, Nov. 2005.

[00213] [12] I. Wong, et al., "Long Range Channel Prediction for Adaptive OFDM Systems," *Proc. of the IEEE Asilomar Conf. on Signals, Systems, and Computers*, vol. 1, pp. 723-736, Pacific Grove, CA, USA, Nov. 7-10, 2004.

[00214] [13] J. G. Proakis, *Communication System Engineering*, Prentice Hall, 1994

[00215] [14] B.D.Van Veen, et al., "Beamforming: a versatile approach to spatial filtering," *IEEE ASSP Magazine*, Apr. 1988.

[00216] [15] R.G. Vaughan, "On optimum combining at the mobile," *IEEE Trans. On Vehic. Tech.*, vol. 37, n.4, pp.181-188, Nov. 1988

[00217] [16] F.Qian, "Partially adaptive beamforming for correlated interference rejection," *IEEE Trans. On Sign. Proc.*, vol. 43, n.2, pp.506-515, Feb.1995

[00218] [17] H.Krim, et. al., "Two decades of array signal processing research," *IEEE Signal Proc. Magazine*, pp.67-94, July 1996

[00219] [19] W.R. Remley, "Digital *beamforming* system", US Patent N. 4,003,016, Jan. 1977

[00220] [18] R.J. Masak, "Beamforming/null-steering adaptive array", US Patent N. 4,771,289, Sep.1988

[00221] [20] K.-B.Yu, et. al., "Adaptive digital *beamforming* architecture and algorithm for nulling mainlobe and multiple sidelobe radar jammers while preserving monopulse ratio angle estimation accuracy", US Patent 5,600,326, Feb.1997

[00222] [21] H.Boche, et al., "Analysis of different precoding/decoding strategies for multiuser beamforming", IEEE Vehic. Tech. Conf., vol.1, Apr. 2003

[00223] [22] M.Schubert, et al., "Joint 'dirty paper' pre-coding and downlink beamforming," vol.2, pp.536-540, Dec. 2002

[00224] [23] H.Boche, et al." A general duality theory for uplink and downlink beamformingc", vol.1, pp.87-91, Dec. 2002

[00225] [24] K. K. Wong, R. D. Murch, and K. B. Letaief, "A joint channel diagonalization for multiuser MIMO antenna systems," *IEEE Trans. Wireless Comm.*, vol. 2, pp. 773-786, Jul 2003;

[00226] [25] Q. H. Spencer, A. L. Swindlehurst, and M. Haardt, "Zero forcing methods for downlink spatial multiplexing in multiuser MIMO channels," *IEEE Trans. Sig. Proc.*, vol. 52, pp. 461-471, Feb. 2004.

## II. DISCLOSURE FROM RELATED APPLICATION SERIAL NO. 12/917,257

**[00227]** Described below are wireless radio frequency (RF) communication systems and methods employing a plurality of distributed transmitting antennas operating cooperatively to create wireless links to given users, while suppressing interference to other users. Coordination across different transmitting antennas is enabled via *user-clustering*. The user cluster is a subset of transmitting antennas whose signal can be reliably detected by given user (i.e., received signal strength above noise or interference level). Every user in the system defines its own user-cluster. The waveforms sent by the transmitting antennas within the same user-cluster coherently combine to create RF energy at the target user's location and points of zero RF interference at the location of any other user reachable by those antennas.

**[00228]** Consider a system with  $M$  transmit antennas within one user-cluster and  $K$  users reachable by those  $M$  antennas, with  $K \leq M$ . We assume the transmitters are aware of the CSI ( $\mathbf{H} \in \mathbb{C}^{K \times M}$ ) between the  $M$  transmit antennas and  $K$  users. For simplicity, every user is assumed to be equipped with a single antenna, but the same method can be extended to multiple receive antennas per user. Consider the channel matrix  $\mathbf{H}$  obtained by combining the channel vectors ( $\mathbf{h}_k \in \mathbb{C}^{1 \times M}$ ) from the  $M$  transmit antennas to the  $K$  users as

$$\mathbf{H} = \begin{bmatrix} \mathbf{h}_1 \\ \vdots \\ \mathbf{h}_k \\ \vdots \\ \mathbf{h}_K \end{bmatrix}.$$

The precoding weights ( $\mathbf{w}_k \in \mathbb{C}^{M \times 1}$ ) that create RF energy to user  $k$  and zero RF energy to all other  $K-1$  users are computed to satisfy the following condition

$$\tilde{\mathbf{H}}_k \mathbf{w}_k = \mathbf{0}^{K \times 1}$$

where  $\tilde{\mathbf{H}}_k$  is the effective channel matrix of user  $k$  obtained by removing the  $k$ -th row of matrix  $\mathbf{H}$  and  $\mathbf{0}^{K \times 1}$  is the vector with all zero entries

**[00229]** In one embodiment, the wireless system is a DIDO system and user clustering is employed to create a wireless communication link to the target user, while pre-cancelling interference to any other user reachable by the antennas lying within the user-cluster. In U.S. Application Serial No. 12/630,627, a DIDO system is described which includes:

- **DIDO clients:** user terminals equipped with one or multiple antennas;
- **DIDO distributed antennas:** transceiver stations operating cooperatively to transmit precoded data streams to multiple users, thereby suppressing inter-user interference;
- **DIDO base transceiver stations (BTS):** centralized processor generating precoded waveforms to the DIDO distributed antennas;

- **DIDO base station network (BSN):** wired backhaul connecting the BTS to the DIDO distributed antennas or to other BTSs.

The DIDO distributed antennas are grouped into different subsets depending on their spatial distribution relative to the location of the BTSs or DIDO clients. We define three types of clusters, as depicted in **Figure 36**:

- **Super-cluster 3640:** is the set of DIDO distributed antennas connected to one or multiple BTSs such that the round-trip latency between all BTSs and the respective users is within the constraint of the DIDO precoding loop;
- **DIDO-cluster 3641:** is the set of DIDO distributed antennas connected to the same BTS. When the super-cluster contains only one BTS, its definition coincides with the DIDO-cluster;
- **User-cluster 3642:** is the set of DIDO distributed antennas that cooperatively transmit precoded data to given user.

**[00230]** For example, the BTSs are local hubs connected to other BTSs and to the DIDO distributed antennas via the BSN. The BSN can be comprised of various network technologies including, but not limited to, digital subscriber lines (DSL), ADSL, VDSL [6], cable modems, fiber rings, T1 lines, hybrid fiber coaxial (HFC) networks, and/or fixed wireless (e.g., WiFi). All BTSs within the same super-cluster share information about DIDO precoding via the BSN such that the round-trip latency is within the DIDO precoding loop.

**[00231]** In **Figure 37**, the dots denote DIDO distributed antennas, the crosses are the users and the dashed lines indicate the user-clusters for users U1 and U8, respectively. The method described hereafter is designed to create a communication link to the target user U1 while creating points of zero RF energy to any other user (U2-U8) inside or outside the user-cluster.

**[00232]** We proposed similar method in [5], where points of zero RF energy were created to remove interference in the overlapping regions between DIDO clusters. Extra antennas were required to transmit signal to the clients within the DIDO cluster while suppressing inter-cluster interference. One embodiment of a method proposed in the present application does not attempt to remove inter-DIDO-cluster interference; rather it assumes the cluster is bound to the client (i.e., user-cluster) and guarantees that no interference (or negligible interference) is generated to any other client in that neighborhood.

**[00233]** One idea associated with the proposed method is that users far enough from the user-cluster are not affected by radiation from the transmit antennas, due to large pathloss. Users close or within the user-cluster receive interference-free signal due to precoding. Moreover, additional transmit antennas can be added to the user-cluster (as shown in **Figure 37**) such that the condition  $K \leq M$  is satisfied.

[00234] One embodiment of a method employing user clustering consists of the following steps:

- a. **Link-quality measurements:** the link quality between every DIDO distributed antenna and every user is reported to the BTS. The link-quality metric consists of signal-to-noise ratio (SNR) or signal-to-interference-plus-noise ratio (SINR).

In one embodiment, the DIDO distributed antennas transmit training signals and the users estimate the received signal quality based on that training. The training signals are designed to be orthogonal in time, frequency or code domains such that the users can distinguish across different transmitters. Alternatively, the DIDO antennas transmit narrowband signals (i.e., single tone) at one particular frequency (i.e., a beacon channel) and the users estimate the link-quality based on that beacon signal. One threshold is defined as the minimum signal amplitude (or power) above the noise level to demodulate data successfully as shown in **Figure 38a**. Any link-quality metric value below this threshold is assumed to be zero. The link-quality metric is quantized over a finite number of bits and fed back to the transmitter.

In a different embodiment, the training signals or beacons are sent from the users and the link quality is estimated at the DIDO transmit antennas (as in **Figure 38b**), assuming reciprocity between uplink (UL) and downlink (DL) pathloss. Note that pathloss reciprocity is a realistic assumption in time division duplexing (TDD) systems (with UL and DL channels at the same frequency) and frequency division duplexing (FDD) systems when the UL and DL frequency bands are relatively close.

Information about the link-quality metrics is shared across different BTSs through the BSN as depicted in **Figure 37** such that all BTSs are aware of the link-quality between every antenna/user couple across different DIDO clusters.

- b. **Definition of user-clusters:** the link-quality metrics of all wireless links in the DIDO clusters are the entries to the *link-quality matrix* shared across all BTSs via the BSN. One example of link-quality matrix for the scenario in **Figure 37** is depicted in **Figure 39**.

The link-quality matrix is used to define the user clusters. For example, **Figure 39** shows the selection of the user cluster for user U8. The subset of transmitters with non-zero link-quality metrics (i.e., *active transmitters*) to user U8 is first identified. These transmitters populate the *user-cluster* for the user U8. Then the sub-matrix containing non-zero entries from the transmitters within the user-cluster to the other users is selected. Note that since the link-quality metrics are only used to select the user cluster, they can be quantized with only two bits (i.e., to identify the state above or below the thresholds in **Figure 38**) thereby reducing feedback overhead.

**[00235]** Another example is depicted in **Figure 40** for user U1. In this case the number of active transmitters is lower than the number of users in the sub-matrix, thereby violating the condition  $K \leq M$ . Therefore, one or more columns are added to the sub-matrix to satisfy that condition. If the number of transmitters exceeds the number of users, the extra antennas can be used for diversity schemes (i.e., antenna or eigenmode selection).

**[00236]** Yet another example is shown in **Figure 41** for user U4. We observe that the sub-matrix can be obtained as combination of two sub-matrices.

c. **CSI report to the BTSSs:** Once the user clusters are selected, the CSI from all transmitters within the user-cluster to every user reached by those transmitters is made available to all BTSSs. The CSI information is shared across all BTSSs via the BSN. In TDD systems, UL/DL channel reciprocity can be exploited to derive the CSI from training over the UL channel. In FDD systems, feedback channels from all users to the BTSSs are required. To reduce the amount of feedback, only the CSI corresponding to the non-zero entries of the link-quality matrix are fed back.

d. **DIDO precoding:** Finally, DIDO precoding is applied to every CSI sub-matrix corresponding to different user clusters (as described, for example, in the related U.S. Patent Applications).

In one embodiment, singular value decomposition (SVD) of the effective channel matrix  $\tilde{\mathbf{H}}_k$  is computed and the precoding weight  $\mathbf{w}_k$  for user  $k$  is defined as the right singular vector corresponding to the null subspace of  $\tilde{\mathbf{H}}_k$ . Alternatively, if  $M > K$  and the SVD decomposes the effective channel matrix as  $\tilde{\mathbf{H}}_k = \mathbf{V}_k \Sigma_k \mathbf{U}_k^H$ , the DIDO precoding weight for user  $k$  is given by

$$\mathbf{w}_k = \mathbf{U}_0 (\mathbf{U}_0^H \cdot \mathbf{h}_k^T)$$

where  $\mathbf{U}_0$  is the matrix with columns being the singular vectors of the null subspace of  $\tilde{\mathbf{H}}_k$ .

From basic linear algebra considerations, we observe that the right singular vector in the null subspace of the matrix  $\tilde{\mathbf{H}}$  is equal to the eigenvector of  $\mathbf{C}$  corresponding to the zero eigenvalue

$$\mathbf{C} = \tilde{\mathbf{H}}^H \tilde{\mathbf{H}} = (\mathbf{V} \Sigma \mathbf{U}^H)^H (\mathbf{V} \Sigma \mathbf{U}^H) = \mathbf{U} \Sigma^2 \mathbf{U}^H$$

where the effective channel matrix is decomposed as  $\tilde{\mathbf{H}} = \mathbf{V} \Sigma \mathbf{U}^H$ , according to the SVD. Then, one alternative to computing the SVD of  $\tilde{\mathbf{H}}_k$  is to calculate the eigenvalue decomposition of  $\mathbf{C}$ . There are several methods to compute eigenvalue decomposition such as the power method. Since we are only interested to the eigenvector corresponding to the null subspace of  $\mathbf{C}$ , we use the inverse power method described by the iteration

$$\mathbf{u}_{i+1} = \frac{(\mathbf{C} - \lambda \mathbf{I})^{-1} \mathbf{u}_i}{\|(\mathbf{C} - \lambda \mathbf{I})^{-1} \mathbf{u}_i\|}$$

where the vector  $(\mathbf{u}_i)$  at the first iteration is a random vector.

6181P526XPCT

Given that the eigenvalue ( $\lambda$ ) of the null subspace is known (i.e., zero) the inverse power method requires only one iteration to converge, thereby reducing computational complexity. Then, we write the precoding weight vector as

$$\mathbf{w} = \mathbf{C}^{-1} \mathbf{u}_1$$

where  $\mathbf{u}_1$  is the vector with real entries equal to 1 (i.e., the precoding weight vector is the sum of the columns of  $\mathbf{C}^{-1}$ ).

The DIDO precoding calculation requires one matrix inversion. There are several numerical solutions to reduce the complexity of matrix inversions such as the Strassen's algorithm [1] or the Coppersmith-Winograd's algorithm [2,3]. Since  $\mathbf{C}$  is Hermitian matrix by definition, an alternative solution is to decompose  $\mathbf{C}$  in its real and imaginary components and compute matrix inversion of a real matrix, according to the method in [4, Section 11.4].

**[00237]** Another feature of the proposed method and system is its reconfigurability. As the client moves across different DIDO clusters as in **Figure 42**, the user-cluster follows its moves. In other words, the subset of transmit antennas is constantly updated as the client changes its position and the effective channel matrix (and corresponding precoding weights) are recomputed.

**[00238]** The method proposed herein works within the super-cluster in **Figure 36**, since the links between the BTSs via the BSN must be low-latency. To suppress interference in the overlapping regions of different super-clusters, it is possible to use our method in [5] that uses extra antennas to create points of zero RF energy in the interfering regions between DIDO clusters.

**[00239]** It should be noted that the terms “user” and “client” are used interchangeably herein.

## References

- [00240]** [1] S. Robinson, “Toward an Optimal Algorithm for Matrix Multiplication”, SIAM News, Volume 38, Number 9, November 2005.
- [00241]** [2] D. Coppersmith and S. Winograd, “Matrix Multiplication via Arithmetic Progression”, J. Symb. Comp. vol.9, p.251-280, 1990.
- [00242]** [3] H. Cohn, R. Kleinberg, B. Szegedy, C. Umans, “Group-theoretic Algorithms for Matrix Multiplication”, p. 379-388, Nov. 2005.
- [00243]** [4] W.H. Press, S.A. Teukolsky, W. T. Vetterling, B.P. Flannery “NUMERICAL RECIPES IN C: THE ART OF SCIENTIFIC COMPUTING”, Cambridge University Press, 1992.
- [00244]** [5] A. Forenza and S.G.Perlman, “INTERFERENCE MANAGEMENT, HANDOFF, POWER CONTROL AND LINK ADAPTATION IN DISTRIBUTED-INPUT DISTRIBUTED-OUTPUT (DIDO) COMMUNICATION SYSTEMS”, Patent Application Serial No. 12/802,988, filed June 16, 2010.

**[00245]** [6] Per-Erik Eriksson and Björn Odenhammar, “VDSL2: Next important broadband technology”, Ericsson Review No. 1, 2006.

### III. SYSTEMS AND METHODS TO EXPLOIT AREAS OF COHERENCE IN WIRELESS SYSTEMS

**[00246]** The capacity of multiple antenna systems (MAS) in practical propagation environments is a function of the spatial diversity available over the wireless link. Spatial diversity is determined by the distribution of scattering objects in the wireless channel as well as the geometry of transmit and receive antenna arrays.

**[00247]** One popular model for MAS channels is the so called clustered channel model, that defines groups of scatterers as clusters located around the transmitters and receivers. In general, the more clusters and the larger their angular spread, the higher spatial diversity and capacity achievable over wireless links. Clustered channel models have been validated through practical measurements [1-2] and variations of those models have been adopted by different indoor (i.e., IEEE 802.11n Technical Group [3] for WLAN) and outdoor (3GPP Technical Specification Group for 3G cellular systems [4]) wireless standards.

**[00248]** Other factors that determine the spatial diversity in wireless channels are the characteristics of the antenna arrays, including: antenna element spacing [5-7], number of antennas [8-9], array aperture [10-11], array geometry [5,12,13], polarization and antenna pattern [14-28].

**[00249]** A unified model describing the effects of antenna array design as well as the characteristics of the propagation channel on the spatial diversity (or degrees of freedom) of wireless links was presented in [29]. The received signal model in [29] is given by

$$\mathbf{y}(\mathbf{q}) = \int \mathbf{C}(\mathbf{q}, \mathbf{p}) \mathbf{x}(\mathbf{p}) d\mathbf{p} + \mathbf{z}(\mathbf{q})$$

where  $\mathbf{x}(\mathbf{p}) \in \mathbb{C}^3$  is the polarized vector describing the transmit signal,  $\mathbf{p}, \mathbf{q} \in \mathbb{R}^3$  are the polarized vector positions describing the transmit and receive arrays, respectively, and  $\mathbf{C}(\cdot, \cdot) \in \mathbb{C}^{3 \times 3}$  is the matrix describing the system response between transmit and receive vector positions given by

$$\mathbf{C}(\mathbf{q}, \mathbf{p}) = \iint \mathbf{A}_r(\mathbf{q}, \hat{\mathbf{m}}) \mathbf{H}(\hat{\mathbf{m}}, \hat{\mathbf{n}}) \mathbf{A}_t(\hat{\mathbf{n}}, \mathbf{p}) d\hat{\mathbf{n}} d\hat{\mathbf{m}}$$

where  $\mathbf{A}_t(\cdot, \cdot), \mathbf{A}_r(\cdot, \cdot) \in \mathbb{C}^{3 \times 3}$  are the transmit and receive array responses respectively and  $\mathbf{H}(\hat{\mathbf{m}}, \hat{\mathbf{n}}) \in \mathbb{C}^{3 \times 3}$  is the channel response matrix with entries being the complex gains between transmit direction  $\hat{\mathbf{n}}$  and receive direction  $\hat{\mathbf{m}}$ . In DIDO systems, user devices may have single or multiple antennas. For the sake of simplicity, we assume single antenna receivers with ideal isotropic patterns and rewrite the system response matrix as

$$\mathbf{C}(\mathbf{q}, \mathbf{p}) = \int \mathbf{H}(\mathbf{q}, \hat{\mathbf{n}}) \mathbf{A}(\hat{\mathbf{n}}, \mathbf{p}) d\hat{\mathbf{n}}$$

where only the transmit antenna pattern  $\mathbf{A}(\hat{\mathbf{n}}, \mathbf{p})$  is considered.

**[00250]** From the Maxwell equations and the far-field term of the Green function, the array response can be approximated as [29]

$$\mathbf{A}(\hat{\mathbf{n}}, \mathbf{p}) = \frac{j\eta e^{j2\pi d_0}}{2\lambda^2 d_0} (\mathbf{I} - \hat{\mathbf{n}}\hat{\mathbf{n}}^H) \mathbf{a}(\hat{\mathbf{n}}, \mathbf{p})$$

with  $\mathbf{p} \in \mathbf{P}$ ,  $\mathbf{P}$  is the space that defines the antenna array and where

$$\mathbf{a}(\hat{\mathbf{n}}, \mathbf{p}) = \exp(-j2\pi \hat{\mathbf{n}}^H \mathbf{p})$$

with  $(\hat{\mathbf{n}}, \mathbf{p}) \in \Omega \times \mathbf{P}$ . For unpolarized antennas, studying the array response is equivalent to study the integral kernel above. Hereafter, we show closed for expressions of the integral kernels for different types of arrays.

### Unpolarized Linear Arrays

**[00251]** For unpolarized linear arrays of length  $L$  (normalized by the wavelength) and antenna elements oriented along the  $z$ -axis and centered at the origin, the integral kernel is given by [29]

$$\mathbf{a}(\cos \theta, p_z) = \exp(-j2\pi p_z \cos \theta).$$

**[00252]** Expanding the above equation into a series of shifted dyads, we obtain that the sinc function have resolution of  $1/L$  and the dimension of the array-limited and approximately wavevector-limited subspace (i.e., degrees of freedom) is

$$D_F = L |\Omega_0|$$

where  $\Omega_0 = \{\cos \theta : \theta \in \Theta\}$ . We observe that for broadside arrays  $|\Omega_0| = |\Theta|$  whereas for endfire  $|\Omega_0| \approx |\Theta|^2/2$ .

### Unpolarized Spherical Arrays

**[00253]** The integral kernel for a spherical array of radius  $R$  (normalized by the wavelength) is given by [29]

$$\mathbf{a}(\hat{\mathbf{n}}, \mathbf{p}) = \exp\{-j2\pi R [\sin \theta \sin \theta' \cos(\phi - \phi') + \cos \theta \cos \theta']\}.$$

**[00254]** Decomposing the above function with sum of spherical Bessel functions of the first kind we obtain the resolution of spherical arrays is  $1/(\pi R^2)$  and the degrees of freedom are given by

$$D_F = A |\Omega| = \pi R^2 |\Omega|$$

**[00255]** where  $A$  is the area of the spherical array and  $|\Omega| \subset [0, \pi) \times [0, 2\pi)$ .

### Areas of Coherence in Wireless Channels

**[00256]** The relation between the resolution of spherical arrays and their area  $A$  is depicted in **Figure 43**. The sphere in the middle is the spherical array of area  $A$ . The projection of the channel clusters on the unit sphere defines different scattering regions of size proportional to the angular spread of the clusters. The area of size  $1/A$  within each cluster, which we call “area of coherence”, denotes the projection of the basis functions of the radiated field of the array and defines the resolution of the array in the wavevector domain.

**[00257]** Comparing **Figure 43** with **Figure 44**, we observe that the size of the area of coherence decreases as the inverse of the size of the array. In fact, larger arrays can focus energy into smaller areas, yielding larger number of degrees of freedom  $D_F$ . Note that to total number of degrees of freedom depends also on the angular spread of the cluster, as shown in the definition above.

**[00258]** **Figure 45** depicts another example where the array size covers even larger area than **Figure 44**, yielding additional degrees of freedom. In DIDO systems, the array aperture can be approximated by the total area covered by all DIDO transmitters (assuming antennas are spaced fractions of wavelength apart). Then **Figure 45** shows that DIDO systems can achieve increasing numbers of degrees of freedom by distributing antennas in space, thereby reducing the size of the areas of coherence. Note that these figures are generated assuming ideal spherical arrays. In practical scenarios, DIDO antennas spread random across wide areas and the resulting shape of the areas of coherence may not be as regular as in the figures.

**[00259]** **Figure 46** shows that, as the array size increases, more clusters are included within the wireless channel as radio waves are scattered by increasing number of objects between DIDO transmitters. Hence, it is possible to excite an increasing number of basis functions (that span the radiated field), yielding additional degrees of freedom, in agreement with the definition above.

**[00260]** The multi-user (MU) multiple antenna systems (MAS) described in this patent application exploit the area of coherence of wireless channels to create multiple simultaneous independent non-interfering data streams to different users. For given channel conditions and user distribution, the basis functions of the radiated field are selected to create independent and simultaneous wireless links to different users in such a way that every user experiences interference-free links. As the MU-MAS is aware of the channel between every transmitter and every user, the precoding transmission is adjusted based on that information to create separate areas of coherence to different users.

**[00261]** In one embodiment of the invention, the MU-MAS employs non-linear precoding, such as dirty-paper coding (DPC) [30-31] or Tomlinson-Harashima (TH) [32-33] precoding. In another embodiment of the invention, the MU-MAS employs non-linear precoding, such as

6181P526XPCT

block diagonalization (BD) as in our previous patent applications [0003-0009] or zero-forcing beamforming (ZF-BF) [34].

**[00262]** To enable precoding, the MU-MAS requires knowledge of the channel state information (CSI). The CSI is made available to the MU-MAS via a feedback channel or estimated over the uplink channel, assuming uplink/downlink channel reciprocity is possible in time division duplex (TDD) systems. One way to reduce the amount of feedback required for CSI, is to use limited feedback techniques [35-37]. In one embodiment, the MU-MAS uses limited feedback techniques to reduce the CSI overhead of the control channel. Codebook design is critical in limited feedback techniques. One embodiment defines the codebook from the basis functions that span the radiated field of the transmit array.

**[00263]** As the users move in space or the propagation environment changes over time due to mobile objects (such as people or cars), the areas of coherence change their locations and shape. This is due to well known Doppler effect in wireless communications. The MU-MAS described in this patent application adjusts the precoding to adapt the areas of coherence constantly for every user as the environment changes due to Doppler effects. This adaptation of the areas of coherence is such to create simultaneous non-interfering channels to different users.

**[00264]** Another embodiment of the invention adaptively selects a subset of antennas of the MU-MAS system to create areas of coherence of different sizes. For example, if the users are sparsely distributed in space (i.e., rural area or times of the day with low usage of wireless resources), only a small subset of antennas is selected and the size of the area of coherence are large relative to the array size as in **Figure 43**. Alternatively, in densely populated areas (i.e., urban areas or time of the day with peak usage of wireless services) more antennas are selected to create small areas of coherence for users in direct vicinity of each other.

**[00265]** In one embodiment of the invention, the MU-MAS is a DIDO system as described in previous patent applications [0003-0009]. The DIDO system uses linear or non-linear precoding and/or limited feedback techniques to create area of coherence to different users.

## Numerical Results

**[00266]** We begin by computing the number of degrees of freedom in conventional multiple-input multiple-output (MIMO) systems as a function of the array size. We consider unpolarized linear arrays and two types of channel models: indoor as in the IEEE 802.11n standard for WiFi systems and outdoor as in the 3GPP-LTE standard for cellular systems. The indoor channel mode in [3] defines the number of clusters in the range [2, 6] and angular spread in the range [15°, 40°]. The outdoor channel model for urban micro defines about 6 clusters and the angular spread at the base station of about 20°.

**[00267]** **Figure 47** shows the degrees of freedom of MIMO systems in practical indoor and outdoor propagation scenarios. For example, considering linear arrays with ten antennas spaced one wavelength apart, the maximum degrees of freedom (or number of spatial channels) available over the wireless link is limited to about 3 for outdoor scenarios and 7 for indoor. Of course, indoor channels provide more degrees of freedom due to the larger angular spread.

**[00268]** Next we compute the degrees of freedom in DIDO systems. We consider the case where the antennas distributed over 3D space, such as downtown urban scenarios where DIDO access points may be distributed on different floors of adjacent building. As such, we model the DIDO transmit antennas (all connected to each other via fiber or DSL backbone) as a spherical array. Also, we assume the clusters are uniformly distributed across the solid angle.

**[00269]** **Figure 48** shows the degrees of freedom in DIDO systems as a function of the array diameter. We observe that for a diameter equal to ten wavelengths, about 1000 degrees of freedom are available in the DIDO system. In theory, it is possible to create up to 1000 non-interfering channels to the users. The increased spatial diversity due to distributed antennas in space is the key to the multiplexing gain provided by DIDO over conventional MIMO systems.

**[00270]** As a comparison, we show the degrees of freedom achievable in suburban environments with DIDO systems. We assume the clusters are distributed within the elevation angles  $[\alpha, \pi - \alpha]$ , and define the solid angle for the clusters as  $|\Omega| = 4\pi \cos \alpha$ . For example, in suburban scenarios with two-story buildings, the elevation angle of the scatterers can be  $\alpha = 60^\circ$ . In that case, the number of degrees of freedom as a function of the wavelength is shown in **Figure 48**.

## References

**[00271]** [1] A. A. M. Saleh and R. A. Valenzuela, “A statistical model for indoor multipath propagation,” IEEE Jour. Select. Areas in Comm., vol.195 SAC-5, no. 2, pp. 128–137, Feb. 1987.

**[00272]** [2] J. W. Wallace and M. A. Jensen, “Statistical characteristics of measured MIMO wireless channel data and comparison to conventional models,” Proc. IEEE Veh. Technol. Conf., vol. 2, no. 7-11, pp. 1078–1082, Oct. 2001.

**[00273]** [3] V. Erceg et al., “TGn channel models,” IEEE 802.11-03/940r4, May 2004.

**[00274]** [4] 3GPP Technical Specification Group, “Spatial channel model, SCM-134 text V6.0,” Spatial Channel Model AHG (Combined ad-hoc from 3GPP and 3GPP2), Apr. 2003.

[00275] [5] D.-S. Shiu, G. J. Foschini, M. J. Gans, and J. M. Kahn, “Fading correlation and its effect on the capacity of multielement antenna systems,” *IEEE Trans. Comm.*, vol. 48, no. 3, pp. 502–513, Mar. 2000.

[00276] [6] V. Pohl, V. Jungnickel, T. Haustein, and C. von Helmolt, “Antenna spacing in MIMO indoor channels,” *Proc. IEEE Veh. Technol. Conf.*, vol. 2, pp. 749–753, May 2002.

[00277] [7] M. Stoytchev, H. Safar, A. L. Moustakas, and S. Simon, “Compact antenna arrays for MIMO applications,” *Proc. IEEE Antennas and Prop. Symp.*, vol. 3, pp. 708–711, July 2001.

[00278] [8] K. Sulonen, P. Suvikunnas, L. Vuokko, J. Kivinen, and P. Vainikainen, “Comparison of MIMO antenna configurations in picocell and microcell environments,” *IEEE Jour. Select. Areas in Comm.*, vol. 21, pp. 703–712, June 2003.

[00279] [9] Shuangqing Wei, D. L. Goeckel, and R. Janaswamy, “On the asymptotic capacity of MIMO systems with fixed length linear antenna arrays,” *Proc. IEEE Int. Conf. on Comm.*, vol. 4, pp. 2633–2637, 2003.

[00280] [10] T. S. Pollock, T. D. Abhayapala, and R. A. Kennedy, “Antenna saturation effects on MIMO capacity,” *Proc. IEEE Int. Conf. on Comm.*, 192 vol. 4, pp. 2301–2305, May 2003.

[00281] [11] M. L. Morris and M. A. Jensen, “The impact of array configuration on MIMO wireless channel capacity,” *Proc. IEEE Antennas and Prop. Symp.*, vol. 3, pp. 214–217, June 2002.

[00282] [12] Liang Xiao, Lin Dal, Hairuo Zhuang, Shidong Zhou, and Yan Yao, “A comparative study of MIMO capacity with different antenna topologies,” *IEEE ICCS’02*, vol. 1, pp. 431–435, Nov. 2002.

[00283] [13] A. Forenza and R. W. Heath Jr., “Impact of antenna geometry on MIMO communication in indoor clustered channels,” *Proc. IEEE Antennas and Prop. Symp.*, vol. 2, pp. 1700–1703, June 2004.

[00284] [14] M. R. Andrews, P. P. Mitra, and R. deCarvalho, “Tripling the capacity of wireless communications using electromagnetic polarization,” *Nature*, vol. 409, pp. 316–318, Jan. 2001.

[00285] [15] D.D. Stancil, A. Berson, J.P. Van’t Hof, R. Negi, S. Sheth, and P. Patel, “Doubling wireless channel capacity using co-polarised, co-located electric and magnetic dipoles,” *Electronics Letters*, vol. 38, pp. 746–747, July 2002.

[00286] [16] T. Svantesson, “On capacity and correlation of multi-antenna systems employing multiple polarizations,” *Proc. IEEE Antennas and Prop. Symp.*, vol. 3, pp. 202–205, June 2002.

[00287] [17] C. Degen and W. Keusgen, "Performance evaluation of MIMO systems using dual-polarized antennas," Proc. IEEE Int. Conf. on Telecommun., vol. 2, pp. 1520–1525, Feb. 2003.

[00288] [18] R. Vaughan, "Switched parasitic elements for antenna diversity," IEEE Trans. Antennas Propagat., vol. 47, pp. 399–405, Feb. 1999.

[00289] [19] P. Mattheijssen, M. H. A. J. Herben, G. Dolmans, and L. Leyten, "Antenna-pattern diversity versus space diversity for use at handhelds," IEEE Trans. on Veh. Technol., vol. 53, pp. 1035–1042, July 2004.

[00290] [20] L. Dong, H. Ling, and R. W. Heath Jr., "Multiple-input multiple-output wireless communication systems using antenna pattern diversity," Proc. IEEE Glob. Telecom. Conf., vol. 1, pp. 997–1001, Nov. 2002.

[00291] [21] J. B. Andersen and B. N. Getu, "The MIMO cube-a compact MIMO antenna," IEEE Proc. of Wireless Personal Multimedia Communications Int. Symp., vol. 1, pp. 112–114, Oct. 2002.

[00292] [22] C. Waldschmidt, C. Kuhnert, S. Schulteis, and W. Wiesbeck, "Compact MIMO-arrays based on polarisation-diversity," Proc. IEEE Antennas and Prop. Symp., vol. 2, pp. 499–502, June 2003.

[00293] [23] C. B. Dietrich Jr, K. Dietze, J. R. Nealy, and W. L. Stutzman, "Spatial, polarization, and pattern diversity for wireless handheld terminals," Proc. IEEE Antennas and Prop. Symp., vol. 49, pp. 1271–1281, Sep. 2001.

[00294] [24] S. Visuri and D. T. Slock, "Colocated antenna arrays: design desiderata for wireless communications," Proc. of Sensor Array and Multichannel Sign. Proc. Workshop, pp. 580–584, Aug. 2002.

[00295] [25] A. Forenza and R. W. Heath Jr., "Benefit of pattern diversity via 2-element array of circular patch antennas in indoor clustered MIMO channels," IEEE Trans. on Communications, vol. 54, no. 5, pp. 943-954, May 2006.

[00296] [26] A. Forenza and R. W. Heath, Jr., "Optimization Methodology for Designing 2-CPAs Exploiting Pattern Diversity in Clustered MIMO Channels", IEEE Trans. on Communications, Vol. 56, no. 10, pp. 1748 -1759, Oct. 2008.

[00297] [27] D. Piazza, N. J. Kirsch, A. Forenza, R. W. Heath, Jr., and K. R. Dandekar, "Design and Evaluation of a Reconfigurable Antenna Array for MIMO Systems," IEEE Transactions on Antennas and Propagation, vol. 56, no. 3, pp. 869-881, March 2008.

[00298] [28] R. Bhagavatula, R. W. Heath, Jr., A. Forenza, and S. Vishwanath, "Sizing up MIMO Arrays," IEEE Vehicular Technology Magazine, vol. 3, no. 4, pp. 31-38, Dec. 2008.

[00299] [29] Ada Poon, R. Brodersen and D. Tse, "Degrees of Freedom in Multiple Antenna Channels: A Signal Space Approach", *IEEE Transactions on Information Theory*, vol. 51(2), Feb. 2005, pp. 523-536.

[00300] [30] M. Costa, "Writing on dirty paper," *IEEE Transactions on Information Theory*, Vol. 29, No. 3, Page(s): 439 - 441, May 1983.

[00301] [31] U. Erez, S. Shamai (Shitz), and R. Zamir, "Capacity and lattice-strategies for cancelling known interference," *Proceedings of International Symposium on Information Theory*, Honolulu, Hawaii, Nov. 2000.

[00302] [32] M. Tomlinson, "New automatic equalizer employing modulo arithmetic," *Electronics Letters*, Page(s): 138 - 139, March 1971.

[00303] [33] H. Miyakawa and H. Harashima, "A method of code conversion for digital communication channels with intersymbol interference," *Transactions of the Institute of Electronic*

[00304] [34] R. A. Monziano and T. W. Miller, *Introduction to Adaptive Arrays*, New York: Wiley, 1980.

[00305] [35] T. Yoo, N. Jindal, and A. Goldsmith, "Multi-antenna broadcast channels with limited feedback and user selection," *IEEE Journal on Sel. Areas in Communications*, vol. 25, pp. 1478-91, July 2007.

[00306] [36] P. Ding, D. J. Love, and M. D. Zoltowski, "On the sum rate of channel subspace feedback for multi-antenna broadcast channels," in Proc., IEEE Globecom, vol. 5, pp. 2699-2703, November 2005.

[00307] [37] N. Jindal, "MIMO broadcast channels with finite-rate feedback," *IEEE Trans. on Info. Theory*, vol. 52, pp. 5045-60, November 2006.

#### IV. SYSTEM AND METHODS FOR PLANNED EVOLUTION AND OBSOLESCENCE OF MULTIUSER SPECTRUM

[00308] The growing demand for high-speed wireless services and the increasing number of cellular telephone subscribers has produced a radical technology revolution in the wireless industry over the past three decades from initial analog voice services (AMPS [1-2]) to standards that support digital voice (GSM [3-4], IS-95 CDMA [5]), data traffic (EDGE [6], EV-DO [7]) and Internet browsing (WiFi [8-9], WiMAX [10-11], 3G [12-13], 4G [14-15]). This wireless technology growth throughout the years has been enabled by two major efforts:

- i) The federal communications commission (FCC) [16] has been allocating new spectrum to support new emerging standards. For example, in the first generation AMPS systems the number of channels allocated by the FCC grew from the initial 333 in 1983 to 416 in

the late 1980s to support the increasing number of cellular clients. More recently, the commercialization of technologies like Wi-Fi, Bluetooth and ZigBee has been possible with the use of the unlicensed ISM band allocated by the FCC back in 1985 [17].

- ii) The wireless industry has been producing new technologies that utilize the limited available spectrum more efficiently to support higher data rate links and increased numbers of subscribers. One big revolution in the wireless world was the migration from the analog AMPS systems to digital D-AMPS and GSM in the 1990s, that enabled much higher call volume for a given frequency band due to improved spectral efficiency. Another radical shift was produced in the early 2000s by spatial processing techniques such as multiple-input multiple-output (MIMO), yielding 4x improvement in data rate over previous wireless networks and adopted by different standards (i.e., IEEE 802.11n for Wi-Fi, IEEE 802.16 for WiMAX, 3GPP for 4G-LTE).

**[00309]** Despite efforts to provide solutions for high-speed wireless connectivity, the wireless industry is facing new challenges: to offer high-definition (HD) video streaming to satisfy the growing demand for services like gaming and to provide wireless coverage everywhere (including rural areas, where building the wireline backbone is costly and impractical). Currently, the most advanced wireless standard systems (i.e., 4G-LTE) cannot provide data rate requirements and latency constraints to support HD streaming services, particularly when the network is overloaded with a high volume of concurrent links. Once again, the main drawbacks have been the limited spectrum availability and lack of spectrally efficient technologies that can truly enhance data rate and provide complete coverage.

**[00310]** A new technology has emerged in recent years called distributed-input distributed-output (DIDO) [18-21] and described in our previous patent applications [0002-0009]. DIDO technology promises orders of magnitude increase in spectral efficiency, making HD wireless streaming services possible in overloaded networks.

**[00311]** At the same time, the US government has been addressing the issue of spectrum scarcity by launching a plan that will free 500MHz of spectrum over the next 10 years. This plan was released on June 28<sup>th</sup>, 2010 with the goal of allowing new emerging wireless technologies to operate in the new frequency bands and providing high-speed wireless coverage in urban and rural areas [22]. As part of this plan, on September 23<sup>rd</sup>, 2010 the FCC opened up about 200MHz of the VHF and UHF spectrum for unlicensed use called “white spaces” [23]. One restriction to operate in those frequency bands is that harmful interference must not be created with existing wireless microphone devices operating in the same band. As such, on July 22<sup>nd</sup>, 2011 the IEEE 802.22 working group finalized the standard for a new wireless system employing cognitive radio technology (or spectrum sensing) with the key feature of dynamically monitoring the

6181P526XPCT

spectrum and operating in the available bands, thereby avoiding harmful interference with coexisting wireless devices [24]. Only recently has there been debates to allocate part of the white spaces to licensed use and open it up to spectrum auction [25].

**[00312]** The coexistence of unlicensed devices within the same frequency bands and spectrum contention for unlicensed versus licensed use have been two major issues for FCC spectrum allocation plans throughout the years. For example, in white spaces, coexistence between wireless microphones and wireless communications devices has been enabled via cognitive radio technology. Cognitive radio, however, can provide only a fraction of the spectral efficiency of other technologies using spatial processing like DIDO. Similarly, the performance of Wi-Fi systems have been degrading significantly over the past decade due to increasing number of access points and the use of Bluetooth/ZigBee devices that operate in the same unlicensed ISM band and generate uncontrolled interference. One shortcoming of the unlicensed spectrum is unregulated use of RF devices that will continue to pollute the spectrum for years to come. RF pollution also prevents the unlicensed spectrum from being used for future licensed operations, thereby limiting important market opportunities for wireless broadband commercial services and spectrum auctions.

**[00313]** We propose a new system and methods that allow dynamic allocation of the wireless spectrum to enable coexistence and evolution of different services and standards. One embodiment of our method dynamically assigns entitlements to RF transceivers to operate in certain parts of the spectrum and enables obsolescence of the same RF devices to provide:

- i) Spectrum reconfigurability to enable new types of wireless operations (i.e., licensed vs. unlicensed) and/or meet new RF power emission limits. This feature allows spectrum auctions whenever is necessary, without need to plan in advance for use of licensed versus unlicensed spectrum. It also allows transmit power levels to be adjusted to meet new power emission levels enforced by the FCC.
- ii) Coexistence of different technologies operating in the same band (i.e., white spaces and wireless microphones, WiFi and Bluetooth/ZigBee) such that the band can be dynamically reallocated as new technologies are created, while avoiding interference with existing technologies.
- iii) Seamless evolution of wireless infrastructure as systems migrate to more advanced technologies that can offer higher spectral efficiency, better coverage and improved performance to support new types of services demanding higher QoS (i.e., HD video streaming).

**[00314]** Hereafter, we describe a system and method for planned evolution and obsolescence of a multiuser spectrum. One embodiment of the system consists of one or multiple

6181P526XPCT

centralized processors (CP) 4901-4904 and one or multiple distributed nodes (DN) 4911-4913 that communicate via wireline or wireless connections as depicted in **Figure 49**. For example, in the context of 4G-LTE networks [26], the centralized processor is the access core gateway (ACGW) connected to several Node B transceivers. In the context of Wi-Fi, the centralized processor is the internet service provider (ISP) and the distributed nodes are Wi-Fi access points connected to the ISP via modems or direct connection to cable or DSL. In another embodiment of the invention, the system is a distributed-input distributed-output (DIDO) system [0002-0009] with one centralized processor (or BTS) and distributed nodes being the DIDO access points (or DIDO distributed antennas connected to the BTS via the BSN).

**[00315]** The DNs 4911-4913 communicate with the CPs 4901-4904. The information exchanged from the DNs to the CP is used to dynamically adjust the configuration of the nodes to the evolving design of the network architecture. In one embodiment, the DNs 4911-4913 share their identification number with the CP. The CP store the identification numbers of all DNs connected through the network into lookup tables or shared database. Those lookup tables or database can be shared with other CPs and that information is synchronized such that all CPs have always access to the most up to date information about all DNs on the network.

**[00316]** For example, the FCC may decide to allocate a certain portion of the spectrum to unlicensed use and the proposed system may be designed to operate within that spectrum. Due to scarcity of spectrum, the FCC may subsequently need to allocate part of that spectrum to licensed use for commercial carriers (i.e., AT&T, Verizon, or Sprint), defense, or public safety. In conventional wireless systems, this coexistence would not be possible, since existing wireless devices operating in the unlicensed band would create harmful interference to the licensed RF transceivers. In our proposed system, the distributed nodes exchange control information with the CPs 4901-4903 to adapt their RF transmission to the evolving band plan. In one embodiment, the DNs 4911-4913 were originally designed to operate over different frequency bands within the available spectrum. As the FCC allocates one or multiple portions of that spectrum to licensed operation, the CPs exchange control information with the unlicensed DNs and reconfigure them to shut down the frequency bands for licensed use, such that the unlicensed DNs do not interfere with the licensed DNs. This scenario is depicted in **Figure 50** where the unlicensed nodes (e.g., 5002) are indicated with solid circles and the licensed nodes with empty circles (e.g., 5001). In another embodiment, the whole spectrum can be allocated to the new licensed service and the control information is used by the CPs to shut down all unlicensed DNs to avoid interference with the licensed DNs. This scenario is shown in **Figure 51** where the obsolete unlicensed nodes are covered with a cross.

**[00317]** By way of another example, it may be necessary to restrict power emissions for certain devices operating at given frequency band to meet the FCC exposure limits [27]. For instance, the wireless system may originally be designed for fixed wireless links with the DNs 4911-4913 connected to outdoor rooftop transceiver antennas. Subsequently, the same system may be updated to support DNs with indoor portable antennas to offer better indoor coverage. The FCC exposure limits of portable devices are more restrictive than rooftop transmitters, due to possibly closer proximity to the human body. In this case, the old DNs designed for outdoor applications can be re-used for indoor applications as long as the transmit power setting is adjusted. In one embodiment of the invention the DNs are designed with predefined sets of transmit power levels and the CPs 4901-4903 send control information to the DNs 4911-4913 to select new power levels as the system is upgraded, thereby meeting the FCC exposure limits. In another embodiment, the DNs are manufactured with only one power emission setting and those DNs exceeding the new power emission levels are shut down remotely by the CP.

**[00318]** In one embodiment, the CPs 4901-4903 monitor periodically all DNs 4911-4913 in the network to define their entitlement to operate as RF transceivers according to a certain standard. Those DNs that are not up to date can be marked as obsolete and removed from the network. For example, the DNs that operate within the current power limit and frequency band are kept active in the network, and all the others are shut down. Note that the DN parameters controlled by the CP are not limited to power emission and frequency band; it can be any parameter that defines the wireless link between the DN and the client devices.

**[00319]** In another embodiment of the invention, the DNs 4911-4913 can be reconfigured to enable the coexistence of different standard systems within the same spectrum. For example, the power emission, frequency band or other configuration parameters of certain DNs operating in the context of WLAN can be adjusted to accommodate the adoption of new DNs designed for WPAN applications, while avoiding harmful interference.

**[00320]** As new wireless standards are developed to enhance data rate and coverage in the wireless network, the DNs 4911-4913 can be updated to support those standards. In one embodiment, the DNs are software defined radios (SDR) equipped with programmable computational capability such as FPGA, DSP, CPU, GPU and/or GPGPU that run algorithms for baseband signal processing. If the standard is upgraded, new baseband algorithms can be remotely uploaded from the CP to the DNs to reflect the new standard. For example, in one embodiment the first standard is CDMA-based and subsequently it is replaced by OFDM technology to support different types of systems. Similarly, the sample rate, power and other parameters can be updated remotely to the DNs. This SDR feature of the DNs allows for

6181P526XPCT

continuous upgrades of the network as new technologies are developed to improve overall system performance.

**[00321]** In another embodiment, the system described herein is a cloud wireless system consisting of multiple CPs, distributed nodes and a network interconnecting the CPs to the DNs. **Figure 52** shows one example of cloud wireless system where the nodes identified with solid circles (e.g., 5203) communicate to CP 5206, the nodes identified with empty circles communicate to CP 5205 and the CPs 5205-5206 communicate between each other all through the network 5201. In one embodiment of the invention, the cloud wireless system is a DIDO system and the DNs are connected to the CP and exchange information to reconfigure periodically or instantly system parameters, and dynamically adjust to the changing conditions of the wireless architecture. In the DIDO system, the CP is the DIDO BTS, the distributed nodes are the DIDO distributed antennas, the network is the BSN and multiple BTSs are interconnected with each other via the DIDO centralized processor as described in our previous patent applications [0002-0009].

#### **[00322]**

All DNs 5202-5203 within the cloud wireless system can be grouped in different sets. These sets of DNs can simultaneously create non-interfering wireless links to the multitude of client devices, while each set supporting a different multiple access techniques (e.g., TDMA, FDMA, CDMA, OFDMA and/or SDMA), different modulations (e.g., QAM, OFDM) and/or coding schemes (e.g., convolutional coding, LDPC, turbo codes). Similarly, every client may be served with different multiple access techniques and/or different modulation/coding schemes. Based on the active clients in the system and the standard they adopt for their wireless links, the CPs 5205-5206 dynamically select the subset of DNs that can support those standards and that are within range of the client devices.

#### **Reference**

**[00323]** [1] Wikipedia, “Advanced Mobile Phone System”  
[http://en.wikipedia.org/wiki/Advanced\\_Mobile\\_Phone\\_System](http://en.wikipedia.org/wiki/Advanced_Mobile_Phone_System)

**[00324]** [2] AT&T, “1946: First Mobile Telephone Call”  
<http://www.corp.att.com/attlabs/reputation/timeline/46mobile.html>

**[00325]** [3] GSMA, “GSM technology”  
<http://www.gsmworld.com/technology/index.htm>

**[00326]** [4] ETSI, “Mobile technologies GSM”  
<http://www.etsi.org/WebsiTe/Technologies/gsm.aspx>

**[00327]** [5] Wikipedia, “IS-95”  
<http://en.wikipedia.org/wiki/IS-95>

6181P526XPCT

[00328] [6] Ericsson, "The evolution of EDGE"  
[http://www.ericsson.com/res/docs/whitepapers/evolution\\_to\\_edge.pdf](http://www.ericsson.com/res/docs/whitepapers/evolution_to_edge.pdf)

[00329] [7] Q. Bi (2004-03). "A Forward Link Performance Study of the 1xEV-DO Rel. 0 System Using Field Measurements and Simulations" (PDF). Lucent Technologies.  
[http://www.cdg.org/resources/white\\_papers/files/Lucent%201xEV-DO%20Rev%20O%20Mar%2004.pdf](http://www.cdg.org/resources/white_papers/files/Lucent%201xEV-DO%20Rev%20O%20Mar%2004.pdf)

[00330] [8] Wi-Fi alliance, <http://www.wi-fi.org/>

[00331] [9] Wi-Fi alliance, "Wi-Fi certified makes it Wi-Fi"  
[http://www.wi-fi.org/files/WFA\\_Certification\\_Overview\\_WP\\_en.pdf](http://www.wi-fi.org/files/WFA_Certification_Overview_WP_en.pdf)

[00332] [10] WiMAX forum, <http://www.wimaxforum.org/>

[00333] [11] C. Eklund, R. B. Marks, K. L. Stanwood and S. Wang, "IEEE Standard 802.16: A Technical Overview of the WirelessMAN™ Air Interface for Broadband Wireless Access"  
[http://ieee802.org/16/docs/02/C80216-02\\_05.pdf](http://ieee802.org/16/docs/02/C80216-02_05.pdf)

[00334] [12] 3GPP, "UMTS", <http://www.3gpp.org/article/umts>

[00335] [13] H. Ekström, A. Furuskär, J. Karlsson, M. Meyer, S. Parkvall, J. Torsner, and M. Wahlqvist "Technical Solutions for the 3G Long-Term Evolution", IEEE Communications Magazine, pp.38-45, Mar. 2006

[00336] [14] 3GPP, "LTE", <http://www.3gpp.org/LTE>

[00337] [15] Motorola, "Long Term Evolution (LTE): A Technical Overview", <http://business.motorola.com/experiencelte/pdf/LTETechnicalOverview.pdf>

[00338] [16] Federal Communications Commission, "Authorization of Spread Spectrum Systems Under Parts 15 and 90 of the FCC Rules and Regulations", June 1985.

[00339] [17] ITU, "ISM band" <http://www.itu.int/ITU-R/terrestrial/faq/index.html#g013>

[00340] [18] S. Perlman and A. Forenza "Distributed-input distributed-output (DIDO) wireless technology: a new approach to multiuser wireless", Aug. 2011  
[http://www.rearden.com/DIDO/DIDO\\_White\\_Paper\\_110727.pdf](http://www.rearden.com/DIDO/DIDO_White_Paper_110727.pdf)

[00341] [19] Bloomberg Businessweek, "Steve Perlman's Wireless Fix", July 27, 2011  
<http://www.businessweek.com/magazine/the-edison-of-silicon-valley-07272011.html>

[00342] [20] Wired, "Has OnLive's Steve Perlman Discovered Holy Grail of Wireless?", June 30, 2011  
<http://www.wired.com/epicenter/2011/06/perlman-holy-grail-wireless/>

[00343] [21] The Wall Street Journal "Silicon Valley Inventor's Radical Rewrite of Wireless", July 28, 2011  
<http://blogs.wsj.com/digits/2011/07/28/silicon-valley-inventors-radical-rewrite-of-wireless/>

6181P526XPCT

[00344] [22] The White House, “Presidential Memorandum: Unleashing the Wireless Broadband Revolution”, June 28, 2010  
<http://www.whitehouse.gov/the-press-office/presidential-memorandum-unleashing-wireless-broadband-revolution>

[00345] [23] FCC, “Open commission meeting”, Sept. 23<sup>rd</sup>, 2010  
<http://reboot.fcc.gov/open-meetings/2010/september>

[00346] [24] IEEE 802.22, “IEEE 802.22 Working Group on Wireless Regional Area Networks”, <http://www.ieee802.org/22/>

[00347] [25] “A bill”, 112th congress, 1<sup>st</sup> session, July 12, 2011  
<http://republicans.energycommerce.house.gov/Media/file/Hearings/Telecom/071511/DiscussionDraft.pdf>

[00348] [26] H. Ekström, A. Furuskär, J. Karlsson, M. Meyer, S. Parkvall, J. Torsner, and M. Wahlqvist “Technical Solutions for the 3G Long-Term Evolution”, IEEE Communications Magazine, pp.38-45, Mar. 2006

[00349] [27] FCC, “Evaluating compliance with FCC guidelines for human exposure to radiofrequency electromagnetic fields,” OET Bulletin 65, Edition 97-01, Aug. 1997

## V. SYSTEM AND METHOD TO COMPENSATE FOR DOPPLER EFFECTS IN DISTRIBUTED-INPUT DISTRIBUTED-OUTPUT WIRELESS SYSTEMS

[00350] In this portion of the detailed description we describe a multiuser (MU) multiple antenna system (MAS) for multiuser wireless transmissions that adaptively reconfigures its parameters to compensate for Doppler effects due to user mobility or changes in the propagation environment. In one embodiment, the MAS is a distributed-input distributed-output (DIDO) system as described the co-pending patent applications [0002-0016] and depicted in **Figure 53**. The DIDO system of one embodiment includes the following components:

- **User Equipment (UE):** The UE 5301 of one embodiment includes an RF transceiver for fixed or mobile clients receiving data streams over the downlink (DL) channel from the DIDO backhaul and transmitting data to the DIDO backhaul via the uplink (UL) channel
- **Base Transceiver Station (BTS):** The BTSs 5310-5314 of one embodiment interface the DIDO backhaul with the wireless channel. BTSs 5310-5314 are access points consisting of DAC/ADC and radio frequency (RF) chain to convert the baseband signal to RF. In some cases, the BTS is a simple RF transceiver equipped with power amplifier/antenna and the RF signal is carried to the BTS via RF-over-fiber technology as described in our patent application [0010].

- **Controller (CTR):** The CTR 5320 in one embodiment is one particular type of BTS designed for certain specialized features such as transmitting training signals for time/frequency synchronization of the BTSs and/or the UEs, receiving/transmitting control information from/to the UEs, receiving the channel state information (CSI) or channel quality information from the UEs.
- **Centralized Processor (CP):** The CP 5340 of one embodiment is a DIDO server interfacing the Internet or other types of external networks 5350 with the DIDO backhaul. The CP computes the DIDO baseband processing and sends the waveforms to the distributed BTSs for DL transmission
- **Base Station Network (BSN):** The BSN 5330 of one embodiment is the network connecting the CP to the distributed BTSs carrying information for either the DL or the UL channel. The BSN is a wireline or a wireless network or a combination of the two. For example, the BSN is a DSL, cable, optical fiber network, or line-of-sight or non-line-of-sight wireless link. Furthermore, the BSN is a proprietary network, or a local area network, or the Internet.

**[00351]** As described in the co-pending applications, the DIDO system creates independent channels to multiple users, such that each user receives interference-free channels. In DIDO systems, this is achieved by employing distributed antennas or BTSs to exploit spatial diversity. In one embodiment, the DIDO system exploits spatial, polarization and/or pattern diversity to increase the degrees of freedom within each channel. The increased degrees of freedom of the wireless link are used to transmit independent data streams to an increased number of UEs (i.e., multiplexing gain) and/or improve coverage (i.e., diversity gain).

**[00352]** The BTSs 5310-5314 are placed anywhere that is convenient where there is access to the Internet or BSN. In one embodiment of the invention, the UEs 5301-5305 are placed randomly between, around and/or surrounded by the BTSs or distributed antennas as depicted in

**Figure 54.**

**[00353]** In one embodiment, the BTSs 5310-5314 send a training signal and/or independent data streams to the UEs 5301 over the DL channel as depicted in **Figure 55**. The training signal is used by the UEs for different purposes, such as time/frequency synchronization, channel estimation and/or estimation of the channel state information (CSI). In one embodiment of the invention, the MU-MAS DL employs non-linear precoding, such as dirty-paper coding (DPC) [1-2] or Tomlinson-Harashima (TH) [3-4] precoding. In another embodiment of the invention, the MU-MAS DL employs non-linear precoding, such as block diagonalization (BD) as described in the co-pending patent applications [0003-0009] or zero-forcing beamforming (ZF-BF) [5]. If the number of BTSs is larger than the UEs, the extra BTSs are used to increase link

## 6181P526XPCT

quality to every UE via diversity schemes such as antenna selection or eigenmode selection described in [0002-0016]. If the number of BTSs is smaller than the UEs, the extra UEs share the wireless links with the other UEs via conventional multiplexing techniques (e.g., TDMA, FDMA, CDMA, OFDMA).

**[00354]** The UL channel is used to transmit data from the UEs 5301 to the CP 5340 and/or the CSI (or channel quality information) employed by the DIDO precoder. In one embodiment, the UL channels from the UEs are multiplexed via conventional multiplexing techniques (e.g., TDMA, FDMA, CDMA, OFDMA) to the CTR as depicted in **Figure 56** or to the closest BTS. In another embodiment of the invention, spatial processing techniques are used to separate the UL channels from the UEs 5301 to the distributed BTSs 5310-5314 as depicted in **Figure 57**. For example, UL streams are transmitted from the client to the DIDO antennas via multiple-input multiple-output (MIMO) multiplexing schemes. The MIMO multiplexing schemes include transmitting independent data streams from the clients and using linear or non-linear receivers at the DIDO antennas to remove co-channel interference. In another embodiment, the downlink weights are used over the uplink to demodulate the uplink streams, assuming UL/DL channel reciprocity holds and the channel does not vary significantly between DL and UL transmission due to Doppler effects. In another embodiment, a maximum ratio combining (MRC) receiver is used over the UL channel to increase signal quality at the DIDO antennas from every client.

**[00355]** The data, control information and CSI sent over the DL/UL channels is shared between the CP 5340 and the BTSs 5310-5314 via the BSN 5330. The known training signals for the DL channel can be stored in memory at the BTSs 5310-5314 to reduce overhead over the BSN 5330. Depending on the type of network (i.e., wireless versus wireline, DSL versus cable or fiber optic), there may not be a sufficient data rate available over the BSN 5330 to exchange information between the CP 5340 and the BTSs 5310-5314, especially when the baseband signal is delivered to the BTSs. For example, let us assume the BTSs transmit 10Mbps independent data streams to every UE over 5MHz bandwidth (depending on the digital modulation and FEC coding scheme used over the wireless link). If 16 bits of quantization are used for the real and 16 for the imaginary components, the baseband signal requires 160Mbps of data throughput from the CP to the BTSs over the BSN. In one embodiment, the CP and the BTSs are equipped with encoders and decoders to compress and decompress information sent over the BSN. In the forward link, the precoded baseband data sent from the CP to the BTSs is compressed to reduce the amount of bits and overhead sent over the BSN. Similarly, in the reverse link, the CSI as well as data (sent over the uplink channel from the UEs to the BTSs) are compressed before being transmitted over the BSN from the BTSs to the CP. Different compression algorithms are

6181P526XPCT

employed to reduce the amount of bits and overhead sent over the BSN, including but not limited to lossless and/or lossy techniques [6].

**[00356]** One feature of DIDO systems employed in one embodiment is making the CP 5340 aware of the CSI or channel quality information between all BTSs 5310-5314 and UEs 5301 to enable precoding. As explained in [0006], the performance of DIDO depends on the rate at which the CSI is delivered to the CP relative to the rate of change of the wireless links. It is well known that variations of the channel complex gain are due to UE mobility and/or changes in the propagation environment that cause Doppler effects. The rate of change of the channel is measured in terms of channel coherence time ( $T_c$ ) that is inversely proportional to the maximum Doppler shift. For DIDO transmissions to perform reliably, the latency due to CSI feedback must be a fraction (e.g., 1/10 or less) of the channel coherence time. In one embodiment, the latency over the CSI feedback loop is measured as the time between the time at which the CSI training is sent and the time the precoded data is demodulated at the UE side, as depicted in **Figure 58**.

**[00357]** In frequency division duplex (FDD) DIDO systems the BTSs 5310-5314 send CSI training to the UEs 5301, that estimate the CSI and feedback to the BTSs. Then the BTSs send the CSI via the BSN to the CP 5340, that computes the DIDO precoded data streams and sends those back to the BTSs via the BSN 5330. Finally the BTSs send precoded streams to the UEs that demodulate the data. Referring to **Figure 58**, the overall latency for the DIDO feedback loop is given by

$$2*T_{DL} + T_{UL} + T_{BSN} + T_{CP}$$

where  $T_{DL}$  and  $T_{UL}$  include the times to build, send and process the downlink and uplink frames, respectively,  $T_{BSN}$  is the round-trip delay over the BSN and  $T_{CP}$  is the time taken by the CP to process the CSI, generate the precoded data streams for the UEs and schedule different UEs for the current transmission. In this case,  $T_{DL}$  is multiplied by 2 to account for the training signal time (from the BTS to the UE) and the feedback signal time (from the UE to the BTS). In time division duplex (TDD), if channel reciprocity can be exploited, the first step is skipped (i.e., transiting a CSI training signal from the BTS to the UE) as the UEs send CSI training to the BTSs that compute the CSI and send it to the CP. Hence, in this embodiment, the overall latency for the DIDO feedback loop is

$$T_{DL} + T_{UL} + T_{BSN} + T_{CP}$$

**[00358]** The latency  $T_{BSN}$  depends on the type of BSN whether dedicated cable, DSL, fiber optic connection or general Internet. Typical values may vary between fractions of 1msec to 50msec. The computational time at the CP can be reduced if the DIDO processing is implemented at the CP on dedicated processors such as ASIC, FPGA, DSP, CPU, GPU and/or GPGPU. Moreover, if the number of BTSs 5310-5314 exceeds the number of UEs 5301, all the

UEs can be served at the same time, thereby removing latency due to multiuser scheduling. Hence, the latency  $T_{CP}$  is negligible compared to  $T_{BSN}$ . Finally, transmit and receive processing for the DL and UL is typically implemented on ASIC, FPGA or DSP with negligible computational time and if the signal bandwidth is relatively large (e.g. more than 1MHz) the frame duration can be made very small (i.e., less than 1msec). Therefore, also  $T_{DL}$  and  $T_{UL}$  are negligible compared to  $T_{BSN}$ .

**[00359]** In one embodiment of the invention, the CP 5340 tracks the Doppler velocity of all UEs 5301 and dynamically assigns the BTSs 5310-5314 with the lowest  $T_{BSN}$  to the UEs with higher Doppler. This adaptation is based on different criteria:

- Type of BSN: For example, dedicated fiber optic links typically experience lower latency than cable modems or DSL. Then the lower latency BSNs are used for high-mobility UEs (e.g., cars on freeways, trains), whereas the higher-latency BSNs are used for the fixed-wireless or low-mobility UEs (e.g., home equipment, pedestrians, cars in residential areas)
- Type of QoS: For example, the BSN can support different types of DIDO or non-DIDO traffic. It is possible to define quality of service (QoS) with different priorities for different types of traffic. For example, the BSN assigns high priority to DIDO traffic and low priority to non-DIDO traffic. Alternatively, high priority QoS is assigned to traffic for high-mobility UEs and low priority QoS to UEs with low-mobility.
- Long-term statistics: For example, the traffic over the BSN may vary significantly depending on the time of the day (e.g., night use for homes and day use for offices). Higher traffic load may result in higher latency. Then, in different times of the day, the BSNs with higher traffic, if it results in higher latency, are used for low-mobility UEs, whereas the BSNs with lower traffic, if it results in lower latency, are used for the high-mobility UEs
- Short-term statistics: For example, any BSN can be affected by temporary network congestion that can result in higher latency. Then the CP can adaptively select the BTSs from congested BSNs, if the congestion cause higher latency, for the low-mobility UEs and the remaining BSNs, if they are lower latency, for the high-mobility UEs.

**[00360]** In another embodiment of the invention, the BTSs 5310-5314 are selected based on the Doppler experienced on each individual BTS-UE link. For example, in the line-of-sight (LOS) link B in **Figure 59**, the maximum Doppler shift is a function of the angle ( $\phi$ ) between the BTS-UE link and the vehicular velocity (v), according to the well known equation

$$f_d = \frac{v}{\lambda} \cdot \cos \phi$$

where  $\lambda$  is the wavelength corresponding to the carrier frequency. Hence, in LOS channels the Doppler shift is maximum for link A and nearly zero for link C in **Figure 59**. In non-LOS (NLOS) the maximum Doppler shift depends on the direction of the multipaths around the UEs, but in general because of the distributed nature of the BTSs in DIDO systems, some BTSs will experience higher Doppler for a given UE (e.g., BTS 5312) whereas other BTSs will experience lower Doppler for that given UE (e.g., BTS 5314).

**[00361]** In one embodiment, the CP tracks the Doppler velocity over every BTS-UE link and selects only the links with the lowest Doppler effect for every UE. Similarly to the techniques described in [0002], the CP 5340 defines the “user cluster” for every UE 5301. The user cluster is the set of BTSs with good link quality (defined based on certain signal-to-noise ratio, SNR, threshold) to the UE and low Doppler (defined, for example, based on a predefined Doppler threshold) as depicted in **Figure 60**. In **Figure 60**, BTSs 5 through 10 all have good SNR to the UE1, but only BTSs 6 through 9 experience low Doppler effect (e.g., below the specified threshold).

**[00362]** The CP of this embodiment records all of the values of SNR and Doppler for every BTS-UE link into a matrix and for each UE it selects the submatrix that satisfies the SNR and Doppler thresholds. In the example depicted in **Figure 61**, the submatrix is identified by the green dotted line surrounding  $C_{2,6}$ ,  $C_{2,7}$ ,  $C_{3,9}$ ,  $C_{4,7}$ ,  $C_{4,8}$ ,  $C_{4,9}$ , and  $C_{5,6}$ . DIDO precoding weights are computed for that UE based on that submatrix. Note that BTSs 5 and 10 are reachable by UEs 2,3,4,5 and 7 as shown in the table in **Figure 61**. Then, to avoid interference to UE1 when transmitting to those other UEs, the BTSs 5 and 10 either must be switched off or assigned to different orthogonal channels based on conventional multiplexing techniques such as TDMA, FDMA, CDMA or OFDMA.

**[00363]** In another embodiment, the adverse effect of Doppler on the performance of DIDO precoding systems is reduced via linear prediction, which is one technique to estimate the complex channel coefficients in the future based on past channel estimates. By way of example and not limitation, different prediction algorithms for single-input single-output (SISO) and OFDM wireless systems were proposed in [7-11]. Knowing the future channel complex coefficients it is possible to reduce the error due to outdated CSI. For example, **Figure 62** shows the channel gain (or CSI) at different times: i)  $t_{CTR}$  is the time at which the CTR in **Figure 58** receives the CSI from the UEs in FDD systems (or equivalently the BTSs estimate the CSI from the UL channel exploiting DL/UL reciprocity in TDD systems); ii)  $t_{CP}$  is the time at which the CSI is delivered to the CP via the BSN; iii)  $t_{BTS}$  is the time at which the CSI is used for precoding over the wireless link. In **Figure 62** we observe that due to the delay  $T_{BSN}$  (also depicted in **Figure 58**), the CSI estimated at time  $t_{CTR}$  will be outdated (i.e., complex channel

## 6181P526XPCT

gain has changed) by the time is used for wireless transmission over the DL channel at time  $t_{BTS}$ . One way to avoid this effect due to Doppler is to run the prediction method at the CP. The CSI estimates available at the CP at time  $t_{CTR}$  is delayed of  $T_{BSN}/2$  due to CTR-to-CP latency and corresponds to the channel gain at time  $t_0$  in **Figure 62**. Then, the CP uses all or part of the CSI estimated before time  $t_0$  and stored in memory to predict the future channel coefficient at time  $t_0+T_{BSN} = t_{CP}$ . If the prediction algorithm has minimal error propagation, the predicted CSI at time  $t_{CP}$  reproduces reliably the channel gain in the future. The time difference between the predicted CSI and the current CSI is called prediction horizon and in SISO systems typically scales with the channel coherence time.

**[00364]** In DIDO systems the prediction algorithm is more complex since it estimates the future channel coefficients both in time and space domains. Linear prediction algorithms exploiting spatio-temporal characteristics of MIMO wireless channels were described in [12-13]. In [13] it was shown that the performance of the prediction algorithms in MIMO systems (measured in terms of mean squared error, or MSE) improves for higher channel coherence time (i.e., reduce Doppler effect) and lower channel coherence distance (due to lower spatial correlation). Hence the prediction horizon (expressed in seconds) of spatial-temporal methods is directly proportional to the channel coherence time and inversely proportional to the channel coherence distance. In DIDO systems the coherence distance is low due to high spatial selectivity produce by the distributed antennas.

**[00365]** Described herein are prediction techniques that exploit temporal and spatial diversity of DIDO systems to predict the vector channel (i.e., CSI from the BTSs to the UEs) in the future. These embodiments exploit spatial diversity available in wireless channels to obtain negligible CSI prediction error and an extended prediction horizon over any existing SISO and MIMO prediction algorithms. One important feature of these techniques is to exploit distributed antennas given that they receive uncorrelated complex channel coefficients from the distributed UEs.

**[00366]** In one embodiment of the invention, the spatial and temporal predictor is combined with estimator in the frequency domain to allow CSI prediction over all the available subcarriers in the system, such as in OFDM systems. In another embodiment of the invention, the DIDO precoding weights are predicted (rather than the CSI) based on previous estimates of the DIDO weights.

## References

**[00367]** [1] M. Costa, “Writing on dirty paper,” *IEEE Transactions on Information Theory*, Vol. 29, No. 3, Page(s): 439 - 441, May 1983.

[00368] [2] U. Erez, S. Shamai (Shitz), and R. Zamir, "Capacity and lattice-strategies for cancelling known interference," *Proceedings of International Symposium on Information Theory*, Honolulu, Hawaii, Nov. 2000.

[00369] [3] M. Tomlinson, "New automatic equalizer employing modulo arithmetic," *Electronics Letters*, Page(s): 138 - 139, March 1971.

[00370] [4] H. Miyakawa and H. Harashima, "A method of code conversion for digital communication channels with intersymbol interference," *Transactions of the Institute of Electronic*

[00371] [5] R. A. Monziano and T. W. Miller, *Introduction to Adaptive Arrays*, New York: Wiley, 1980.

[00372] [6] Guy E. Bleloch, "Introduction to Data Compression", Carnegie Mellon University Tech. Report Sept. 2010

[00373] [7] A. Duel-Hallen, S. Hu, and H. Hallen, "Long-Range Prediction of Fading Signals," *IEEE Signal Processing Mag.*, vol. 17, no. 3, pp. 62–75, May 2000.

[00374] [8] A. Forenza and R. W. Heath, Jr., "Link Adaptation and Channel Prediction in Wireless OFDM Systems," in *Proc. IEEE Midwest Symp. on Circuits and Sys.*, Aug 2002, pp. 211–214.

[00375] [9] M. Sternad and D. Aronsson, "Channel estimation and prediction for adaptive OFDM downlinks [vehicular applications]," in *Proc. IEEE Vehicular Technology Conference*, vol. 2, Oct 2003, pp. 1283–1287.

[00376] [10] D. Schafhuber and G. Matz, "MMSE and Adaptive Prediction of Time-Varying Channels for OFDM Systems," *IEEE Trans. Wireless Commun.*, vol. 4, no. 2, pp. 593–602, Mar 2005.

[00377] [11] I. C. Wong and B. L. Evans, "Joint Channel Estimation and Prediction for OFDM Systems," in *Proc. IEEE Global Telecommunications Conference*, St. Louis, MO, Dec 2005.

[00378] [12] M. Guillaud and D. Slock, "A specular approach to MIMO frequencyselective channel tracking and prediction," in *Proc. IEEE Signal Processing Advances in Wireless Communications*, July 2004, pp. 59–63.

[00379] [13] Wong, I.C. Evans, B.L., "Exploiting Spatio-Temporal Correlations in MIMO Wireless Channel Prediction", IEEE Globecom Conf., pp.1-5, Dec. 2006

[00380] Embodiments of the invention may include various steps as set forth above. The steps may be embodied in machine-executable instructions which cause a general-purpose or special-purpose processor to perform certain steps. For example, the various components within the Base Stations/APs and Client Devices described above may be implemented as software

6181P526XPCT

executed on a general purpose or special purpose processor. To avoid obscuring the pertinent aspects of the invention, various well known personal computer components such as computer memory, hard drive, input devices, etc., have been left out of the figures.

**[00381]** Alternatively, in one embodiment, the various functional modules illustrated herein and the associated steps may be performed by specific hardware components that contain hardwired logic for performing the steps, such as an application-specific integrated circuit (“ASIC”) or by any combination of programmed computer components and custom hardware components.

**[00382]** In one embodiment, certain modules such as the Coding, Modulation and Signal Processing Logic 903 described above may be implemented on a programmable digital signal processor (“DSP”) (or group of DSPs) such as a DSP using a Texas Instruments’ TMS320x architecture (e.g., a TMS320C6000, TMS320C5000, . . . etc). The DSP in this embodiment may be embedded within an add-on card to a personal computer such as, for example, a PCI card. Of course, a variety of different DSP architectures may be used while still complying with the underlying principles of the invention.

**[00383]** Elements of the present invention may also be provided as a machine-readable medium for storing the machine-executable instructions. The machine-readable medium may include, but is not limited to, flash memory, optical disks, CD-ROMs, DVD ROMs, RAMs, EPROMs, EEPROMs, magnetic or optical cards, propagation media or other type of machine-readable media suitable for storing electronic instructions. For example, the present invention may be downloaded as a computer program which may be transferred from a remote computer (e.g., a server) to a requesting computer (e.g., a client) by way of data signals embodied in a carrier wave or other propagation medium via a communication link (e.g., a modem or network connection).

**[00384]** Throughout the foregoing description, for the purposes of explanation, numerous specific details were set forth in order to provide a thorough understanding of the present system and method. It will be apparent, however, to one skilled in the art that the system and method may be practiced without some of these specific details. Accordingly, the scope and spirit of the present invention should be judged in terms of the claims which follow.

**[00385]** Moreover, throughout the foregoing description, numerous publications were cited to provide a more thorough understanding of the present invention. All of these cited references are incorporated into the present application by reference.

**CLAIMS**

1. A multiuser (MU) multiple antenna system (MAS) comprising:  
one or more centralized units communicatively coupled to multiple distributed transceiver stations or antennas via a network;  
the network comprising wireline or wireless links or a combination of both, employed as a backhaul communication channel;  
the one or more centralized units communication with the distributed transceiver stations or antennas over the network to adaptively reconfigure communications between the distributed transceiver stations or antennas and users to compensate for Doppler effects due to user mobility or changes in the propagation environment; wherein the MU-MAS system comprises one or more sets of user equipment (UE), base transceiver stations (BTSs), controllers (CTRs), centralized processors (CPs) and base station networks (BSNs); and  
wherein the CP adaptively selects the BTSs to be used for low- or high- mobility UEs based on latency over the BSN.
2. The system as in claim 1 employing distributed antennas that exploits spatial, polarization and/or pattern diversity to enhance data rate and/or coverage to one or multiple users in wireless systems.
3. The system as in claim 1 wherein the UEs are located around or in between the distributed antennas or surrounded by the distributed antennas.
4. The system as in claim 1 wherein MU-MAS employs complex weights at the receiver of the uplink channel to demodulate independent streams (e.g. data or CSI) from the UEs.
5. The system as in claim 4 wherein the complex weights of the uplink receiver are derived from the downlink precoding weights or computed via maximum ratio combining receiver.
6. The system as in claim 1 wherein the CP and the BTSs are equipped with encoders/decoders to compress/decompress information exchanged among them over the BSN.

7. The system in claim 6 wherein the precoded baseband data streams are compressed, before being transmitted from/to the BTS to/from the MU-MAS distributed antennas, to reduce overhead over the BSN.

8. The system as in claim 1 wherein the adaptation is based on the type of high versus low data rate BSN, or QoS, or average traffic statistics (e.g., daytime or nighttime use of different networks), or instantaneous traffic statistics (e.g., temporary network congestions) over the BSN.

9. A method implemented within a multiuser (MU) multiple antenna system (MAS) to compensate for Doppler effects comprising, the MU-MAS system comprising at least one centralized unit communicatively coupled to multiple distributed base transceiver stations (BTSs) over a network, the method comprising:

measuring Doppler velocity of a first mobile user relative to the plurality of BTSs; and

the centralized unit communicating with the BTSs over the network to adaptively reconfigure communications between the BTSs and users, wherein adaptively reconfiguring includes dynamically assigning the first mobile user to a first BTS of the plurality of BTSs or to a first set of BTSs based on the measured Doppler velocity for the first BTS relative to other BTSs.

10. The method as in claim 9 wherein if the first mobile user has a measured Doppler velocity which is relatively higher than a second mobile user, then dynamically assigning comprises assigning the first mobile user to a first BTS or to a first set of BTSs and assigning the second mobile user to a second BTS or to a second set of BTSs, the first BTS or the first set of BTSs having a relatively lower latency associated therewith than the second BTS or second set of BTSs.

11. The method as in claim 9 wherein the latency includes (a) time taken to transmit a first training signal from the first mobile user to a BTS, (b) round-trip delay over a base station network (BSN) connecting the BTSs to a centralized processor (CP), and (c) time taken by the CP to process channel state information (CSI) for the wireless channel between the BTSs and the first mobile user, generate precoded data streams for the first mobile user based on the CSI, and schedule transmissions to different mobile users including the first user for the current transmission.

12. The method as in claim 11 wherein the latency further includes time taken to transmit a second training signal from the BTS to the first mobile user.

13. The method as in claim 9 wherein dynamically assigning further comprises assigning based on a combination of link quality of a communication channel between each BTS and the first mobile user and the measured Doppler velocity associated with each BTS with respect to the first user.

14. The method as in claim 13 wherein, for a given Doppler velocity, the BTS having the relatively higher link quality is selected.

15. The method as in claim 13 wherein for a given link quality, the BTS having the relatively lower Doppler velocity is selected.

16. The method as in claim 9 further comprising:

estimating future complex channel coefficients based on past complex channel coefficients to compensate for the adverse effect of Doppler on communication between the BTSs and the first mobile user.

17. The method as in claim 16 wherein linear prediction is employed for estimation.

18. The method as in claim 9 wherein the first mobile user is dynamically assigned to the first BTS or a first set of BTSs based on both the Doppler velocity and channel state information (CSI) defining quality of communication channels between the mobile user and each of the BTSs within the plurality.

19. The method as in claim 18 further comprising:

building a matrix of Doppler velocities and link qualities for each of the BTSs within the plurality with respect to the first mobile user; and

selecting a BTS which has a Doppler velocity below a specified threshold and link quality above a specified threshold.

20. A multiuser (MU) multiple antenna system (MAS) to compensate for Doppler effects comprising:

a plurality of base transceiver stations (BTSs);

a network coupling the plurality of BTSs to at least one centralized processor (CP);

a first mobile user establishing a communication link with each of the BTSs;

the centralized processor (CP) communicating with the BTSS over the network to adaptively reconfigure communications between the BTSS and users, wherein adaptively reconfiguring includes measuring Doppler velocity of a first mobile user relative to each of the BTSS and dynamically assigning the first mobile user to a first BTSS of the plurality of BTSS based on the measured Doppler velocity for the first BTSS relative to other BTSS.

21. The system as in claim 20 wherein if the first mobile user has a measured Doppler velocity which is relatively higher than a second mobile user, then dynamically assigning comprises assigning the first mobile user to a first BTSS and assigning the second mobile user to a second BTSS, the first BTSS having a relatively lower latency associated therewith than the second BTSS.

22. The system as in claim 20 wherein the latency includes (a) time taken to transmit a first training signal from the first mobile user to a BTSS, (b) round-trip delay over a base station network (BSN) connecting the BTSS to a centralized processor (CP), and (c) time taken by the CP to process channel state information (CSI) for the wireless channel between the BTSS and the first mobile user, generate precoded data streams for the first mobile user based on the CSI, and schedule transmissions to different mobile users including the first user for the current transmission.

23. The system as in claim 22 wherein the latency further includes time taken to transmit a second training signal from the BTSS to the first mobile user.

24. The system as in claim 20 wherein dynamically assigning further comprises assigning based on a combination of link quality of a communication channel between each BTSS and the first mobile user and the measured Doppler velocity associated with each BTSS with respect to the first user.

25. The system as in claim 24 wherein, for a given Doppler velocity, the BTSS having the relatively higher link quality is selected.

26. The system as in claim 24 wherein for a given link quality, the BTSS having the relatively lower Doppler velocity is selected.

## 6181P526XPCT

27. The system as in claim 20 wherein the CP estimates future complex channel coefficients based on past complex channel coefficients to compensate for the adverse effect of Doppler on communication between the BTSs and the first mobile user.

28. The system as in claim 27 wherein linear prediction is employed for estimation.

29. The system as in claim 20 wherein the first mobile user is dynamically assigned to the first BTS based on both the Doppler Velocity and channel state information (CSI) defining quality of communication channels between the mobile user and each of the BTSs within the plurality.

30. The system as in claim 29 wherein the CP performs the additional operations of:  
building a matrix of Doppler velocities and link qualities for each of the BTSs within the plurality with respect to the first mobile user; and  
selecting a BTS which has a Doppler velocity below a specified threshold and link quality above a specified threshold.

31. A multiuser (MU) multiple antenna system (MAS) comprising:  
one or more centralized units communicatively coupled to multiple distributed transceiver stations or antennas via a network;  
the network comprising wireline or wireless links or a combination of both, employed as a backhaul communication channel;  
the one or more centralized units communicating with the distributed transceiver stations or antennas over the network to adaptively reconfigure communications between the distributed transceiver stations or antennas and users to compensate for Doppler effects due to user mobility or changes in the propagation environment;  
wherein the MU-MAS system comprises one or more sets of user equipment (UE), base transceiver stations (BTSs), controllers (CTRs), centralized processors (CPs) and base station networks (BSNs); and

wherein the CP adaptively selects the BTSs to be used for low- or high-mobility UEs based on the Doppler velocities of every BTS-UE link.

32. The system as in claim 31 employing distributed antennas that exploits spatial, polarization and/or pattern diversity to enhance data rate and/or coverage to one or multiple users in wireless systems.

33. The system as in claim 31 wherein the UEs are located around or in between the distributed antennas or surrounded by the distributed antennas.

34. The system as in claim 31 wherein MU-MAS employs complex weights at the receiver of the uplink channel to demodulate independent streams (e.g. data or CSI) from the UEs.

35. The system as in claim 34 wherein the complex weights of the uplink receiver are derived from the downlink precoding weights or computed via maximum ratio combining receiver.

36. The system as in claim 31 wherein the CP and the BTSs are equipped with encoders/decoders to compress/decompress information exchanged among them over the BSN.

37. The system in claim 36 wherein the precoded baseband data streams are compressed, before being transmitted from/to the BTS to/from the MU-MAS distributed antennas, to reduce overhead over the BSN.

38. A multiuser (MU) multiple antenna system (MAS) comprising:

one or more centralized units communicatively coupled to multiple distributed transceiver stations or antennas via a network;

the network comprising wireline or wireless links or a combination of both, employed as a backhaul communication channel;

the one or more centralized units communicating with the distributed transceiver stations or antennas over the network to adaptively reconfigure communications between the distributed transceiver stations or antennas and users to compensate for Doppler effects due to user mobility or changes in the propagation environment;

wherein the MU-MAS system comprises one or more sets of user equipment (UE), base transceiver stations (BTSs), controllers (CTRs), centralized processors (CPs) and base station networks (BSNs); and

wherein linear prediction is employed to estimate the CSI or MU-MAS precoding weights in the future, thereby eliminating the adverse effect of Doppler on the performance of the MU-MAS.

39. The system as in claim 38 wherein the linear prediction is employed in the time, frequency and/or space domains.

40. The system as in claim 38 employing distributed antennas that exploits spatial, polarization and/or pattern diversity to enhance data rate and/or coverage to one or multiple users in wireless systems.

41. The system as in claim 38 wherein the UEs are located around or in between the distributed antennas or surrounded by the distributed antennas.

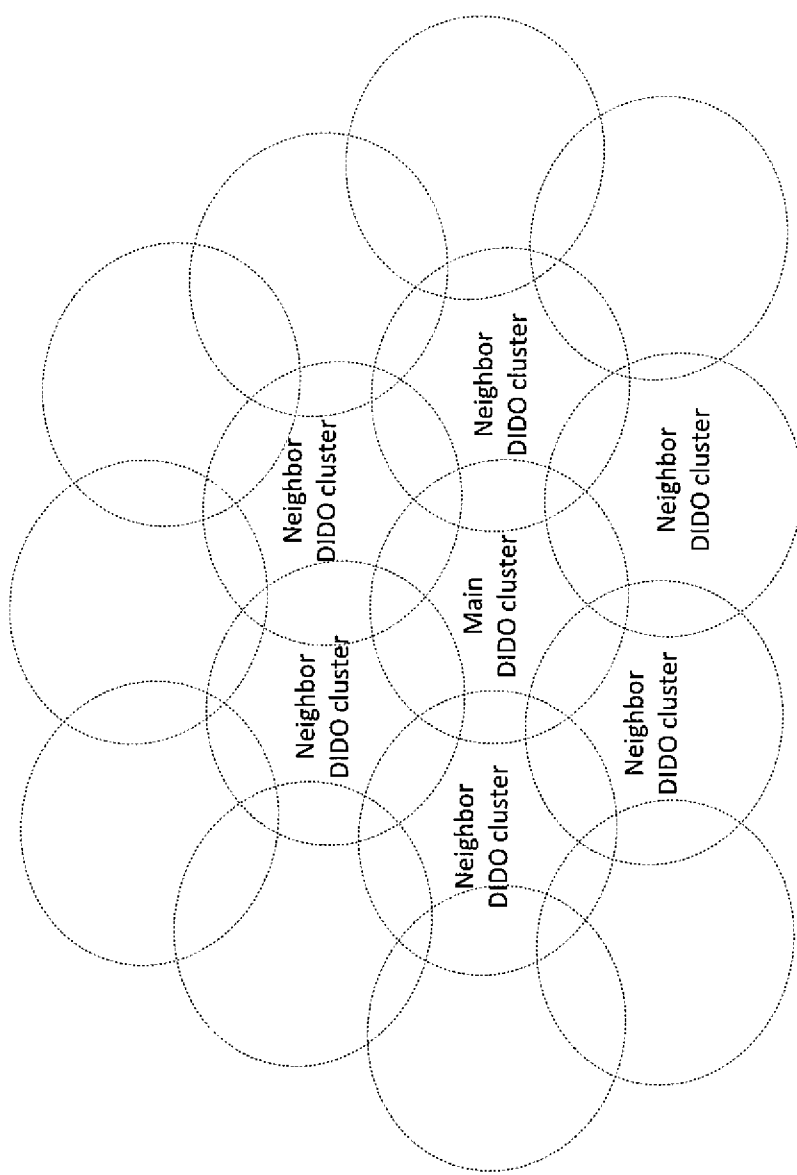
## 6181P526XPCT

42. The system as in claim 38 wherein MU-MAS employs complex weights at the receiver of the uplink channel to demodulate independent streams (e.g. data or CSI) from the UEs.

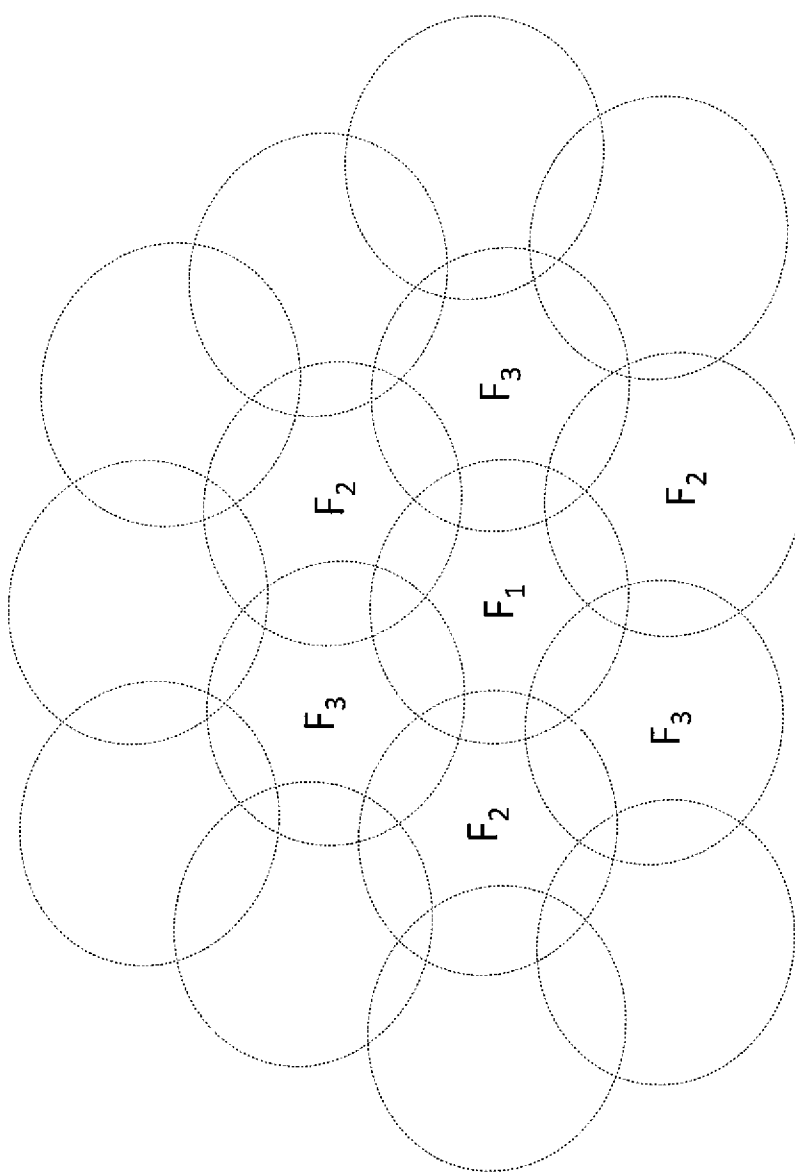
43. The system as in claim 42 wherein the complex weights of the uplink receiver are derived from the downlink precoding weights or computed via maximum ratio combining receiver.

44. The system as in claim 38 wherein the CP and the BTSSs are equipped with encoders/decoders to compress/decompress information exchanged among them over the BSN.

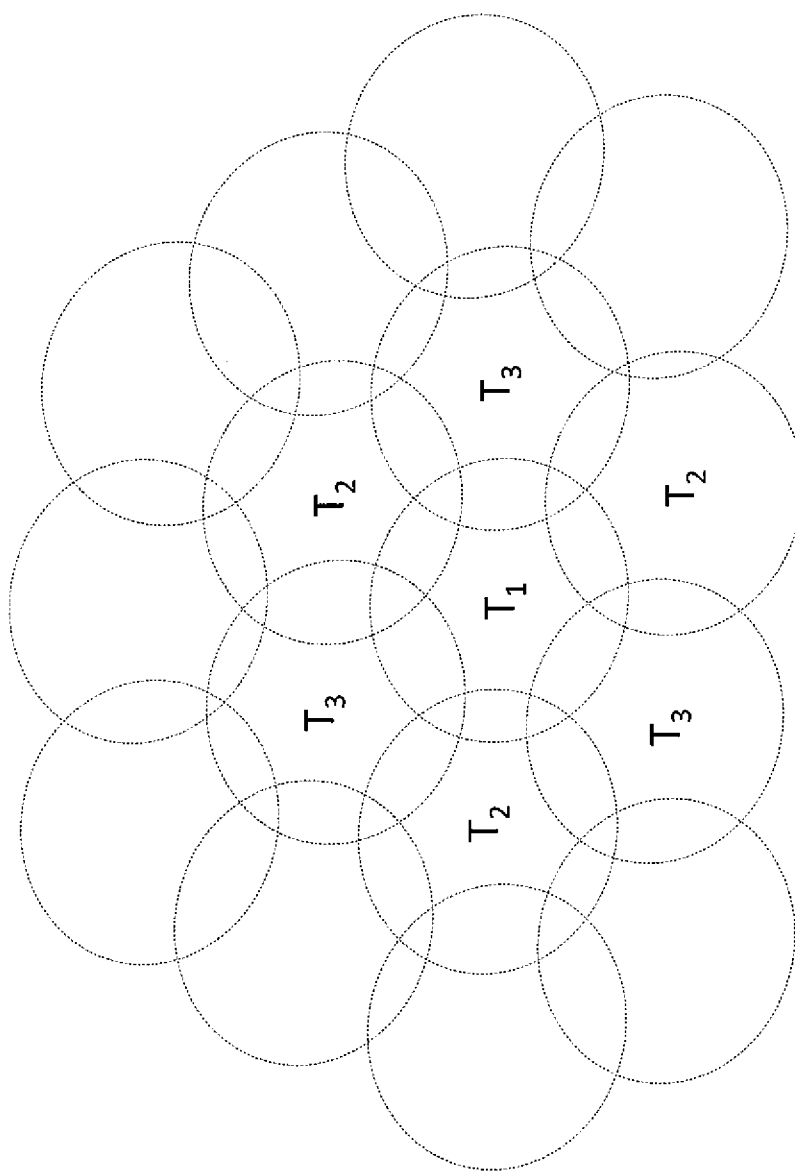
45. The system in claim 44 wherein the precoded baseband data streams are compressed, before being transmitted from/to the BTS to/from the MU-MAS distributed antennas, to reduce overhead over the BSN.



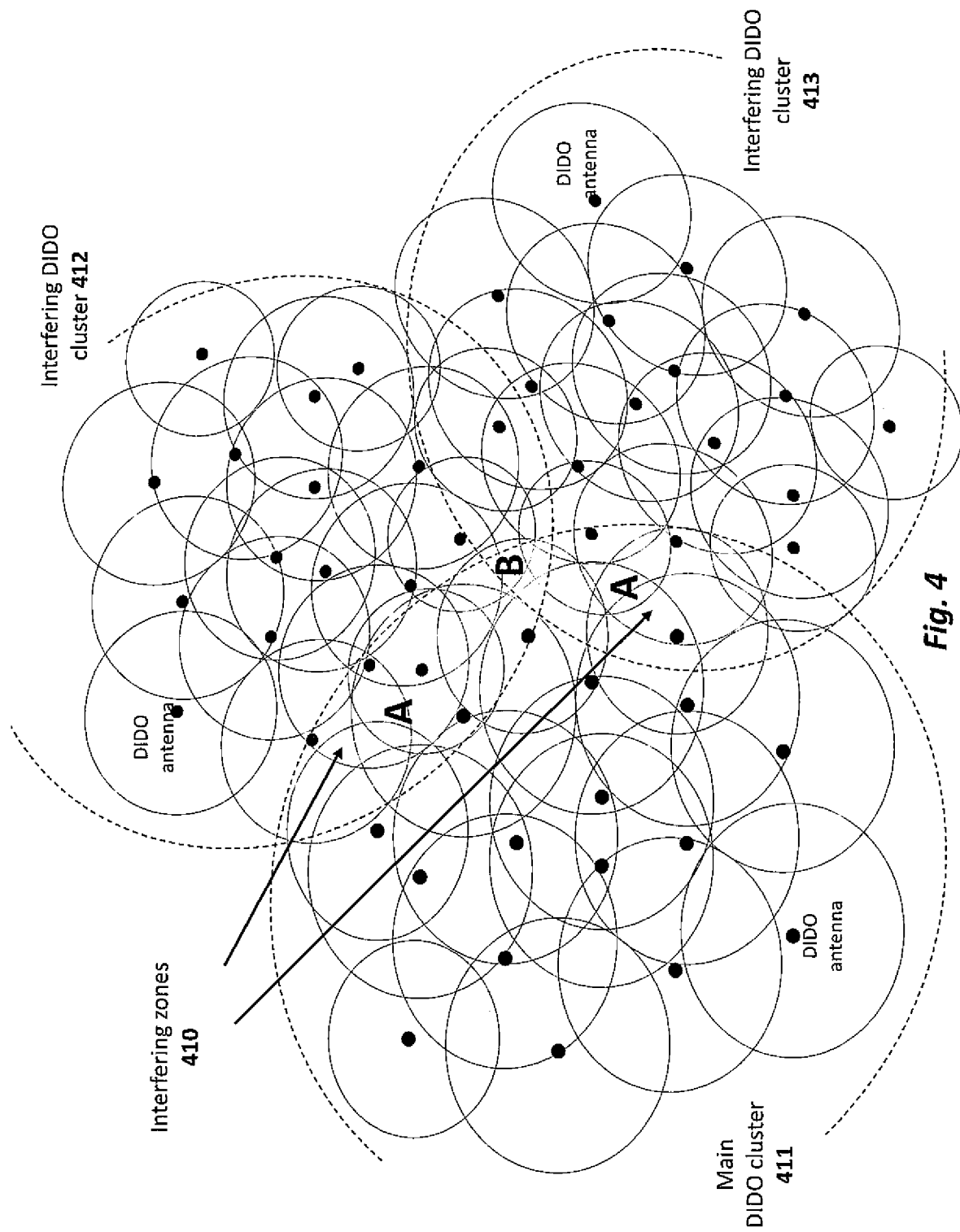
**Fig. 1**



*Fig. 2*



*Fig. 3*



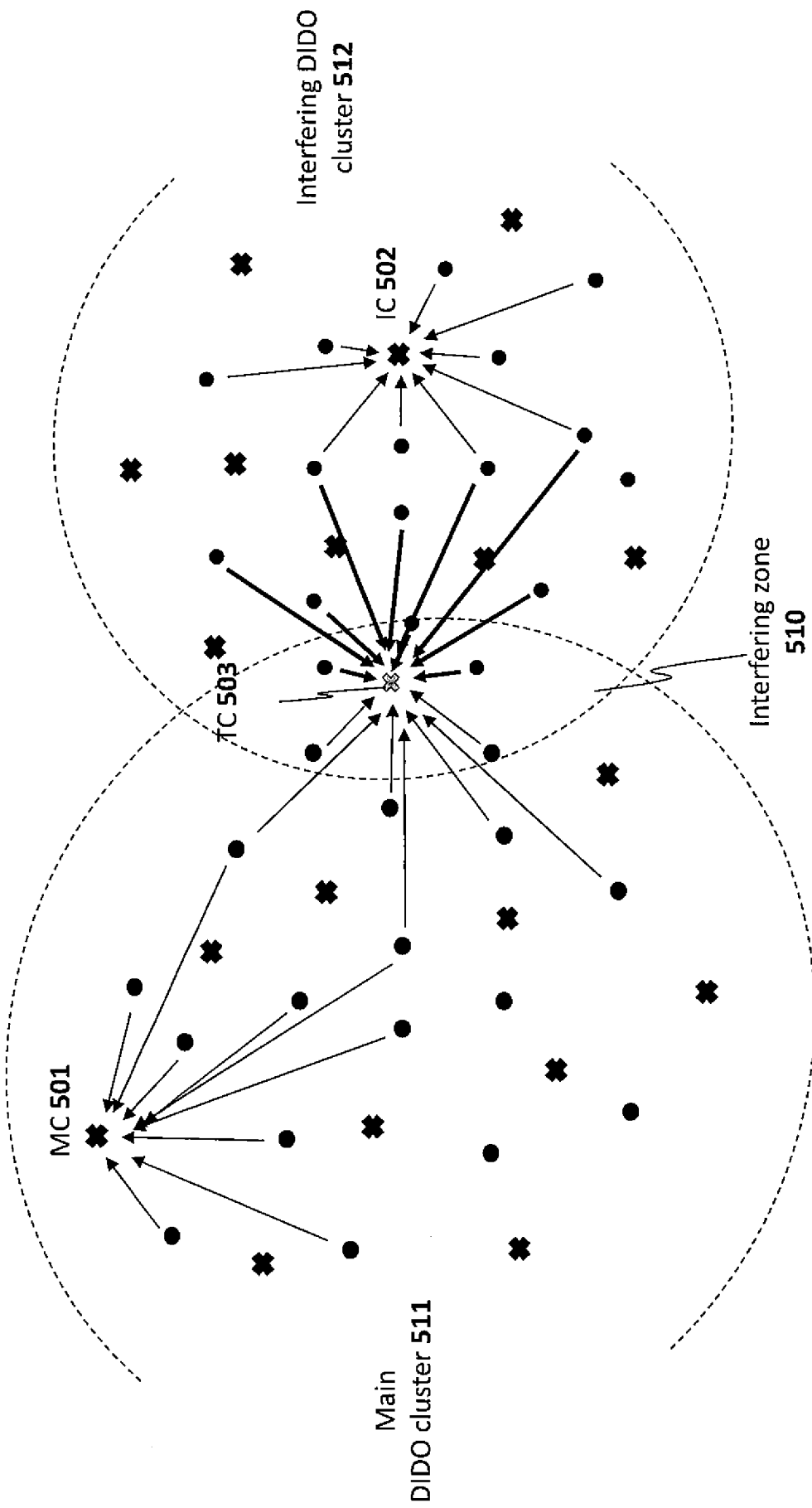


**Fig. 5**

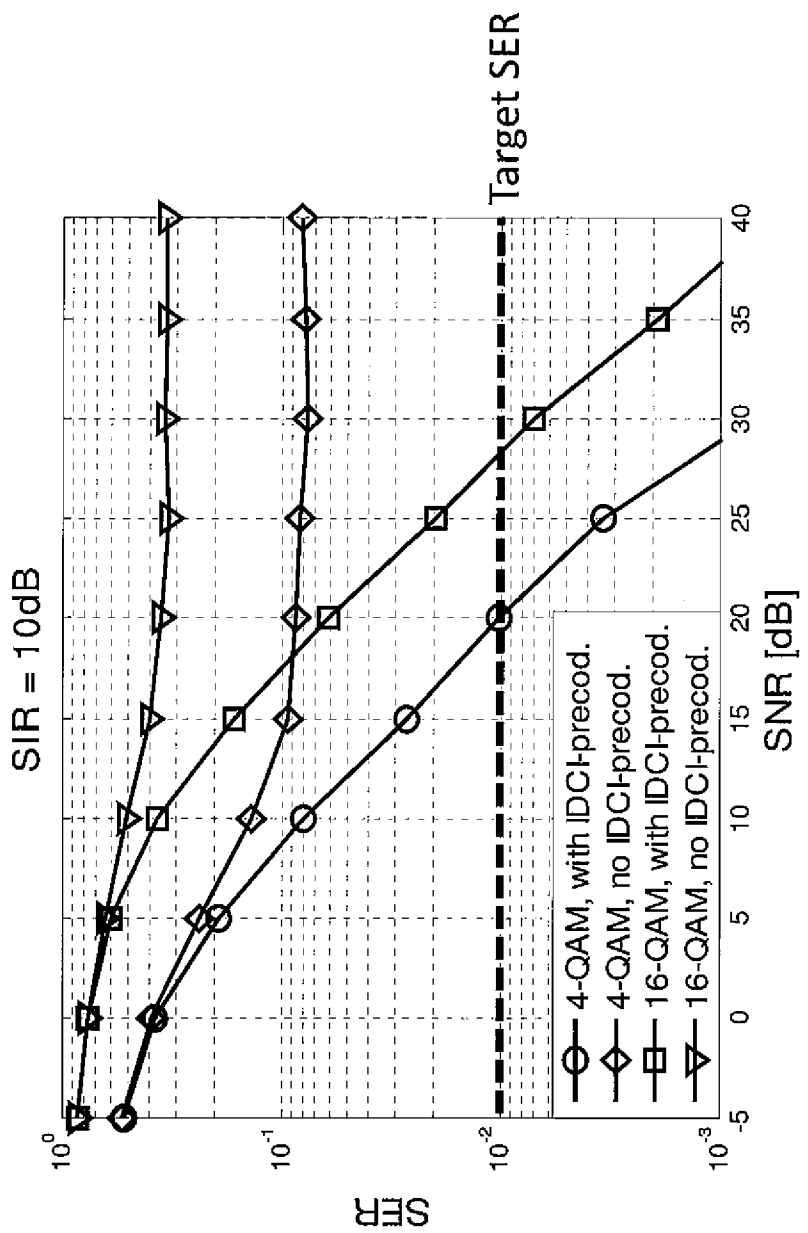


**Fig. 6**

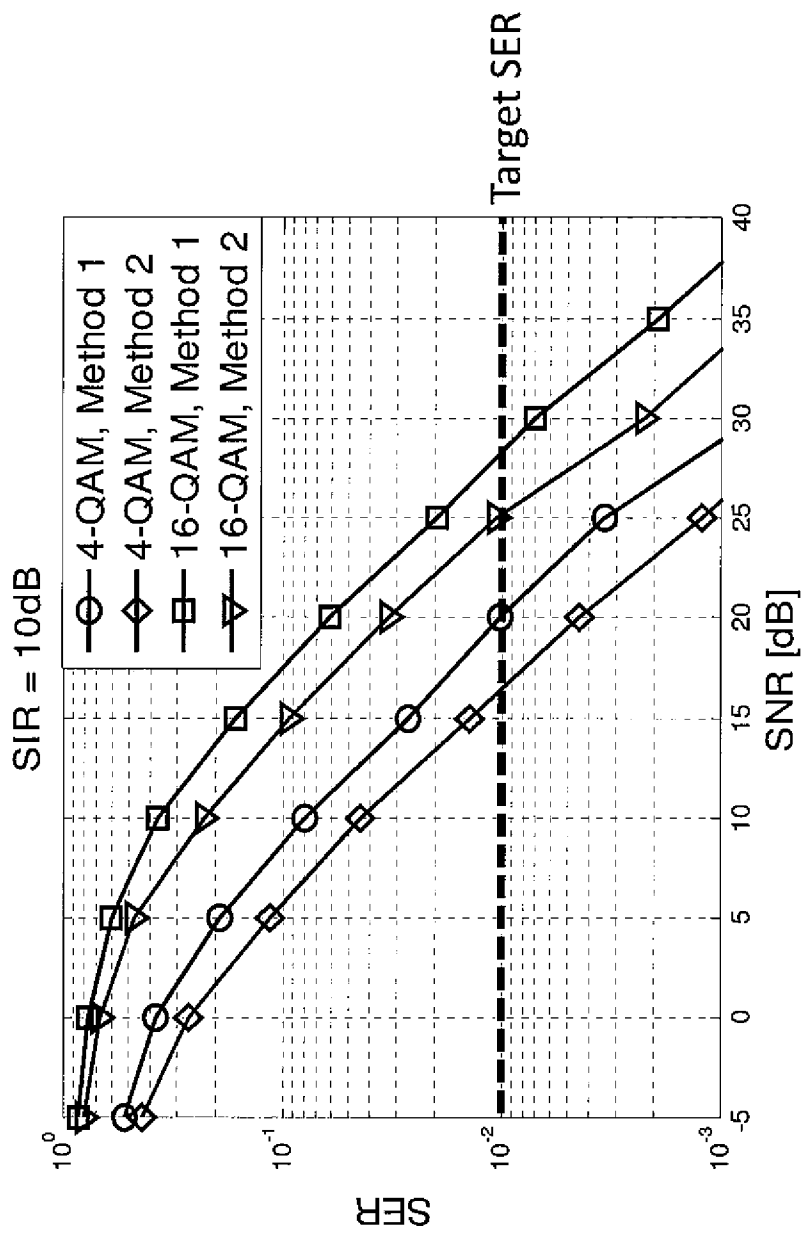


*Fig. 7*

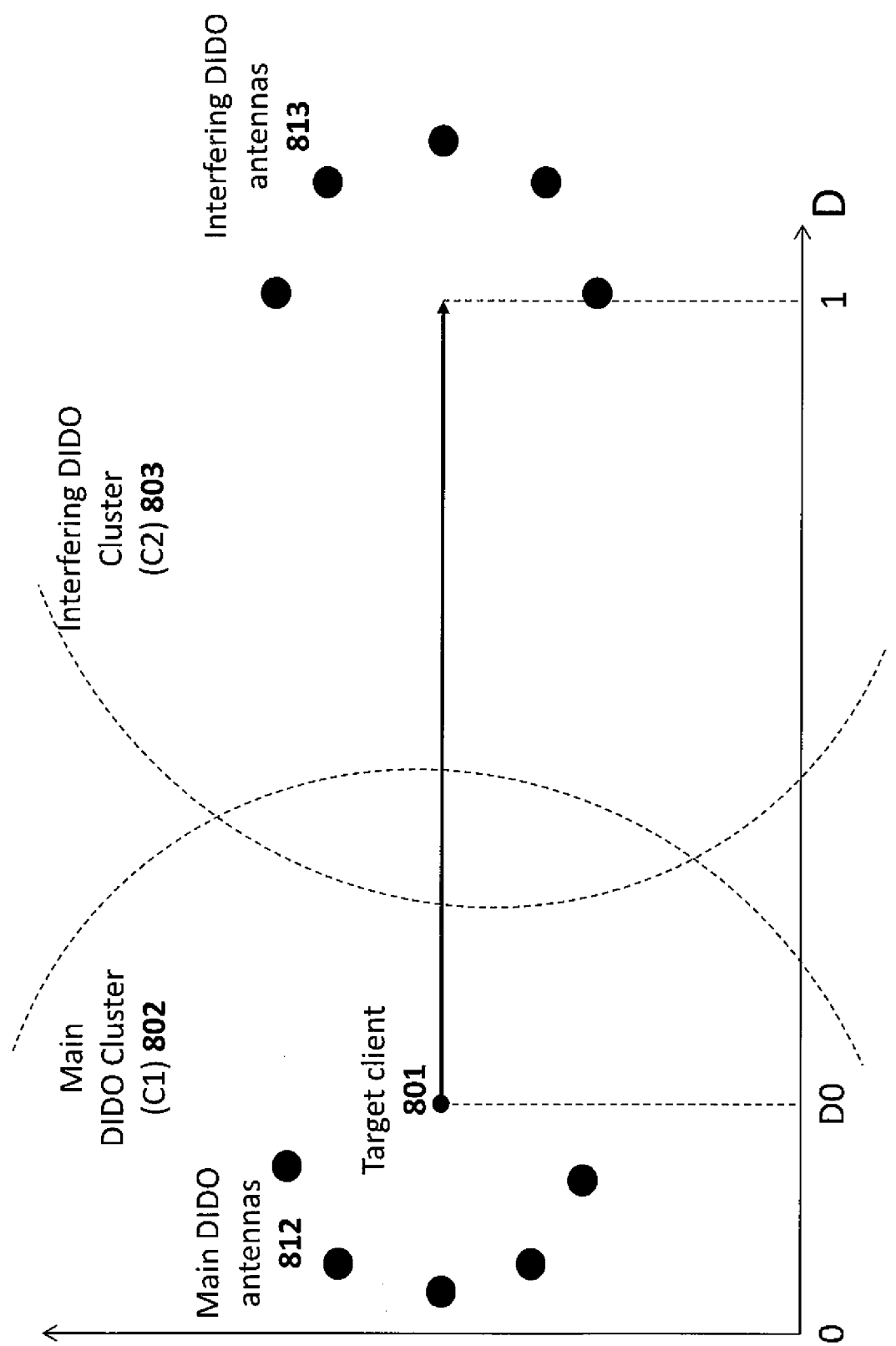


*Fig. 8*

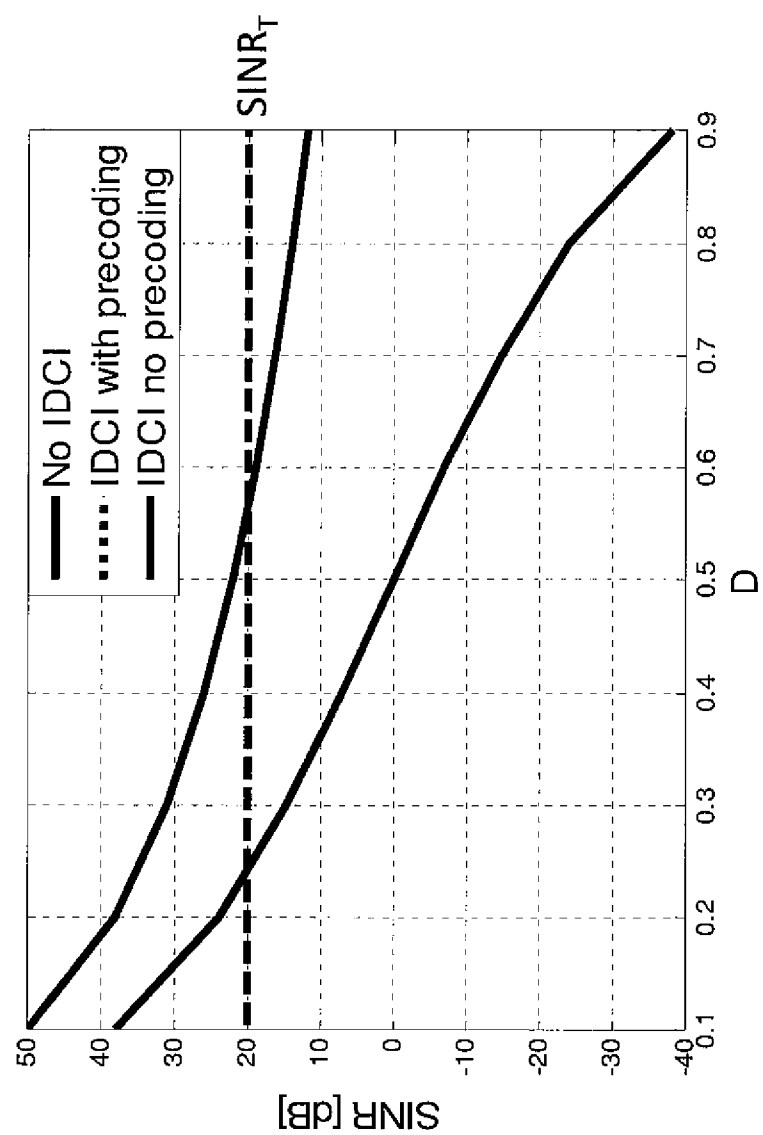
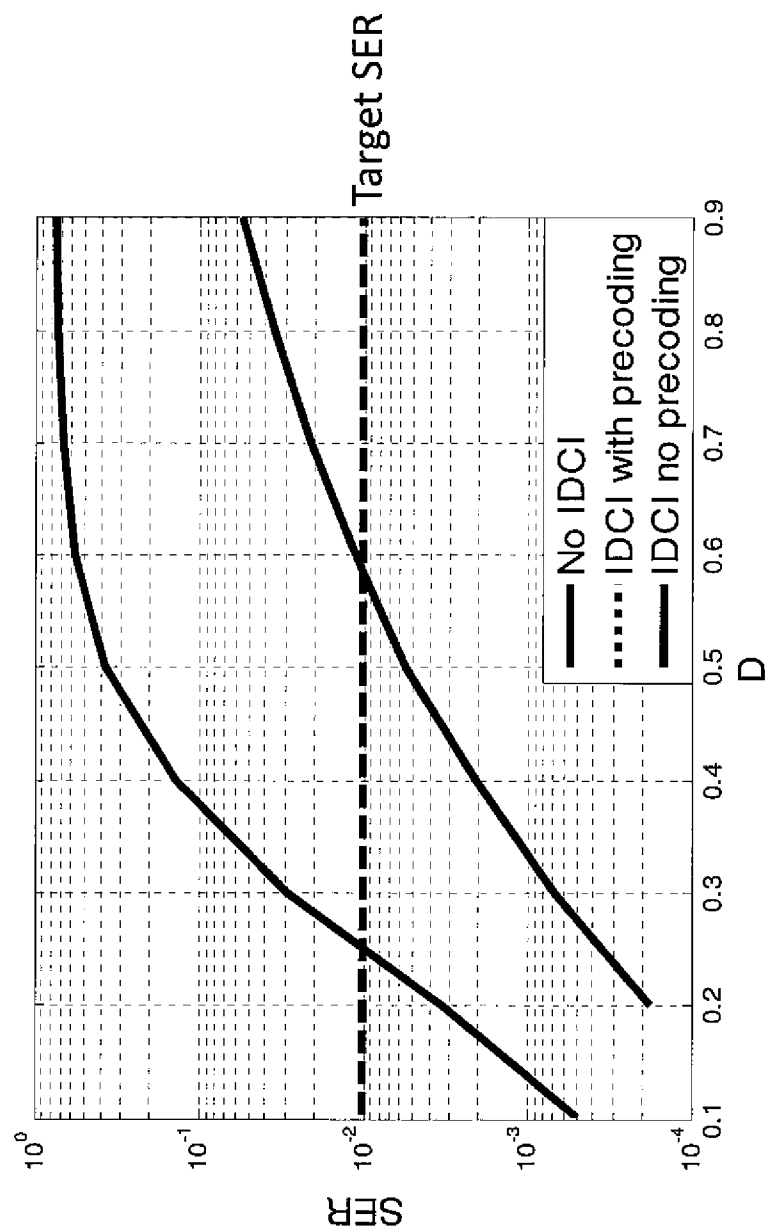
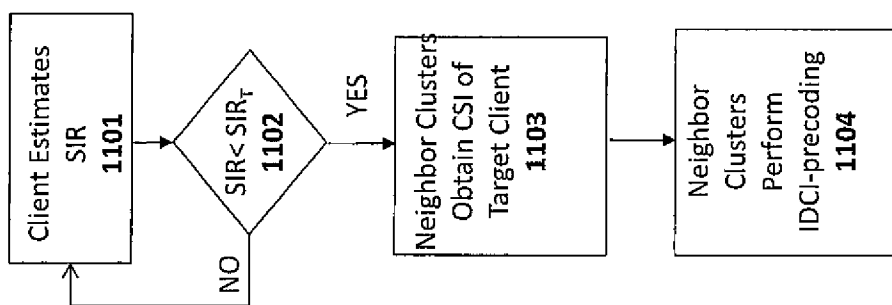


Fig. 9



*Fig. 10*



**Fig. 11**

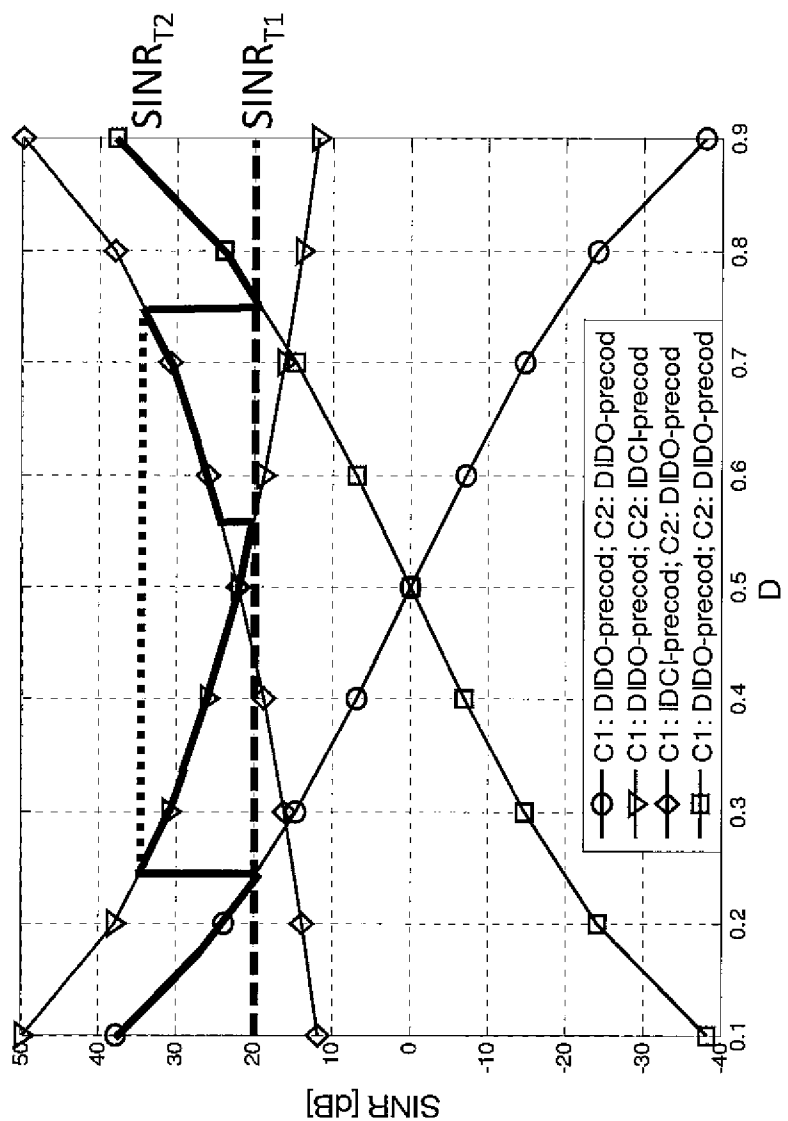


**Fig. 12**

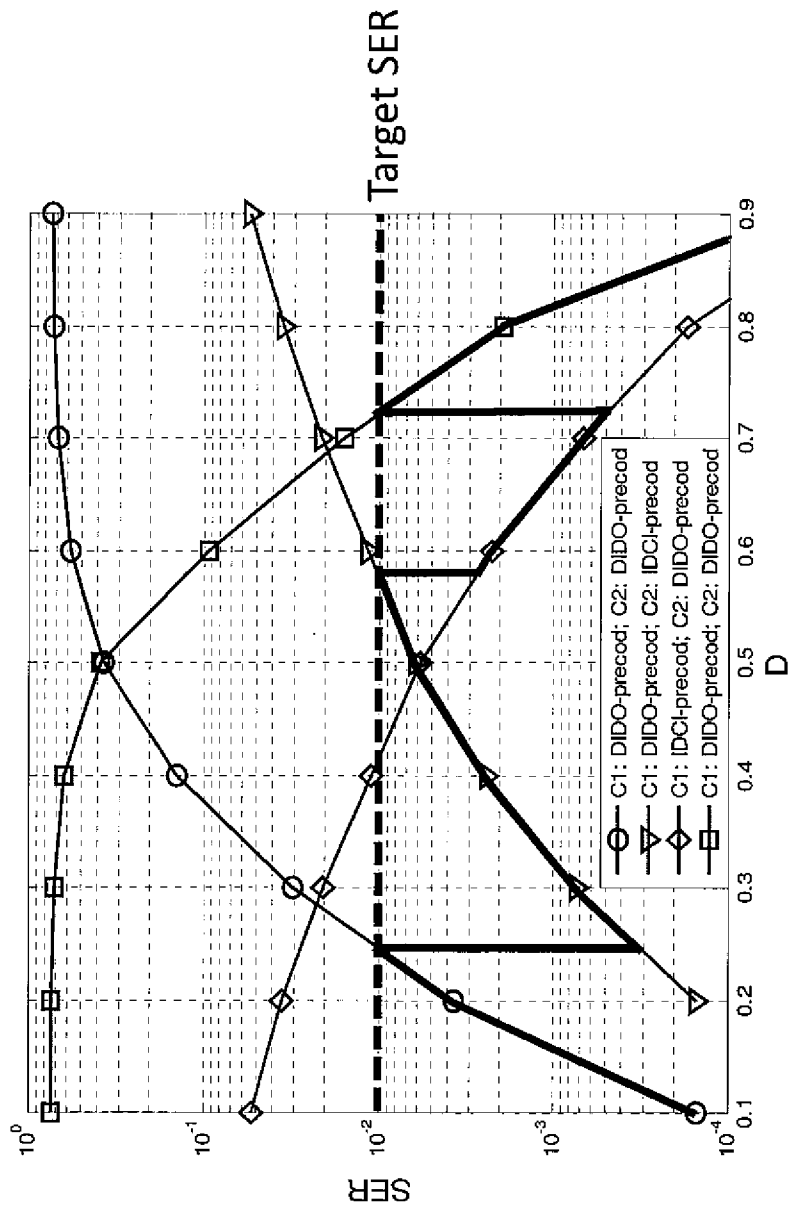
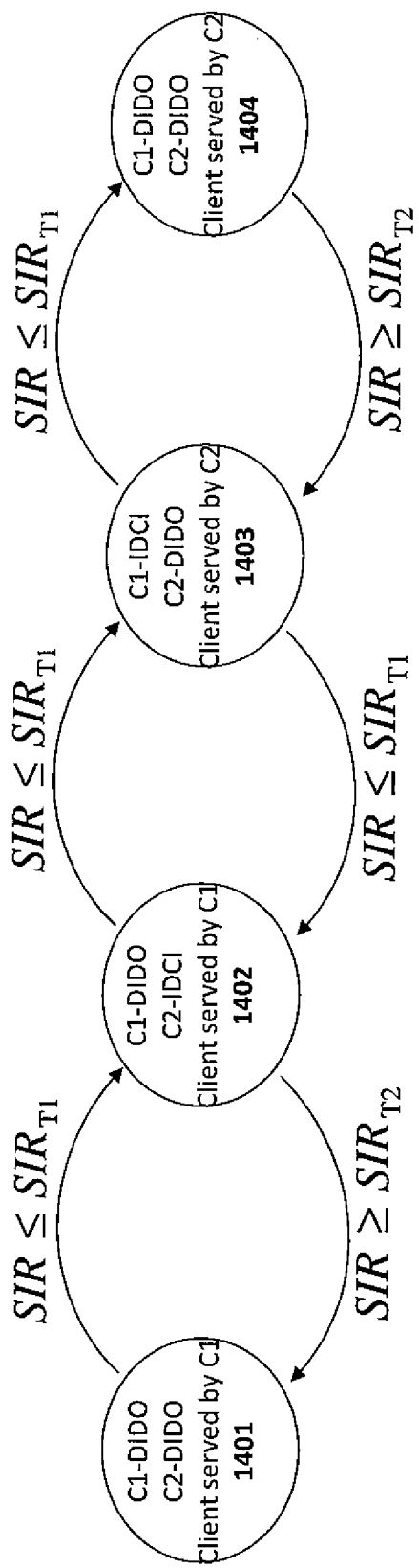


Fig. 13



**Fig. 14**

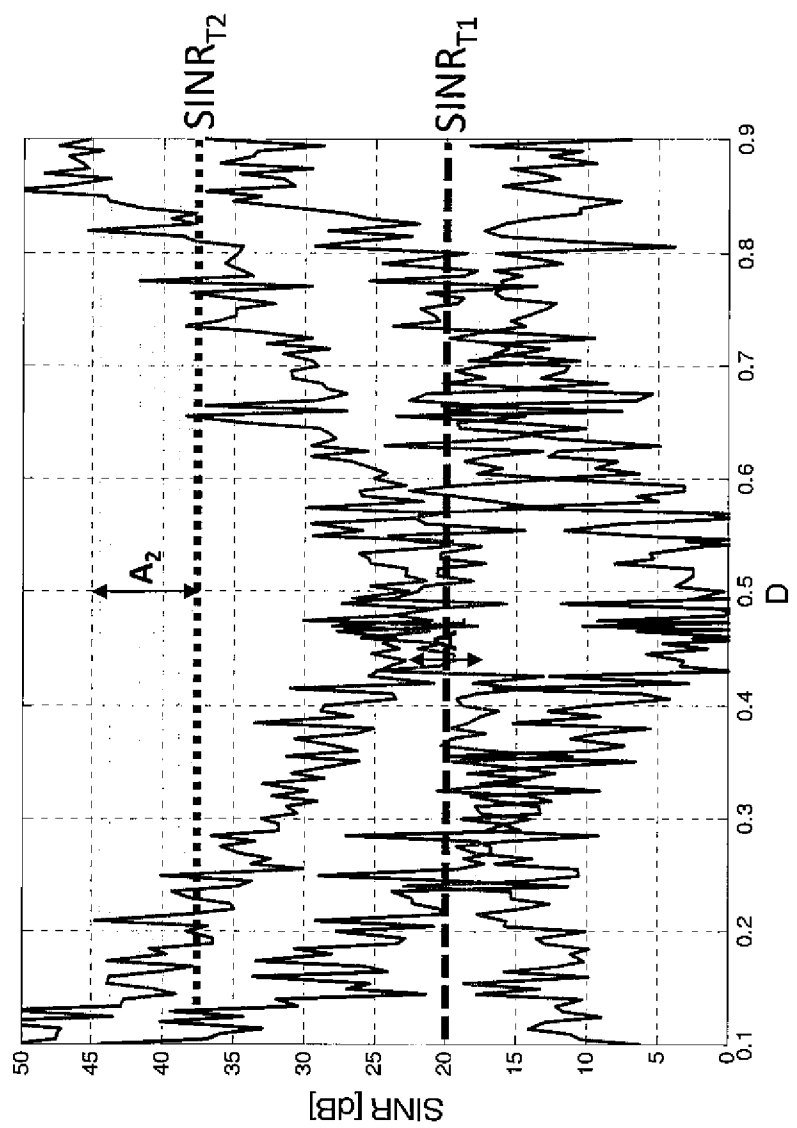
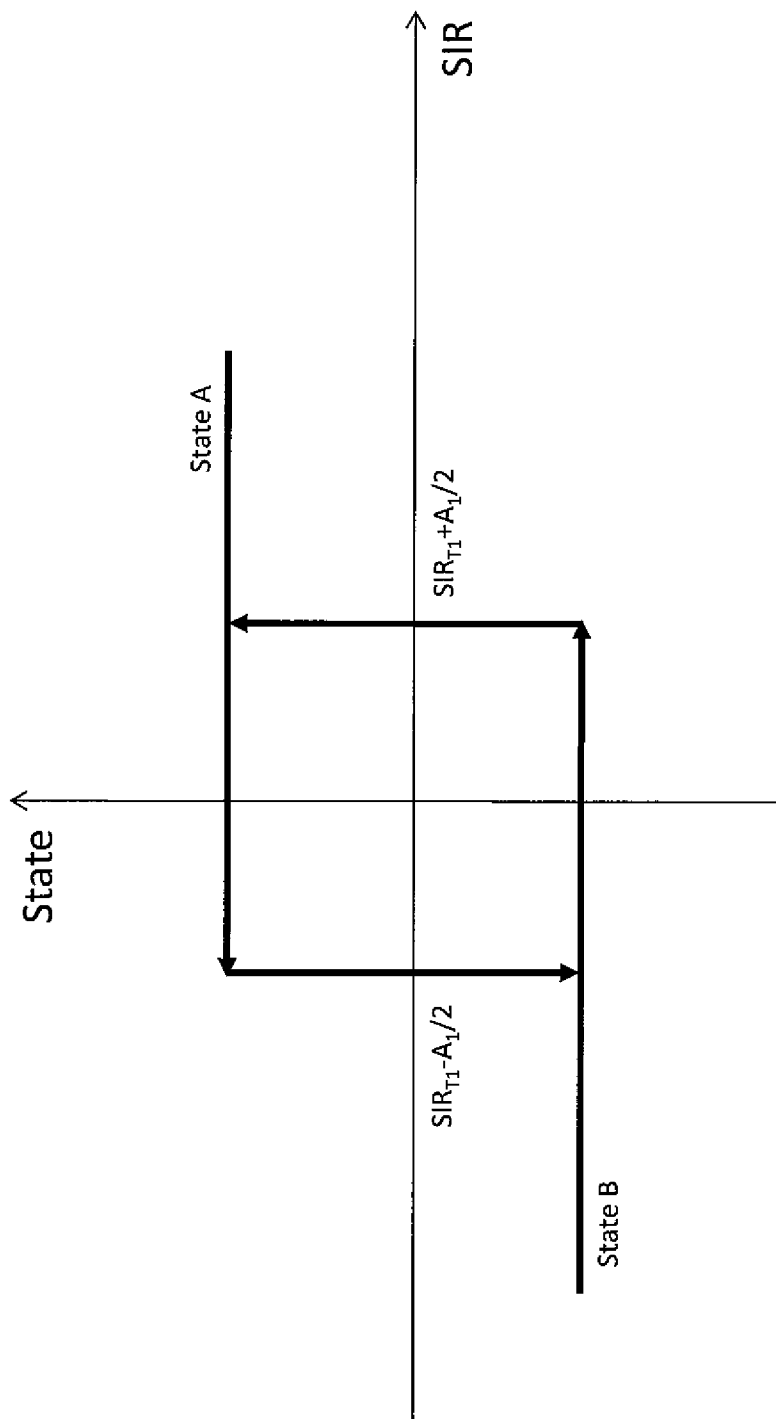
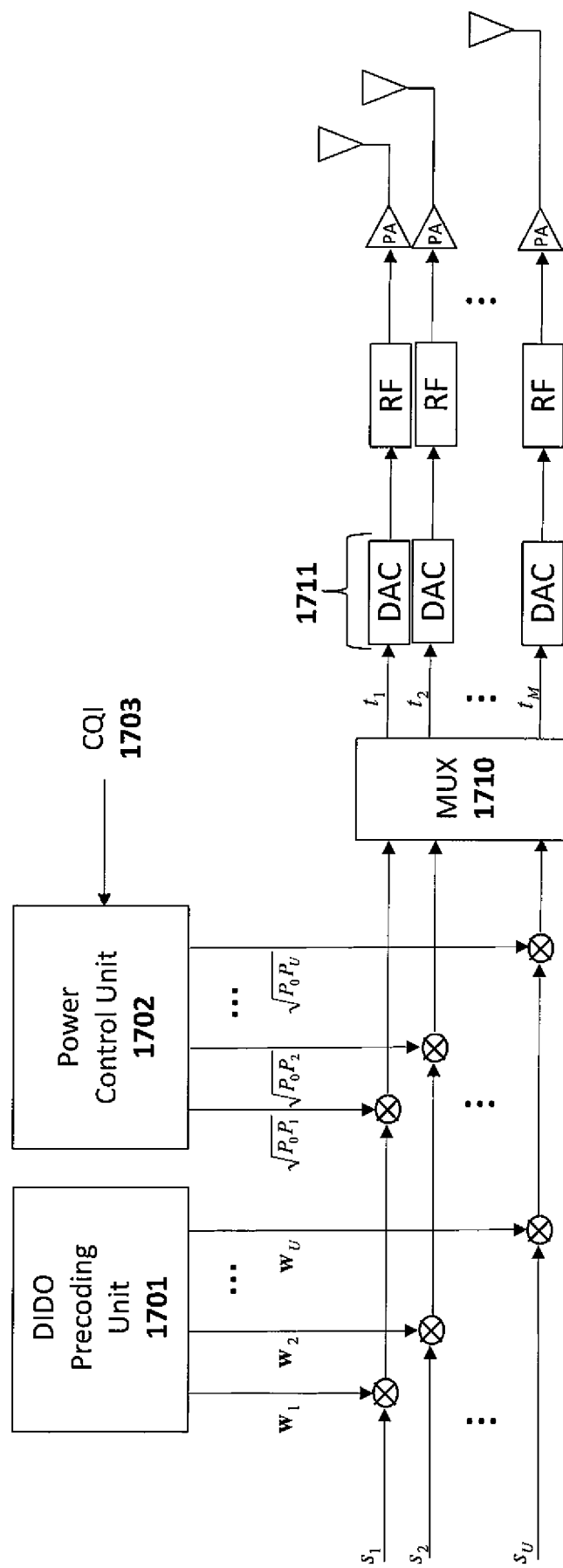


Fig. 15



*Fig. 16*

*Fig. 17*

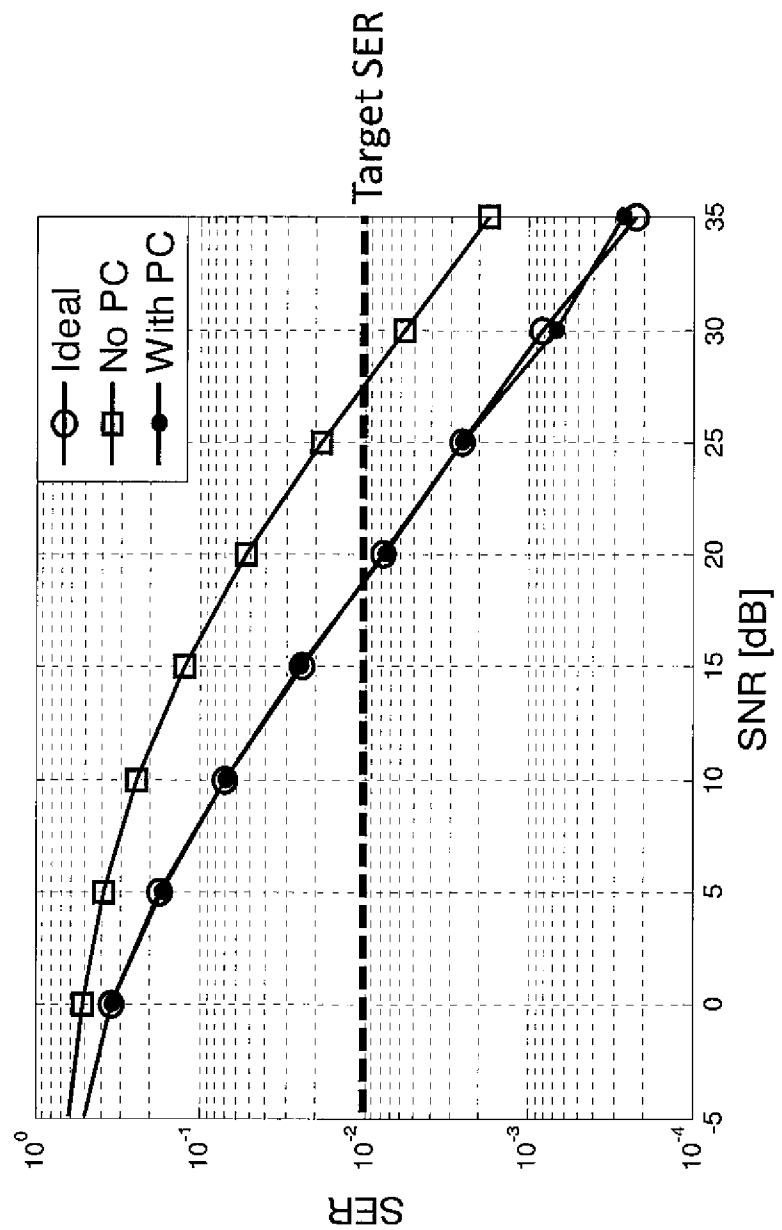


Fig. 18

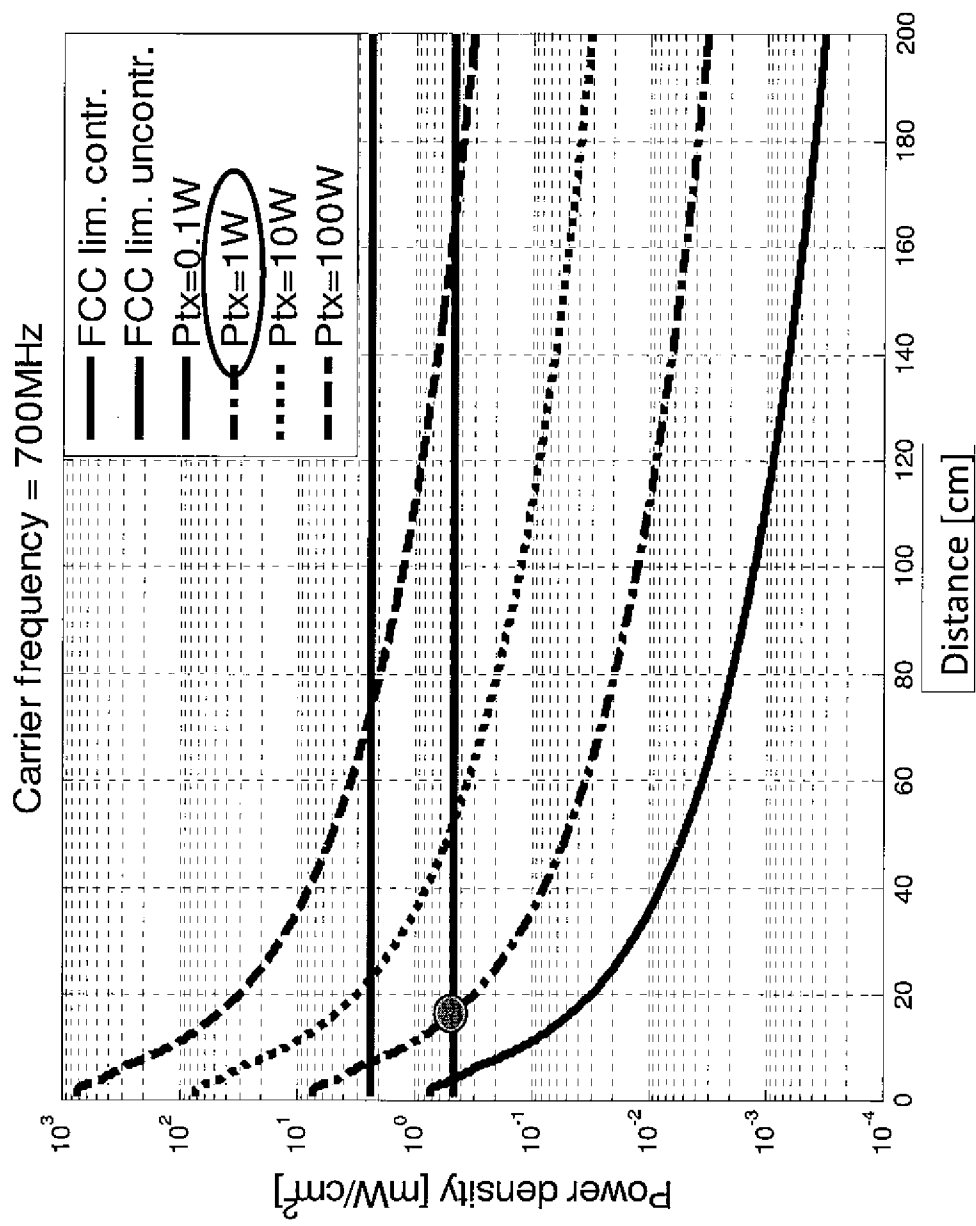
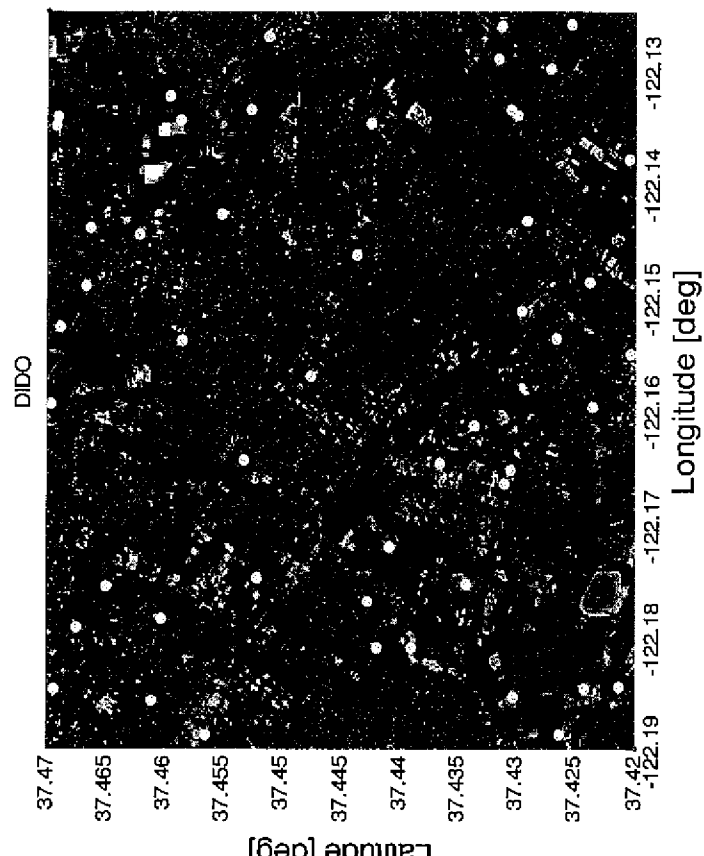


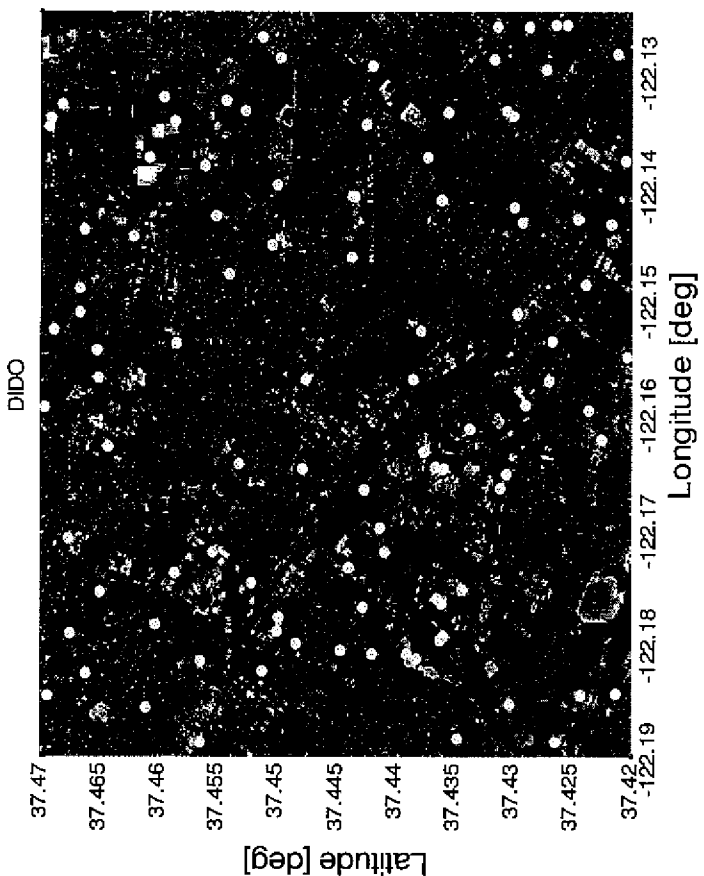
Fig. 19

$N_{HP}=50, N_{LP}=50$

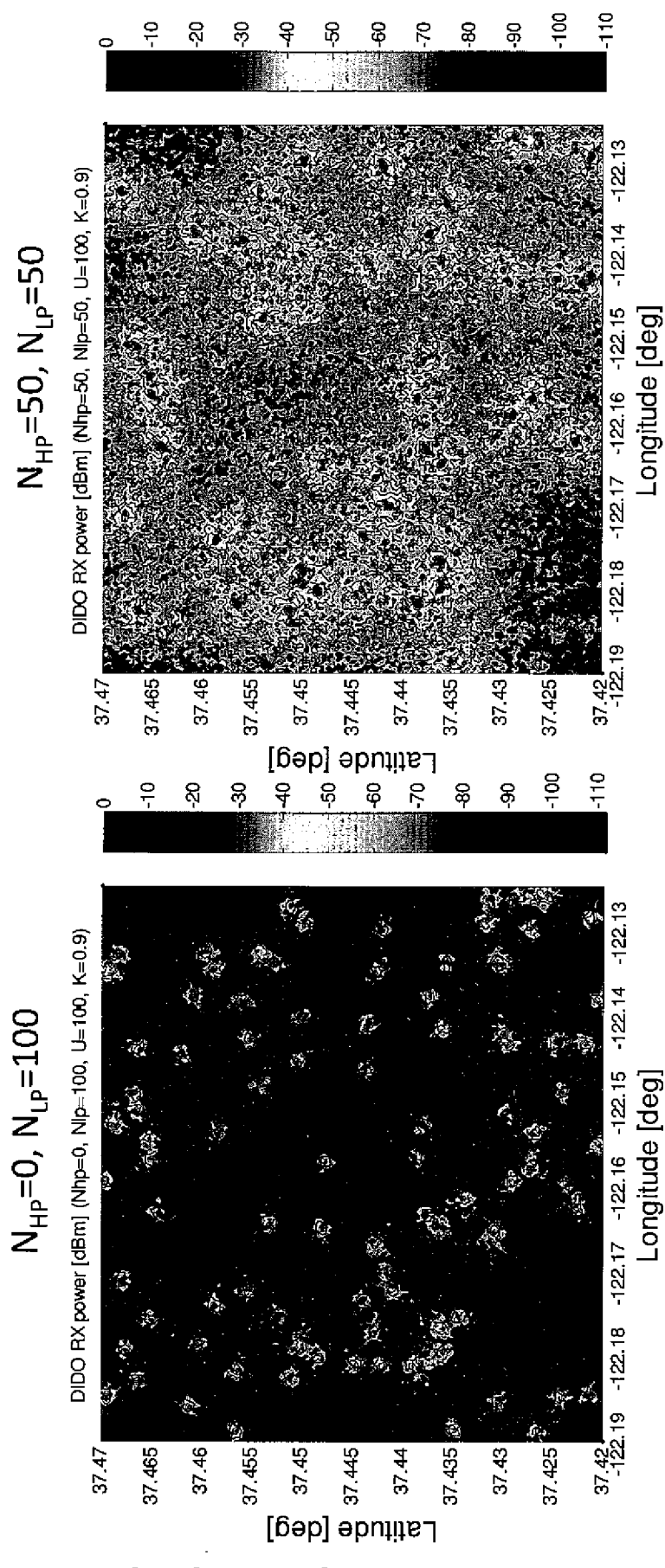


**Fig. 20b**

$N_{HP}=0, N_{LP}=100$



**Fig. 20a**

**Fig. 21a****Fig. 21b**

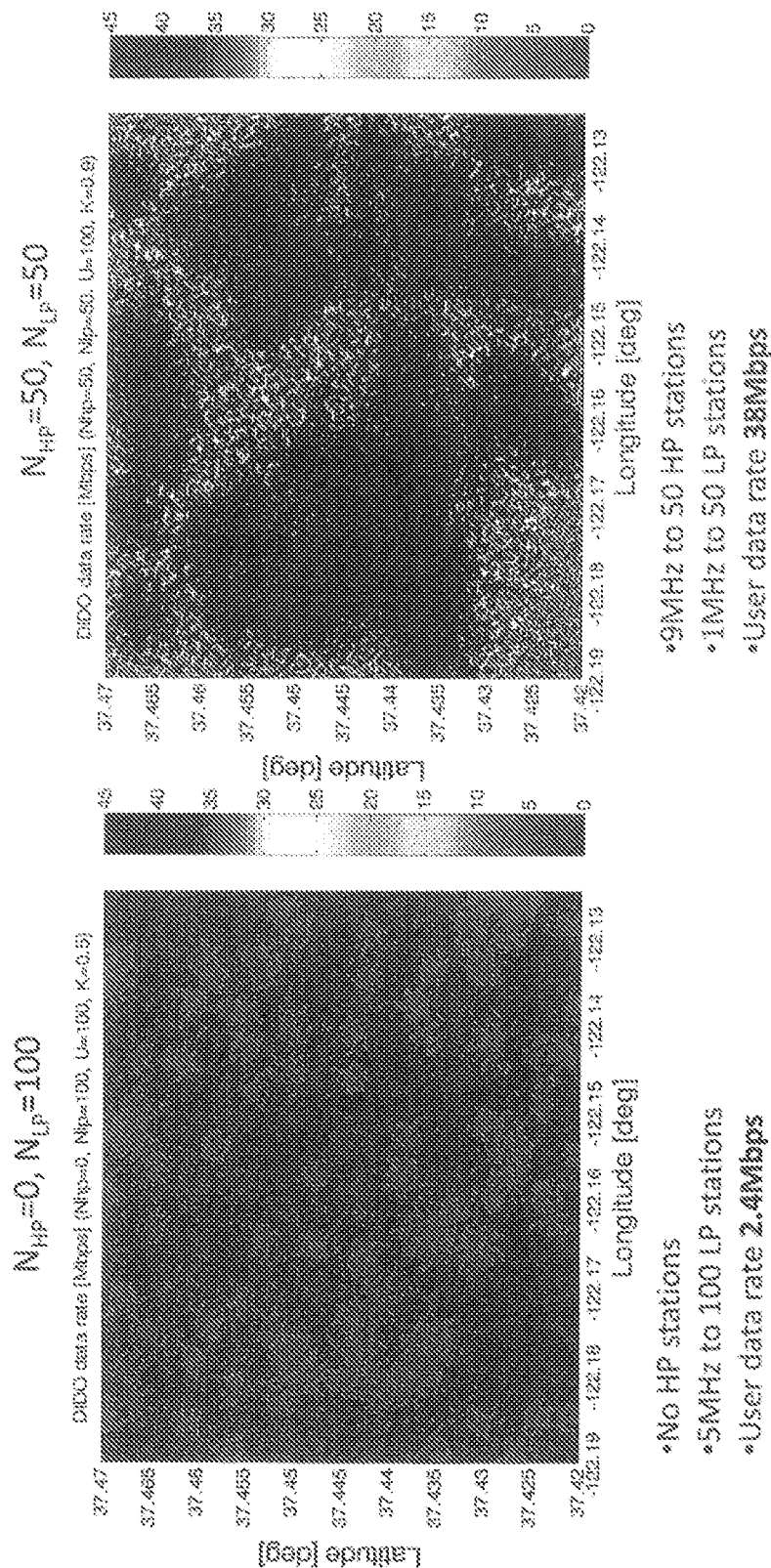


Fig. 22a

Fig. 22b

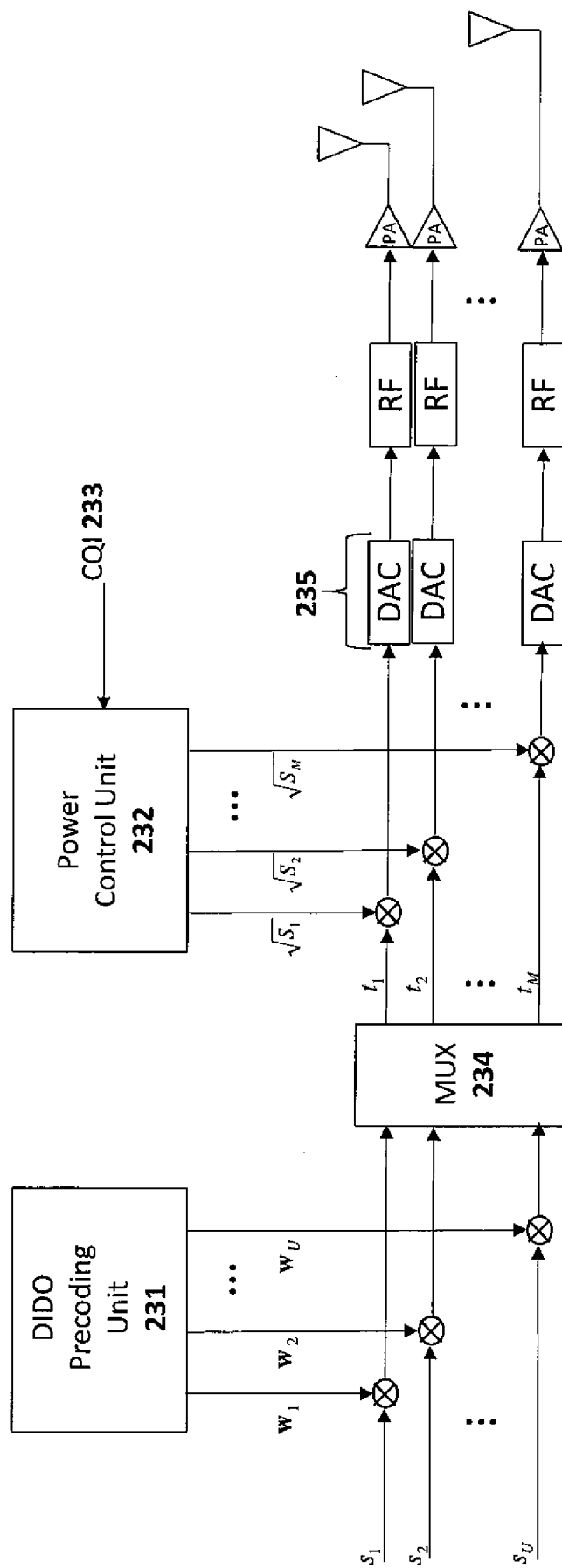


Fig. 23

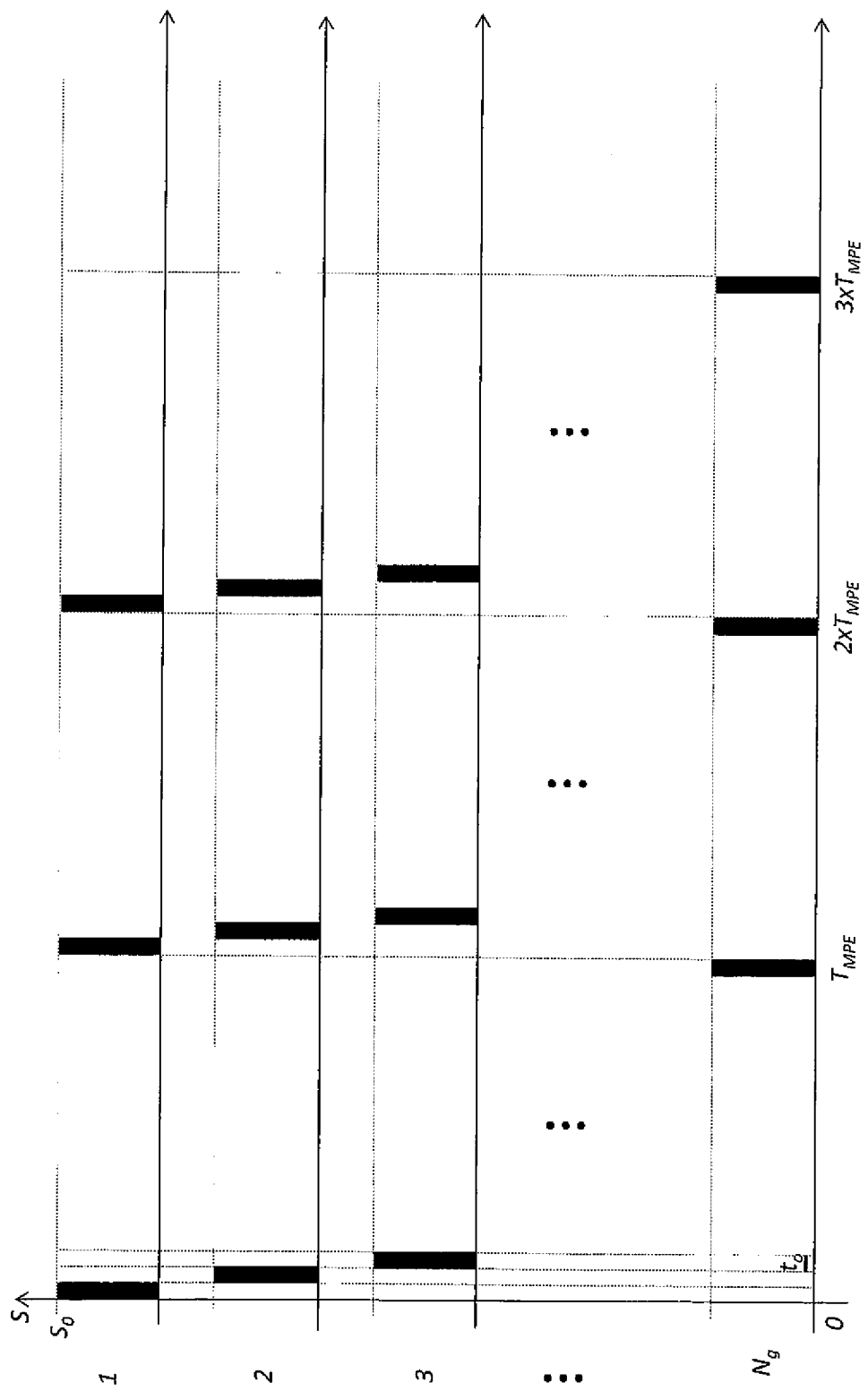


Fig. 24

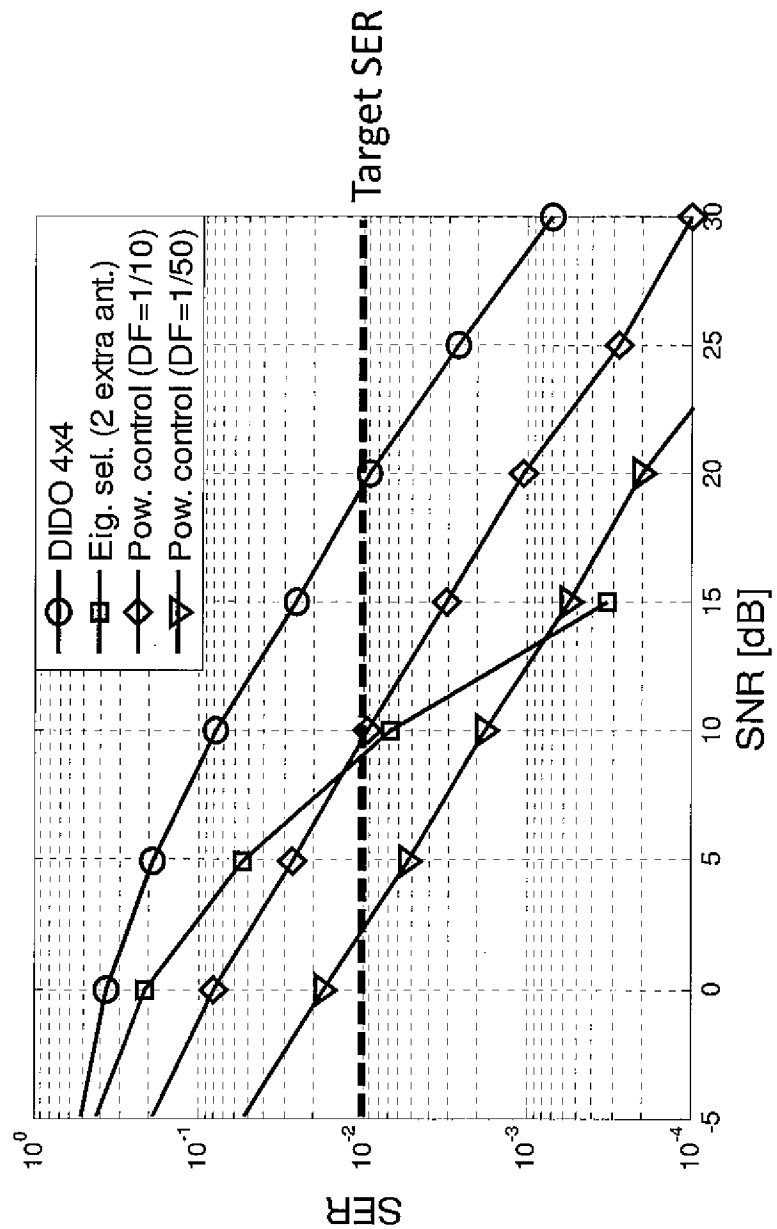


Fig. 25

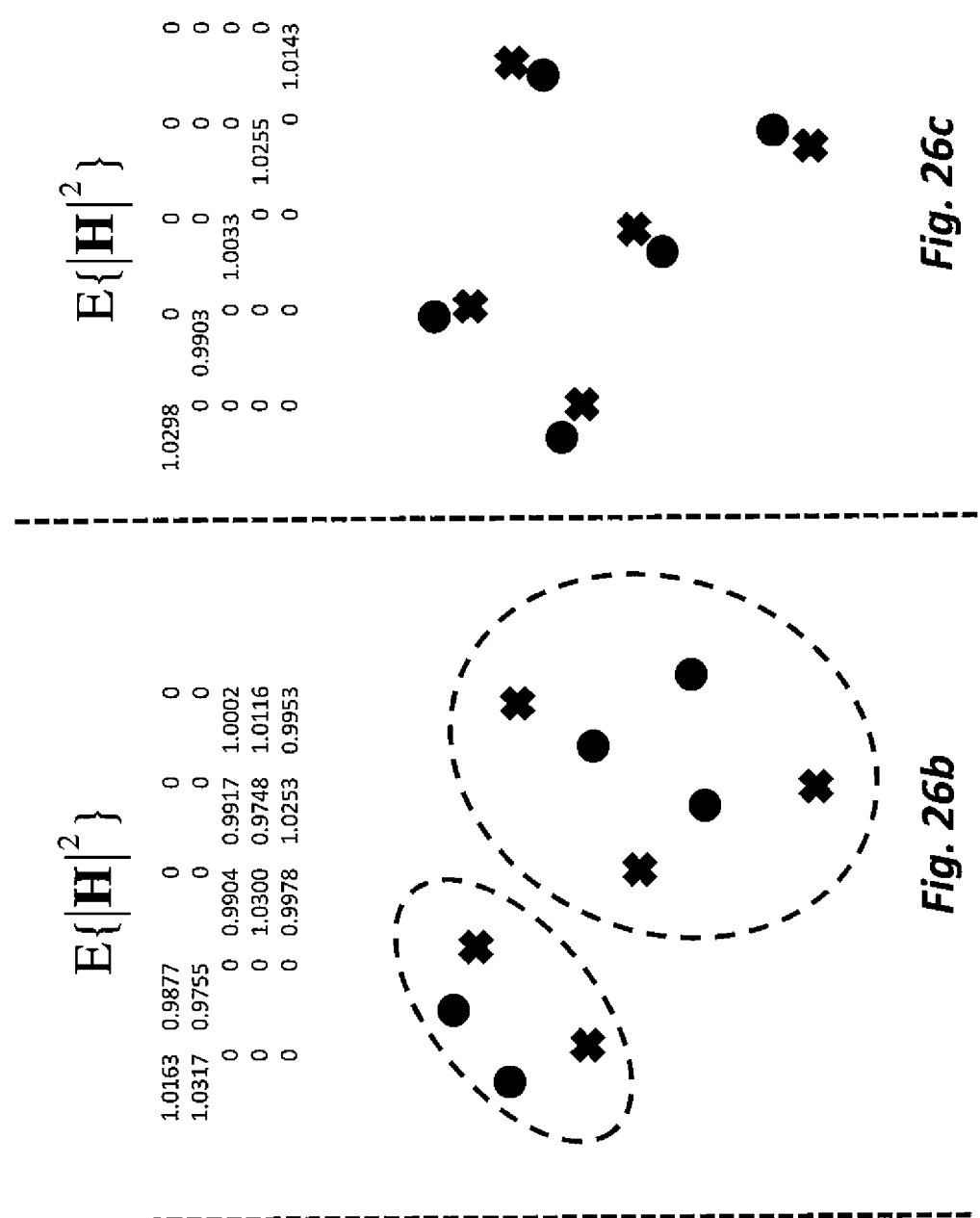


Fig. 26a

Fig. 26b

Fig. 26c

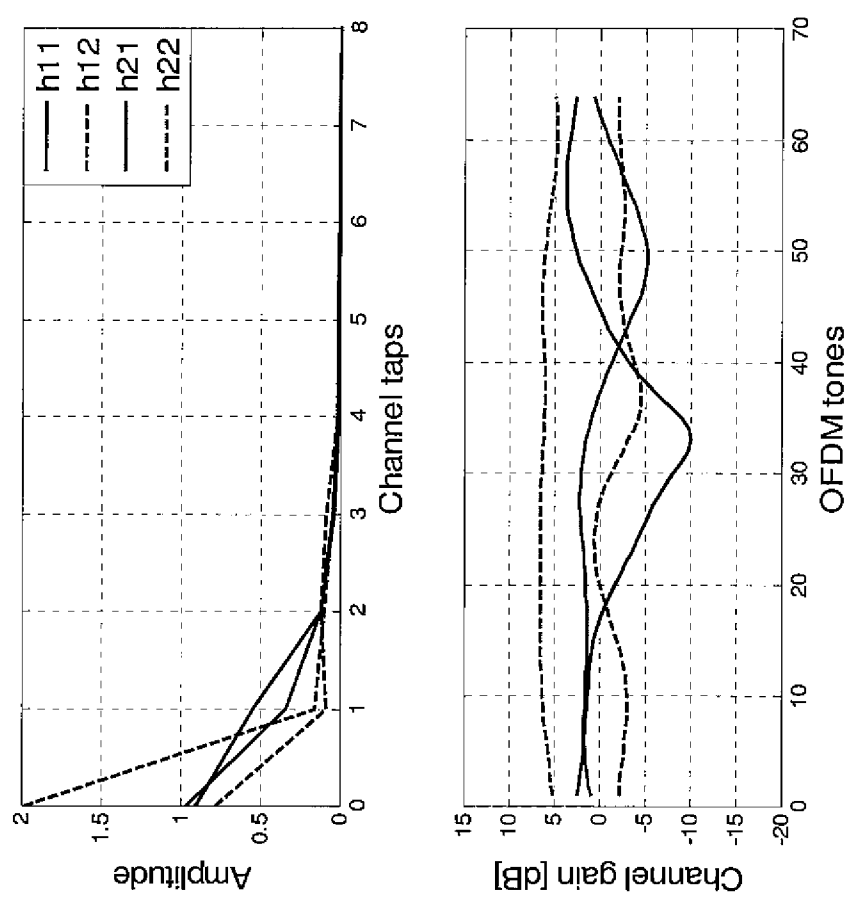


Fig. 27

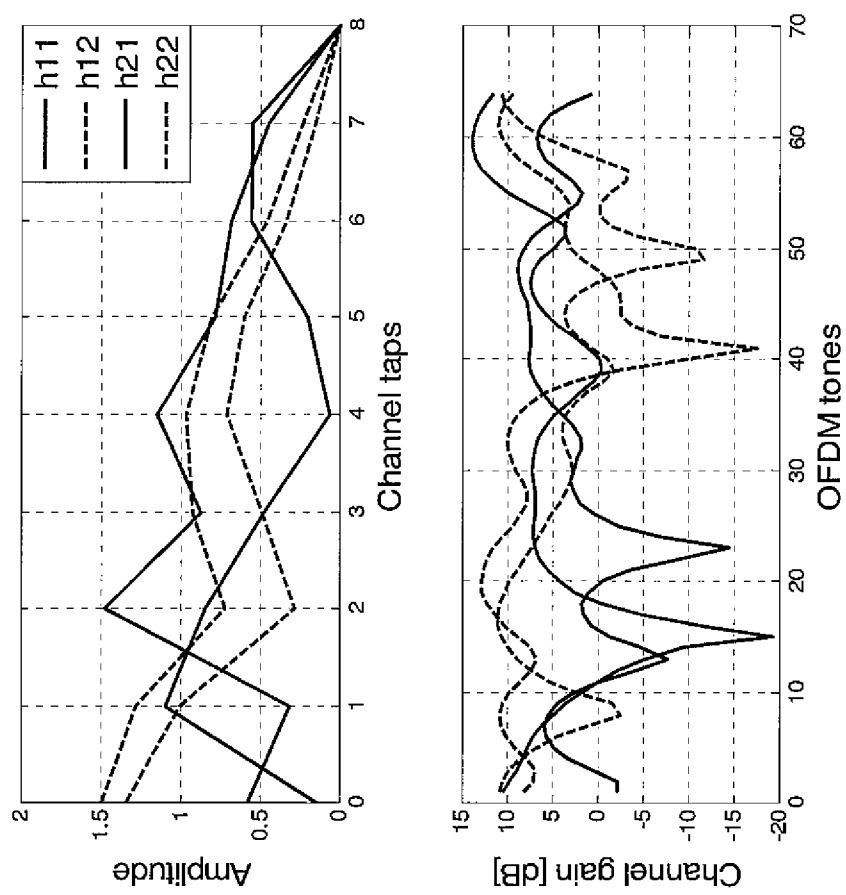


Fig. 28

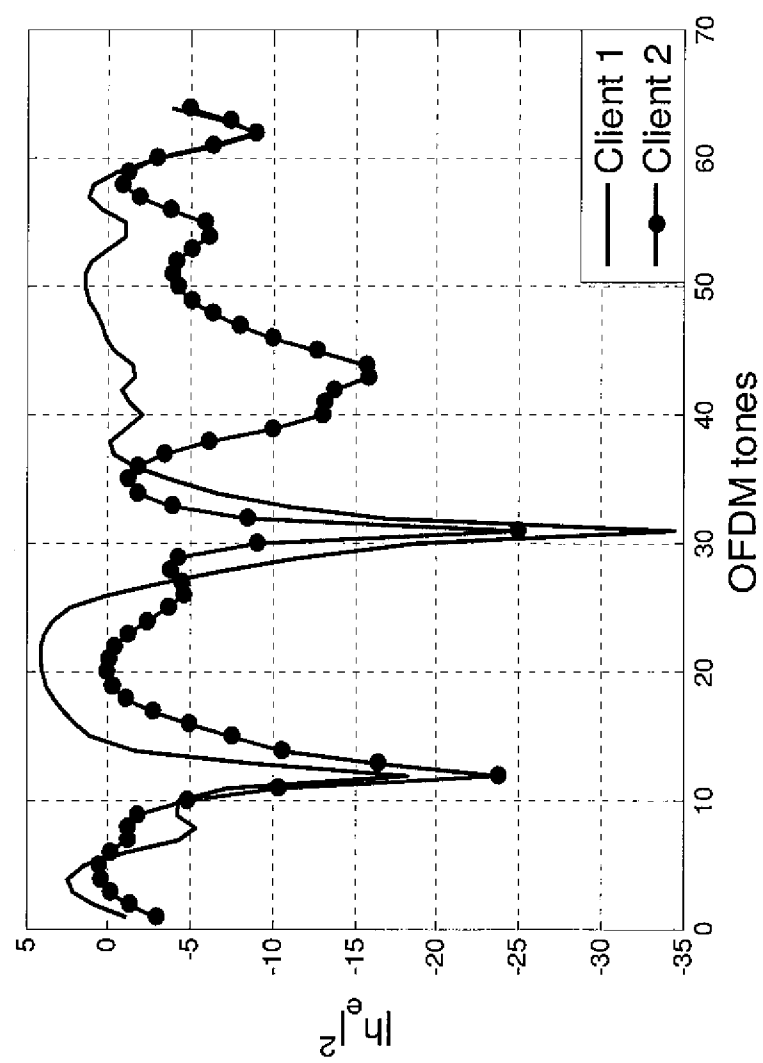


Fig. 29

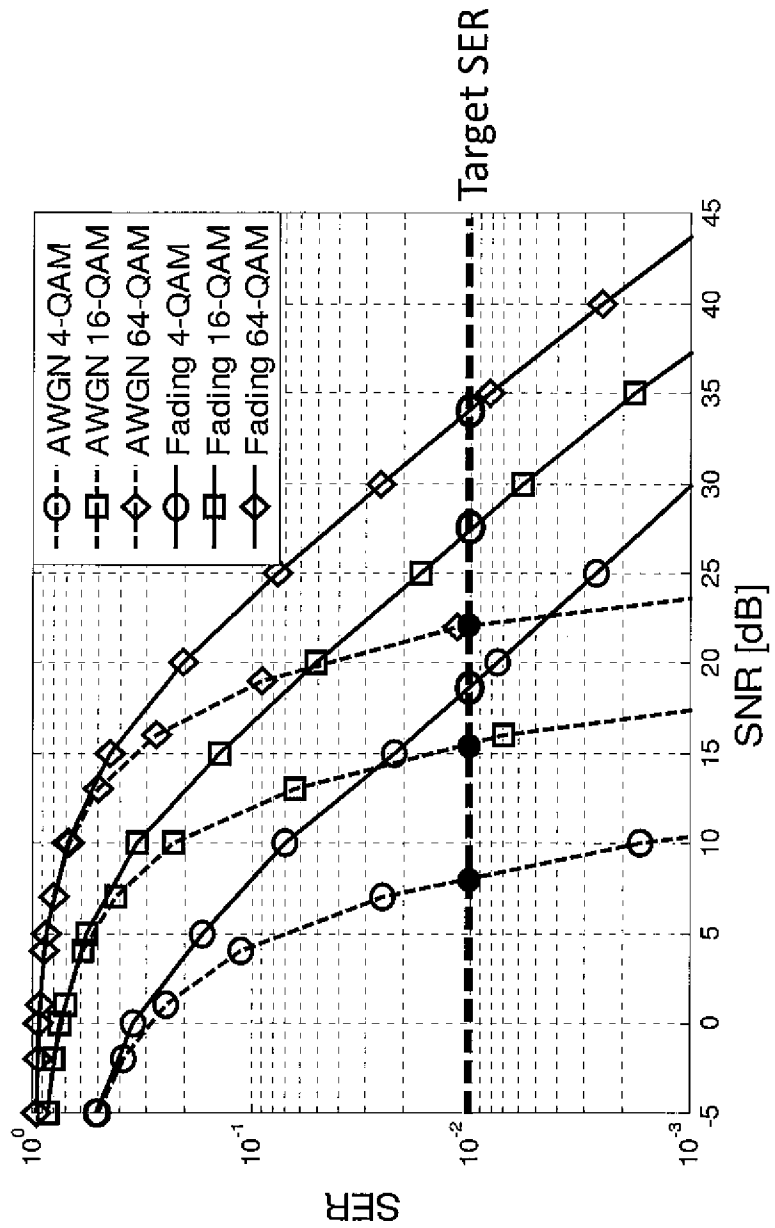
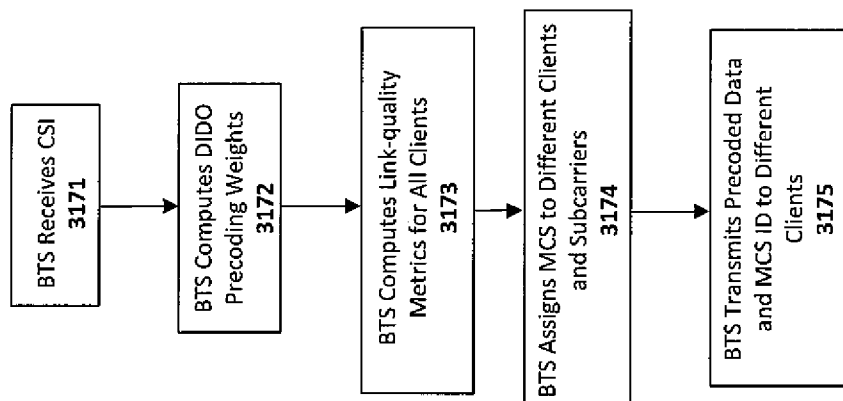


Fig. 30



**Fig. 31**

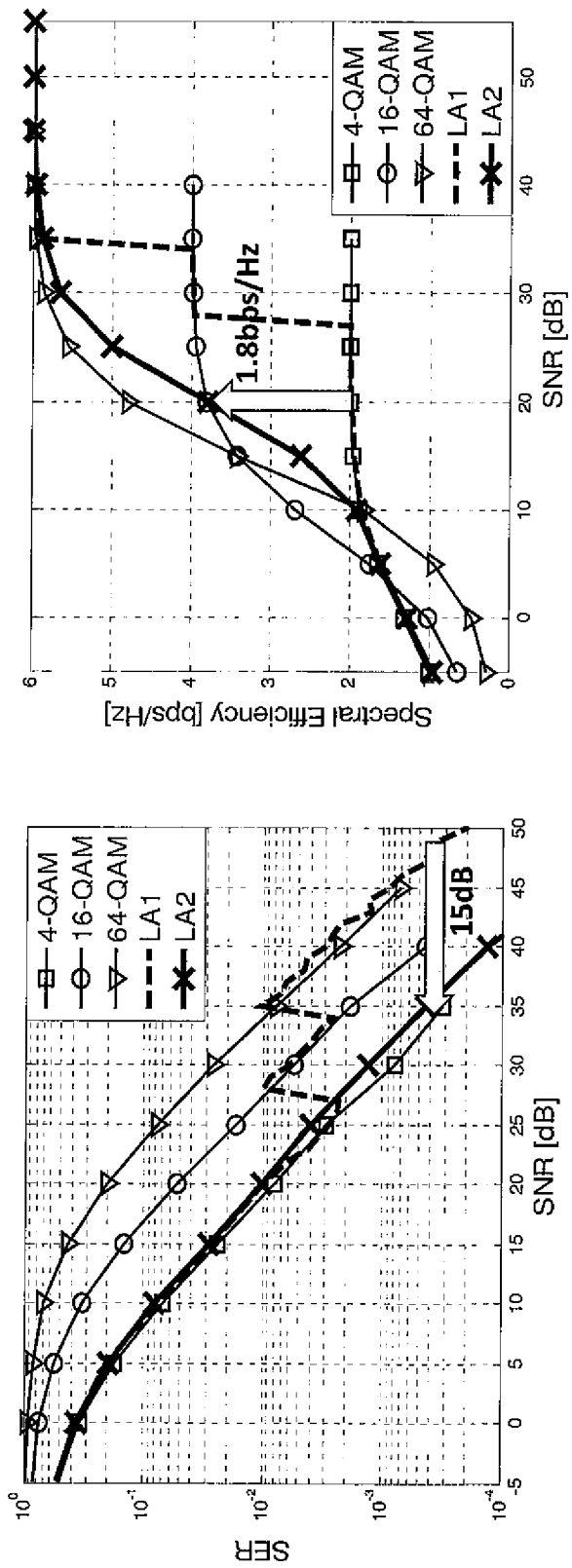


Fig. 32

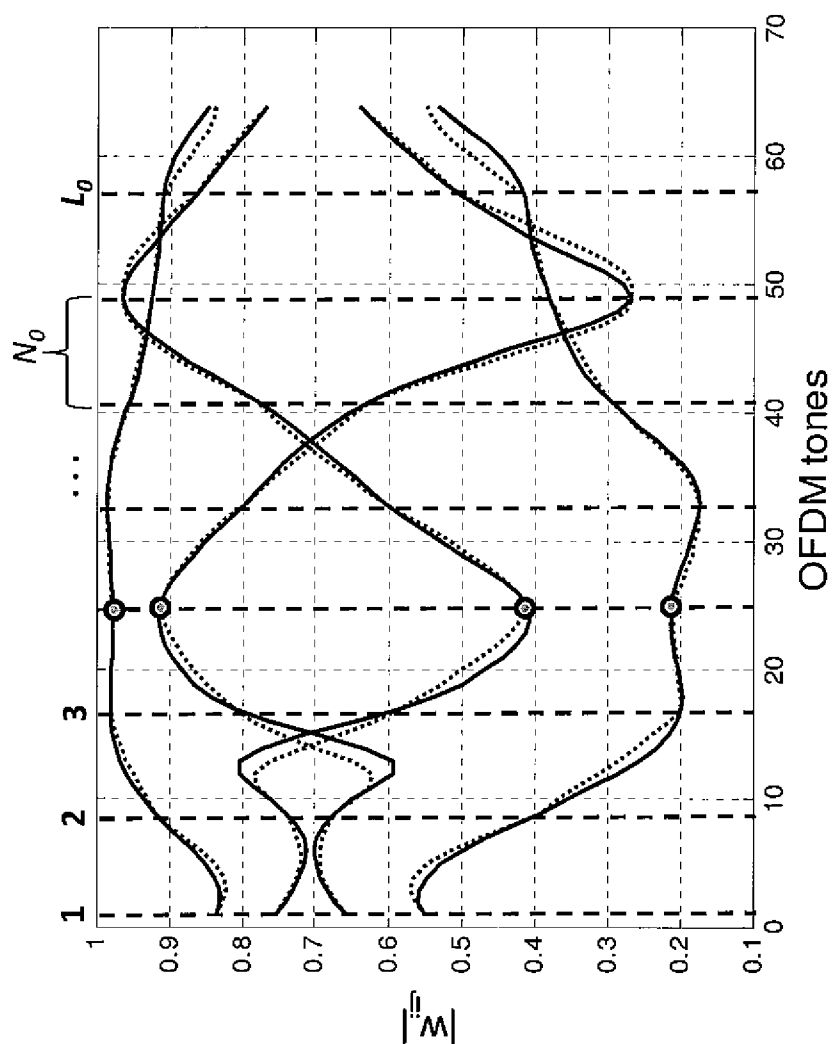


Fig. 33

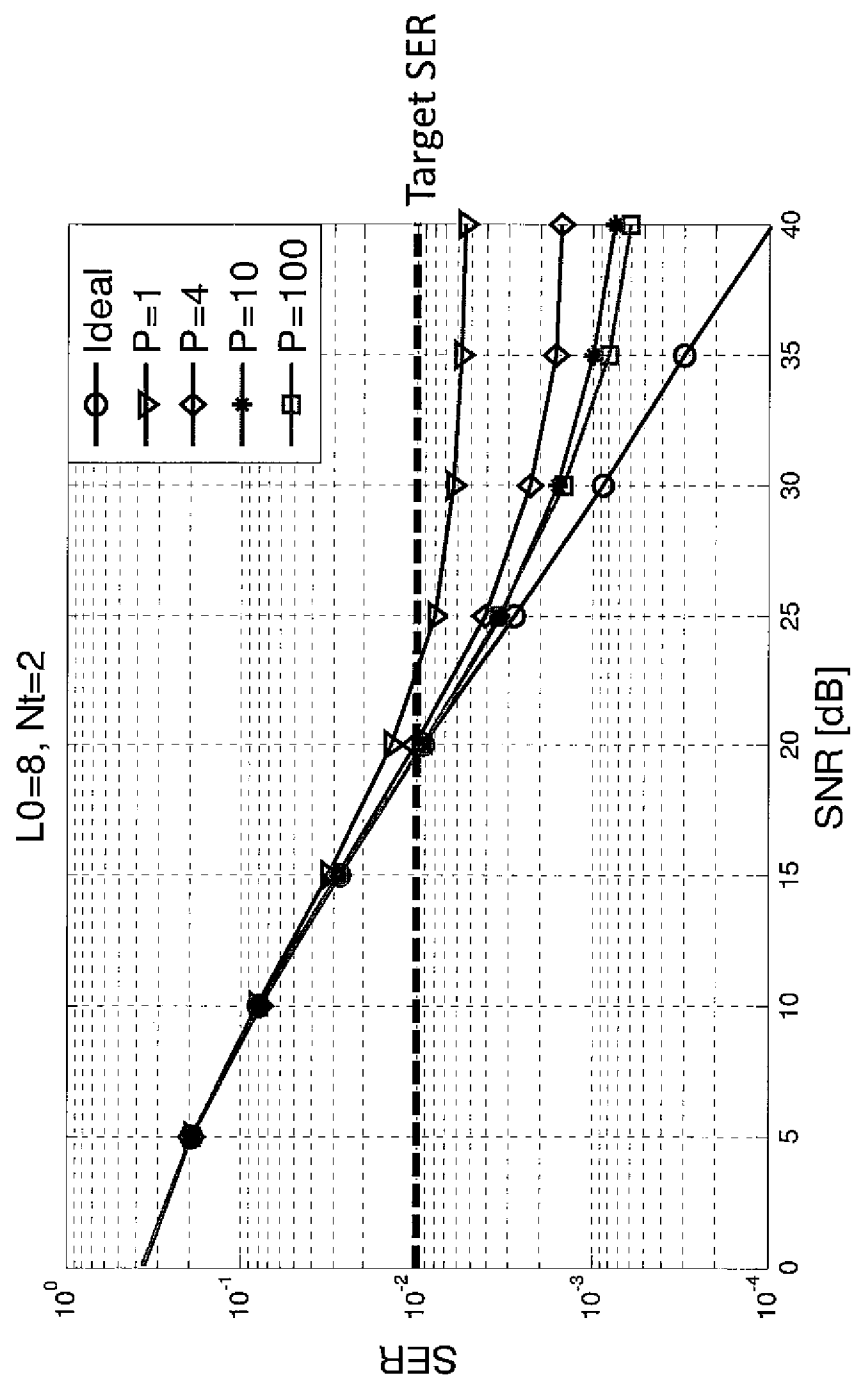


Fig. 34

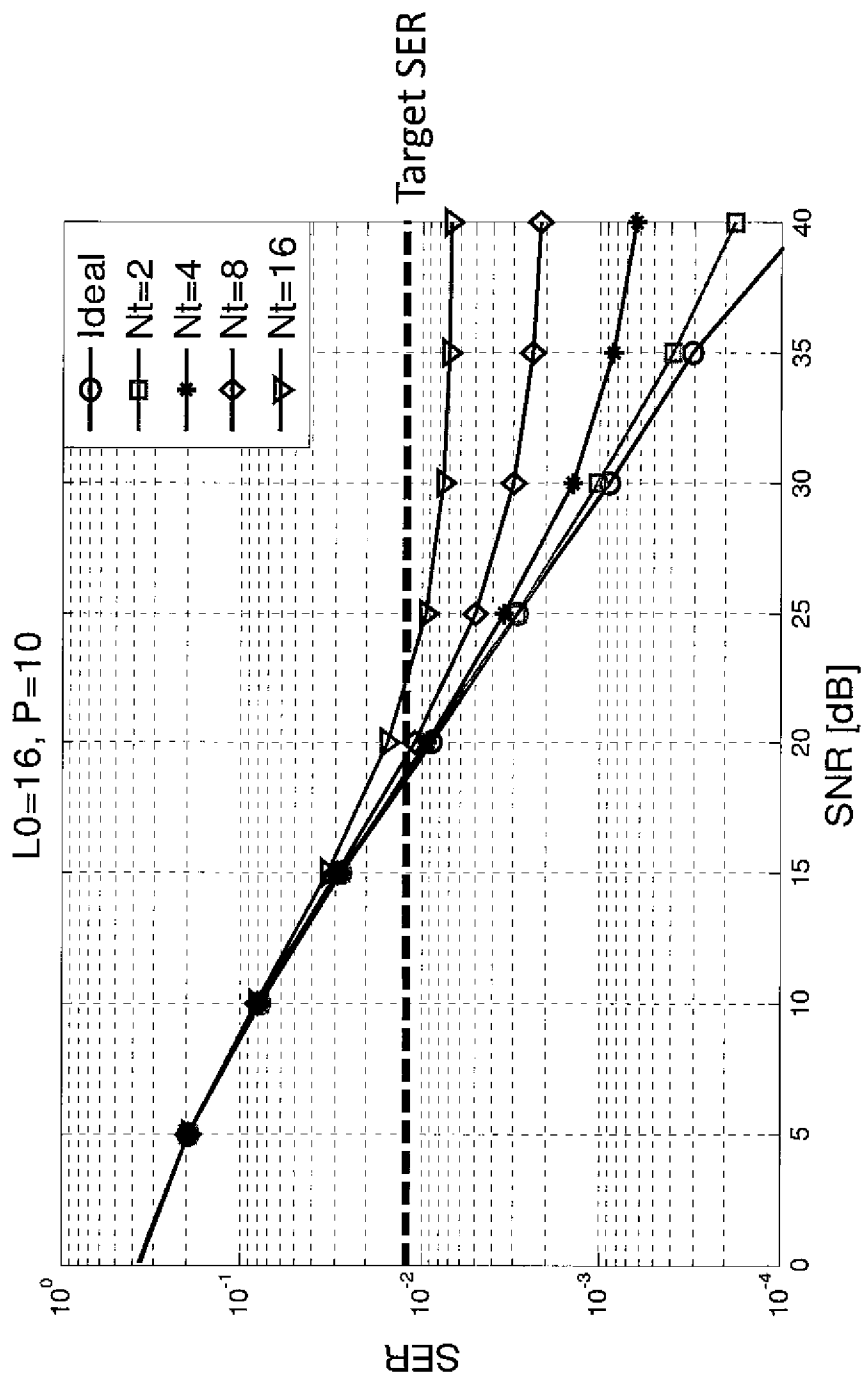


Fig. 35

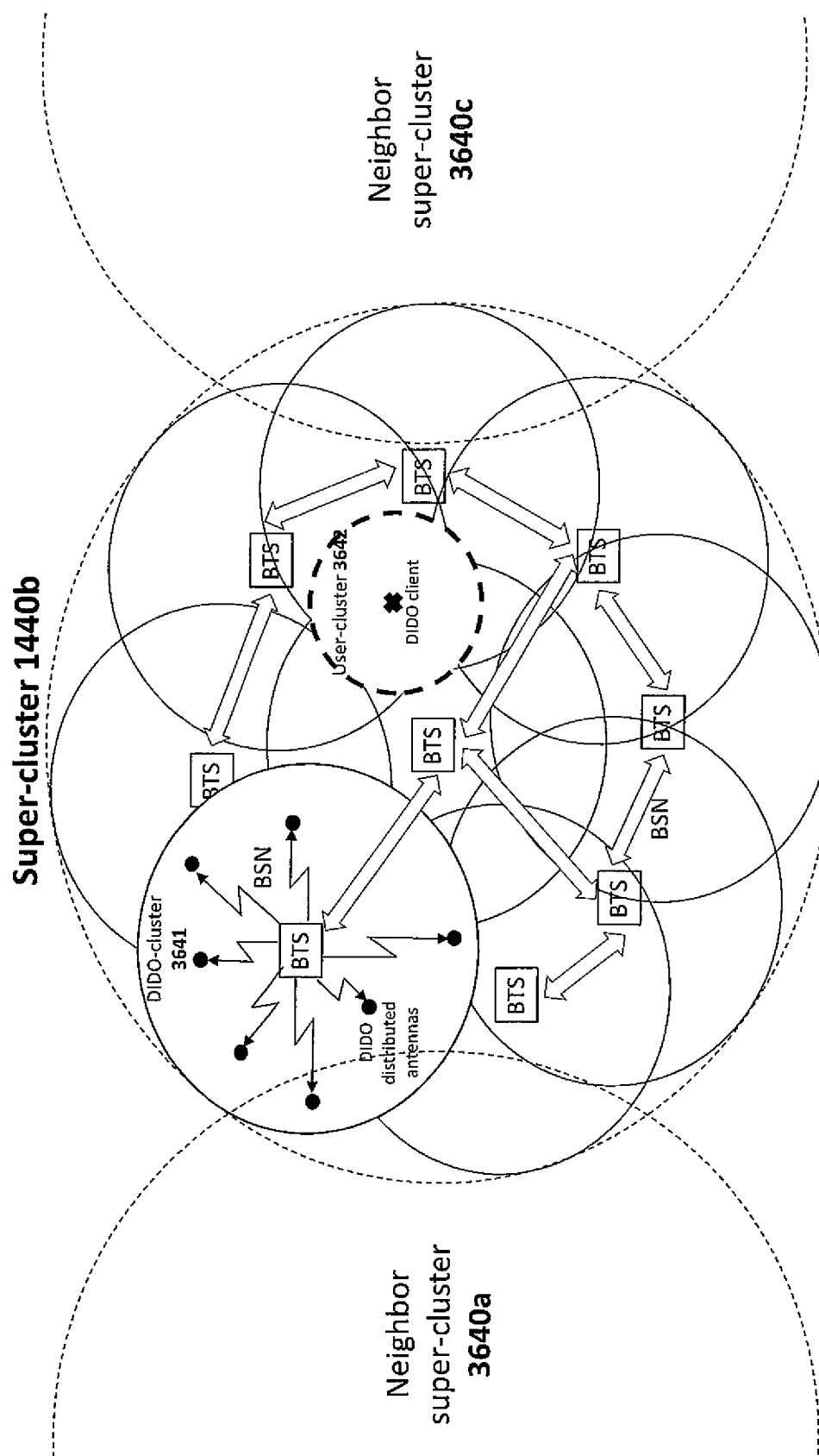


Fig. 36

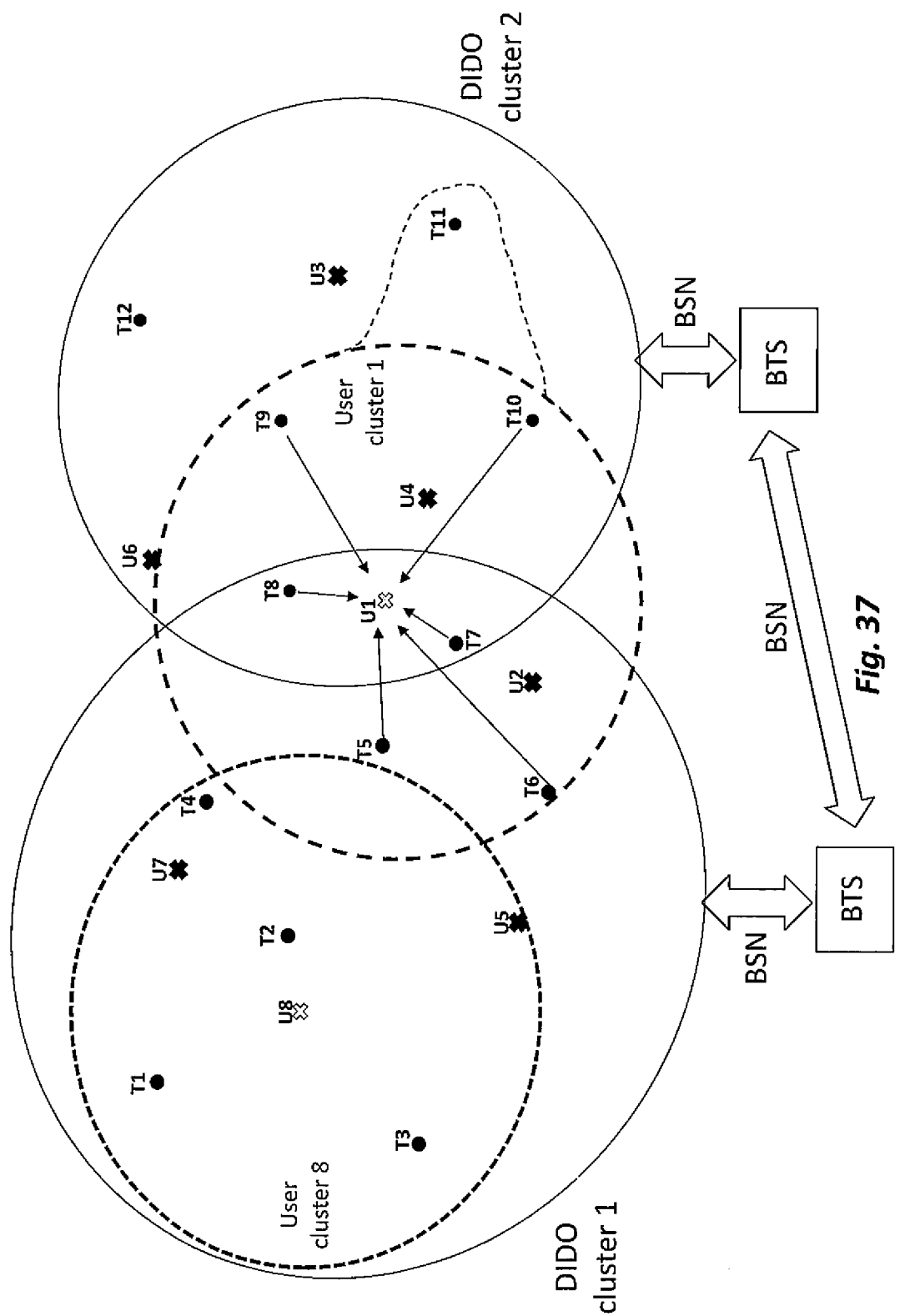
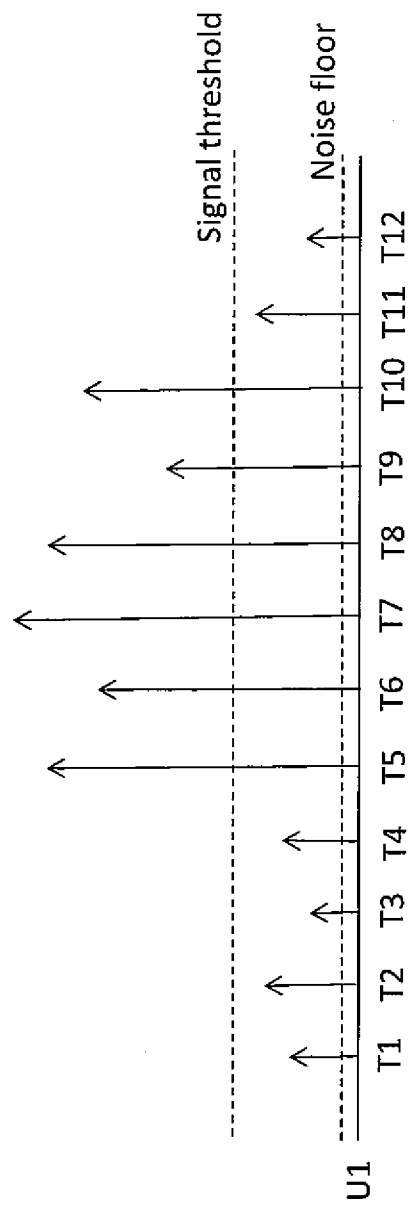
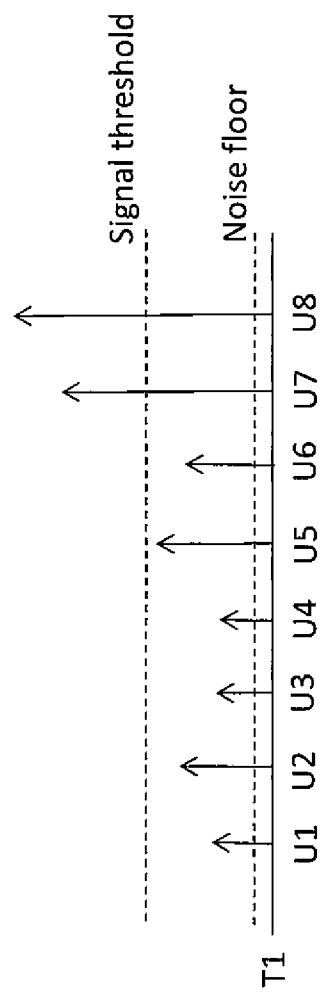


Fig. 37



**Fig. 38a**



**Fig. 38b**

	T1	T2	T3	T4	T5	T6	T7	T8	T9	T10	T11	T12
U1	0	0	0	0	$C_{3,5}$	$C_{4,5}$	$C_{5,5}$	$C_{6,5}$	$C_{7,5}$	$C_{8,5}$	$C_{9,5}$	$C_{10,5}$
U2	0	0	0	0	$C_{2,5}$	$C_{3,6}$	$C_{4,6}$	$C_{5,6}$	$C_{6,6}$	$C_{7,6}$	$C_{8,6}$	$C_{9,6}$
U3	0	0	0	0	0	0	0	$C_{2,5}$	$C_{3,5}$	$C_{4,5}$	$C_{5,5}$	$C_{6,5}$
U4	0	0	0	0	0	0	$C_{4,7}$	$C_{5,8}$	$C_{6,9}$	$C_{7,10}$	$C_{8,11}$	$C_{9,12}$
U5	0	$C_{5,2}$	$C_{5,3}$	0	$C_{5,5}$	$C_{5,6}$	0	0	0	0	0	0
U6	0	0	0	$C_{6,4}$	0	0	$C_{6,5}$	$C_{6,6}$	0	0	0	$C_{6,12}$
U7	$C_{7,1}$	$C_{7,2}$	$C_{7,3}$	0	$C_{7,4}$	$C_{7,5}$	0	0	0	0	0	0
U8	$C_{8,1}$	$C_{8,2}$	$C_{8,3}$	$C_{8,4}$	$C_{8,5}$	$C_{8,6}$	$C_{8,7}$	$C_{8,8}$	$C_{8,9}$	$C_{8,10}$	$C_{8,11}$	$C_{8,12}$

Fig. 39

	T1	T2	T3	T4	T5	T6	T7	T8	T9	T10	T11	T12
U1	0	0	0	0	0	$C_{1,3}$	$C_{1,4}$	$C_{1,5}$	$C_{1,6}$	$C_{1,7}$	$C_{1,8}$	$C_{1,9}$
U2	0	0	0	0	0	$C_{2,5}$	$C_{2,6}$	$C_{2,7}$	0	0	0	0
U3	0	0	0	0	0	0	0	$C_{3,5}$	$C_{3,6}$	$C_{3,7}$	$C_{3,8}$	$C_{3,9}$
U4	0	0	0	0	0	0	$C_{4,7}$	$C_{4,8}$	$C_{4,9}$	0	0	0
U5	0	0	$C_{5,2}$	$C_{5,3}$	0	$C_{5,5}$	$C_{5,6}$	0	0	0	0	0
U6	0	0	0	0	$C_{6,4}$	0	0	$C_{6,3}$	$C_{6,5}$	0	0	$C_{6,2}$
U7	$C_{7,1}$	$C_{7,2}$	0	$C_{7,4}$	$C_{7,5}$	0	0	0	0	0	0	0
U8	$C_{8,1}$	$C_{8,2}$	$C_{8,3}$	$C_{8,4}$	0	0	0	0	0	0	0	0

Fig. 40

	T1	T2	T3	T4	T5	T6	T7	T8	T9	T10	T11	T12
U1	0	0	0	0	$C_{1,5}$	$C_{1,6}$	$C_{1,7}$	$C_{1,8}$	$C_{1,9}$	$C_{1,10}$	0	0
U2	0	0	0	0	$C_{2,5}$	$C_{2,6}$	$C_{2,7}$	0	0	0	0	0
U3	0	0	0	0	0	0	0	0	$C_{3,5}$	$C_{3,6}$	$C_{3,11}$	$C_{3,12}$
U4	0	0	0	0	0	0	$C_{4,7}$	$C_{4,8}$	$C_{4,9}$	$C_{4,10}$	0	0
U5	0	$C_{5,2}$	$C_{5,3}$	0	$C_{5,5}$	0	0	0	0	0	0	0
U6	0	0	0	$C_{6,4}$	0	0	$C_{6,5}$	$C_{6,6}$	0	0	0	$C_{6,12}$
U7	$C_{7,1}$	$C_{7,2}$	0	0	$C_{7,5}$	$C_{7,6}$	0	0	0	0	0	0
U8	$C_{8,1}$	$C_{8,2}$	$C_{8,3}$	0	0	0	0	$C_{8,6}$	0	0	0	0

Fig. 41

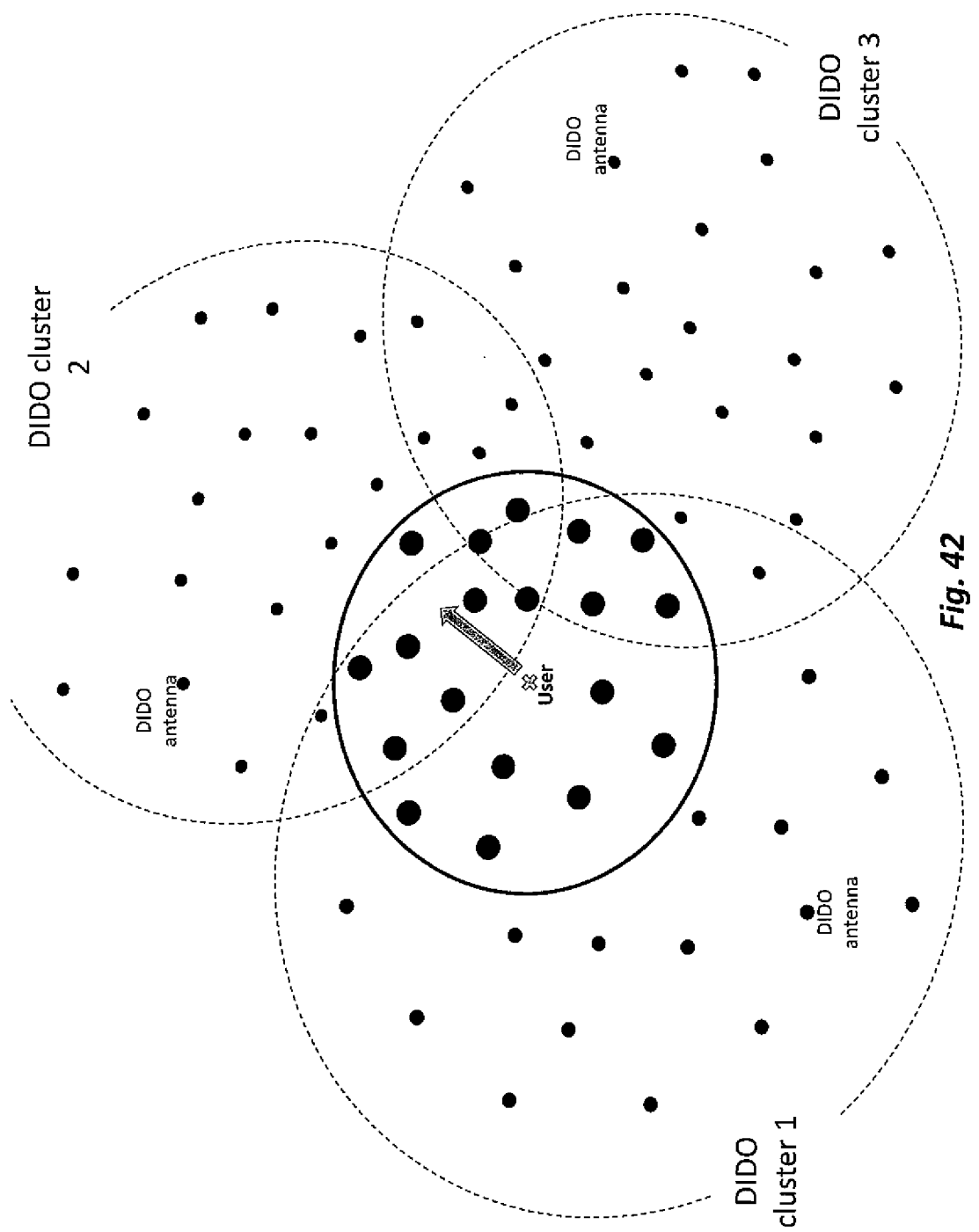


Fig. 42

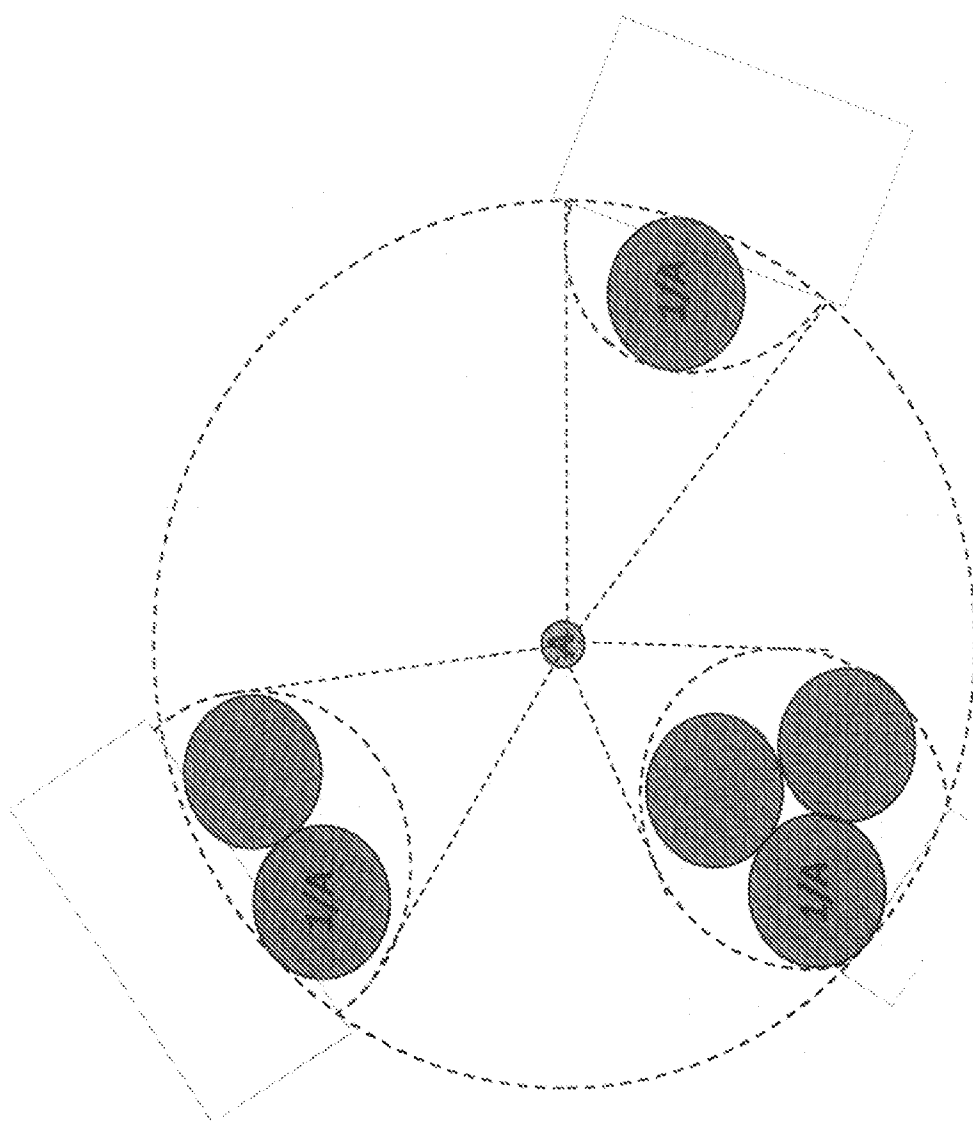


Fig. 43

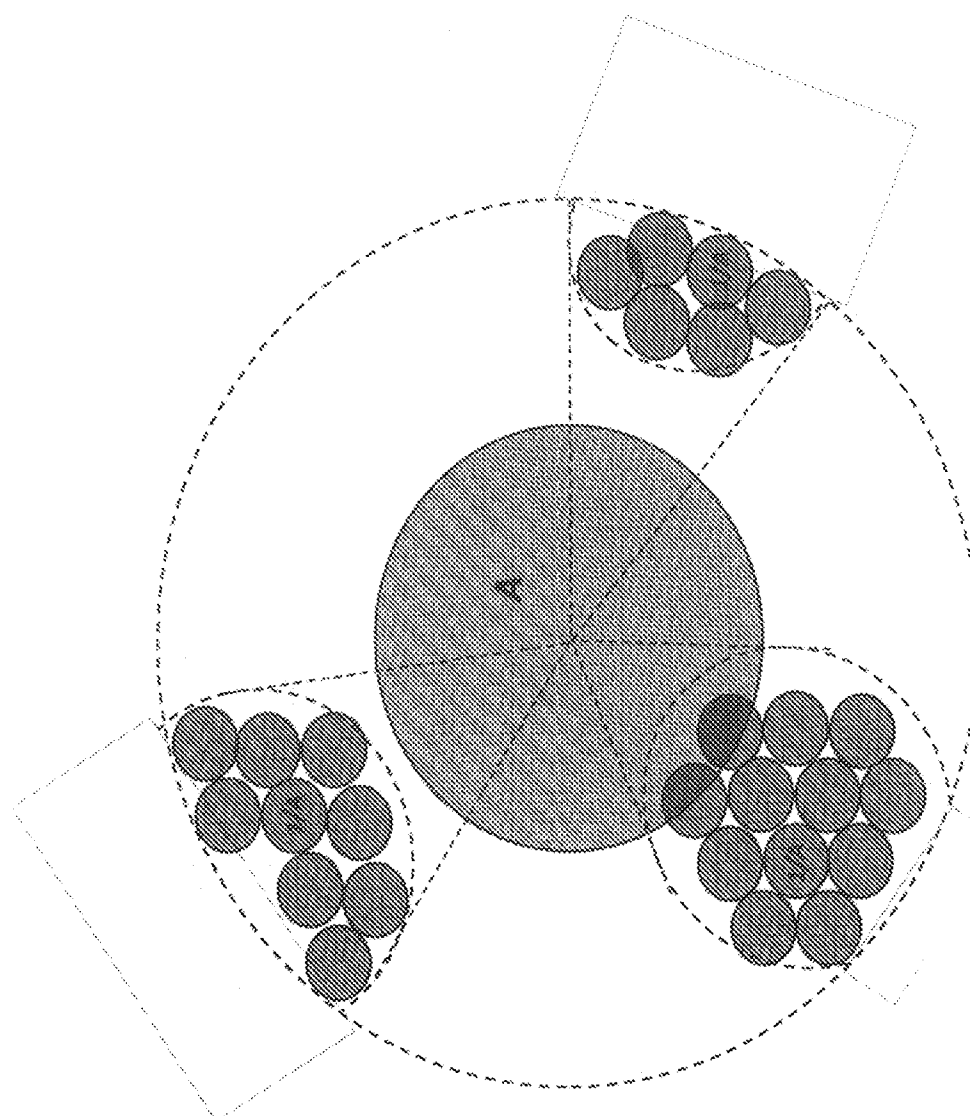


Fig. 44

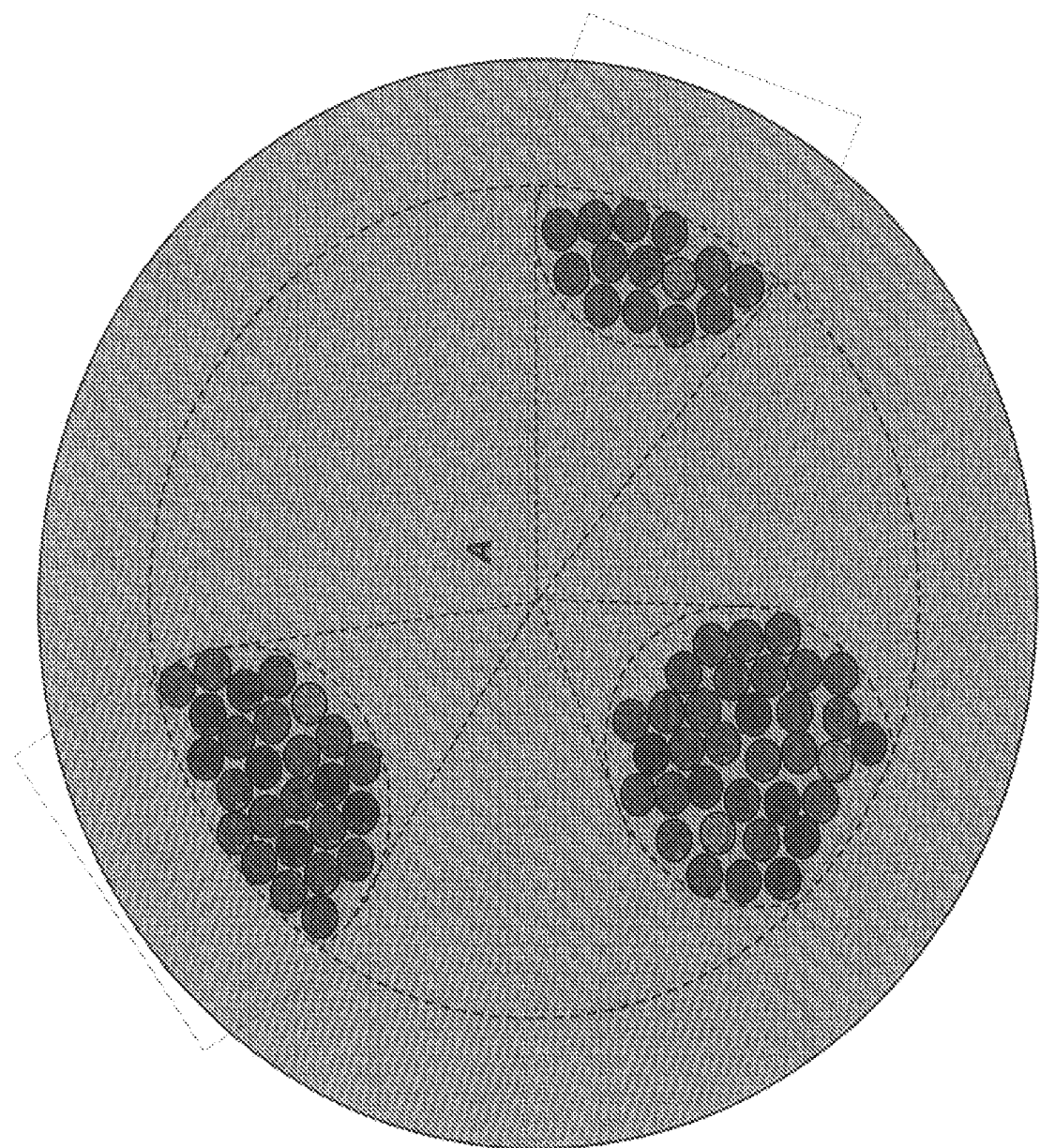


Fig. 45

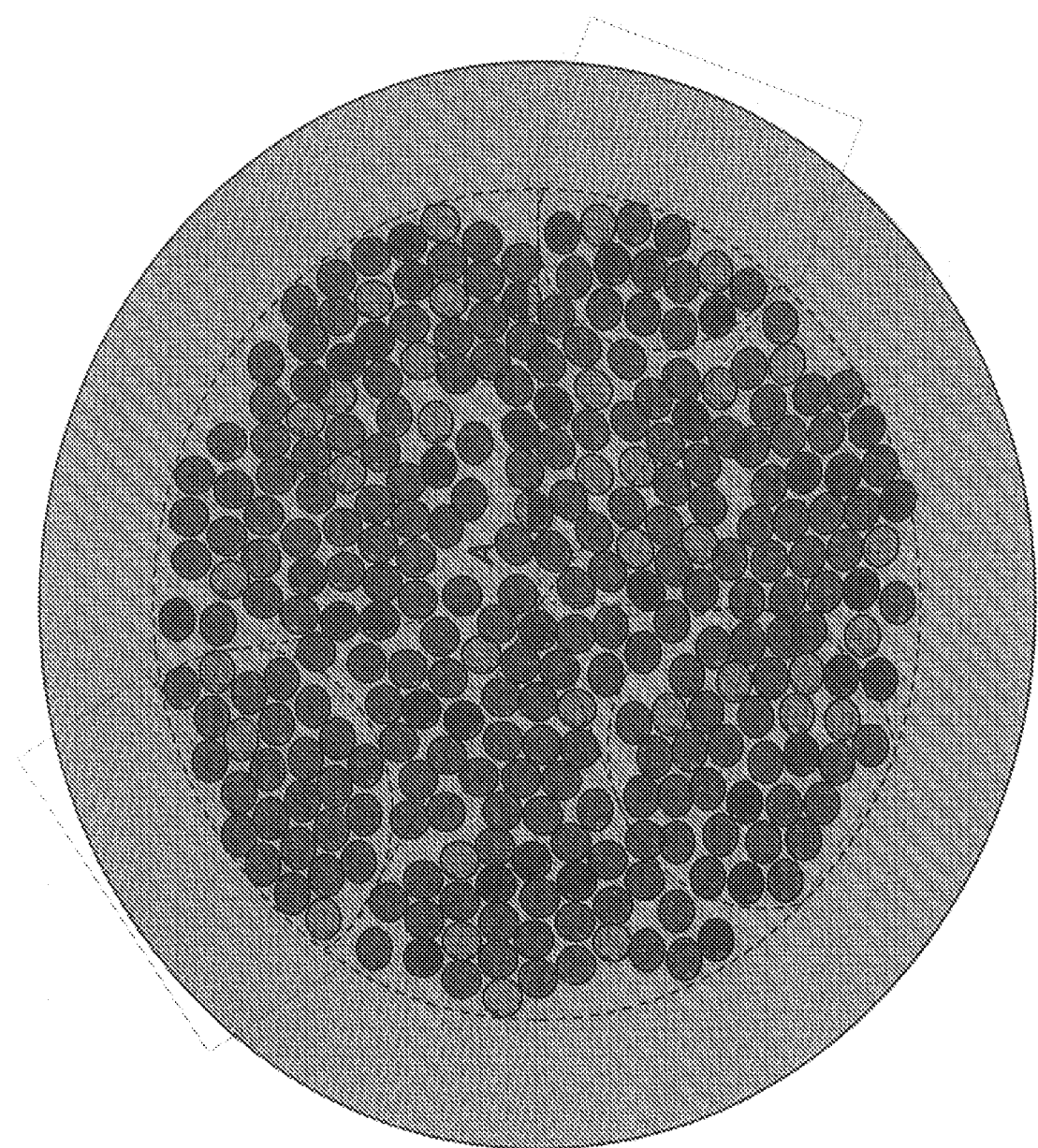
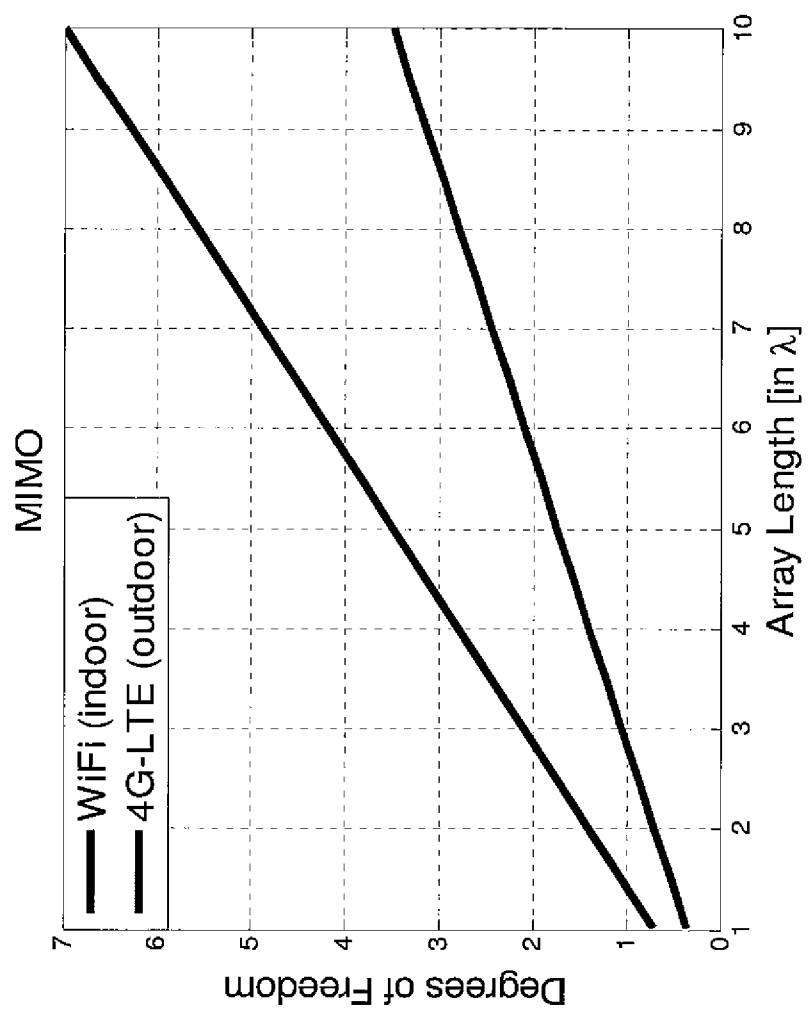
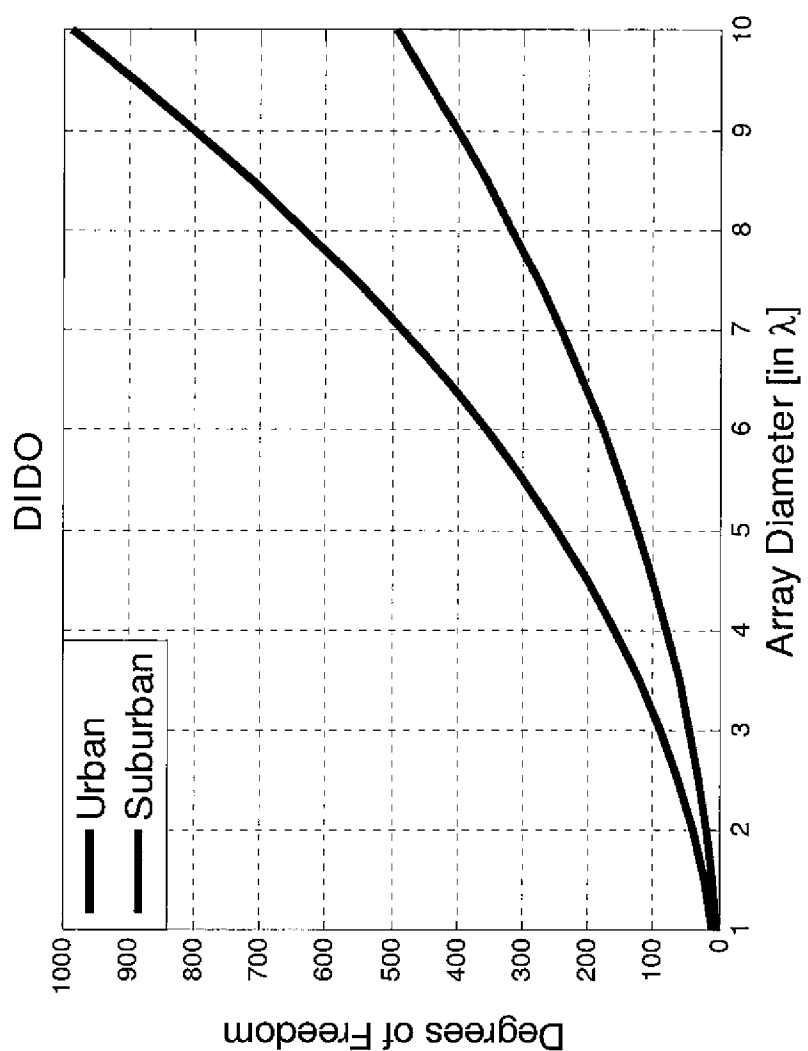


Fig. 46



**Fig. 47**



*Fig. 48*

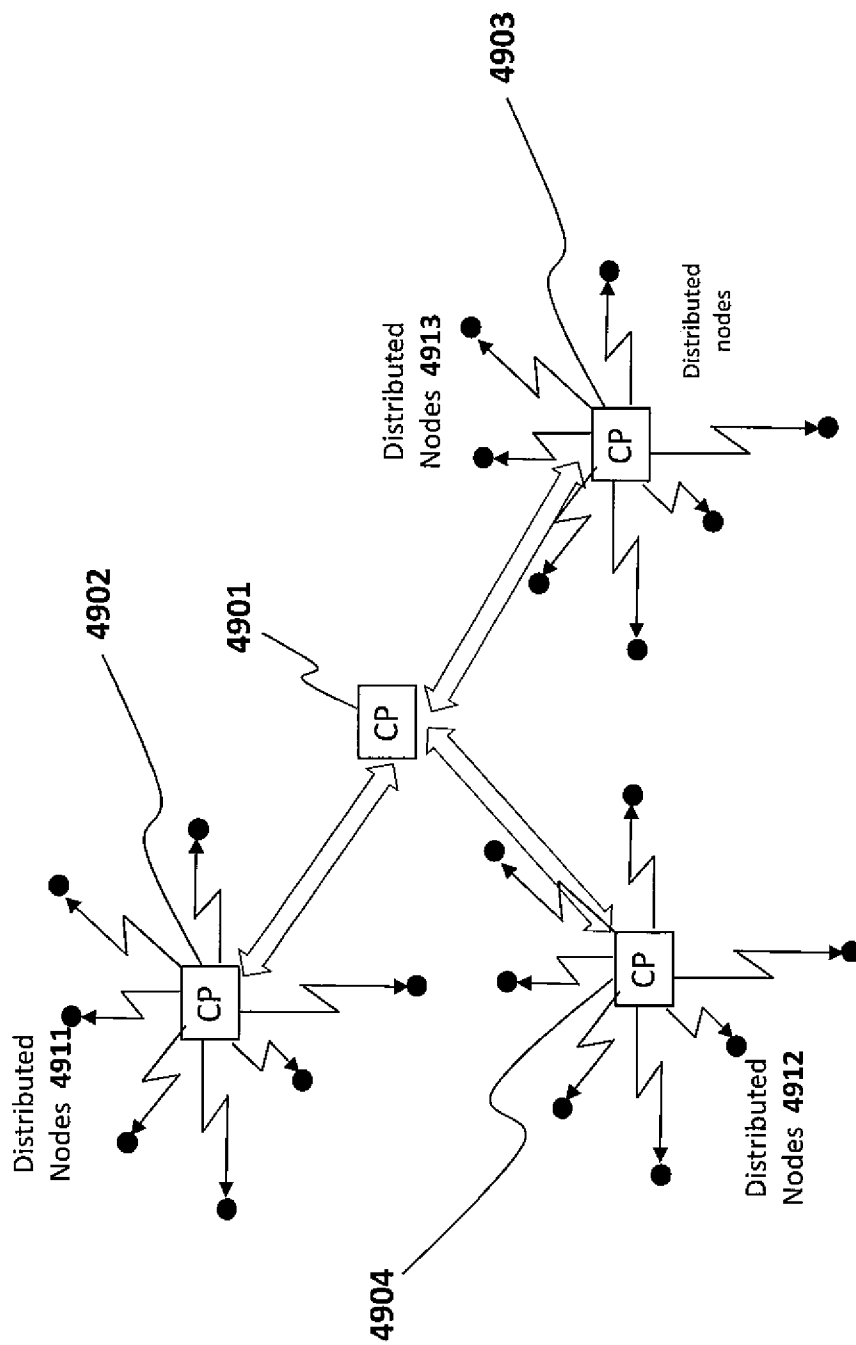
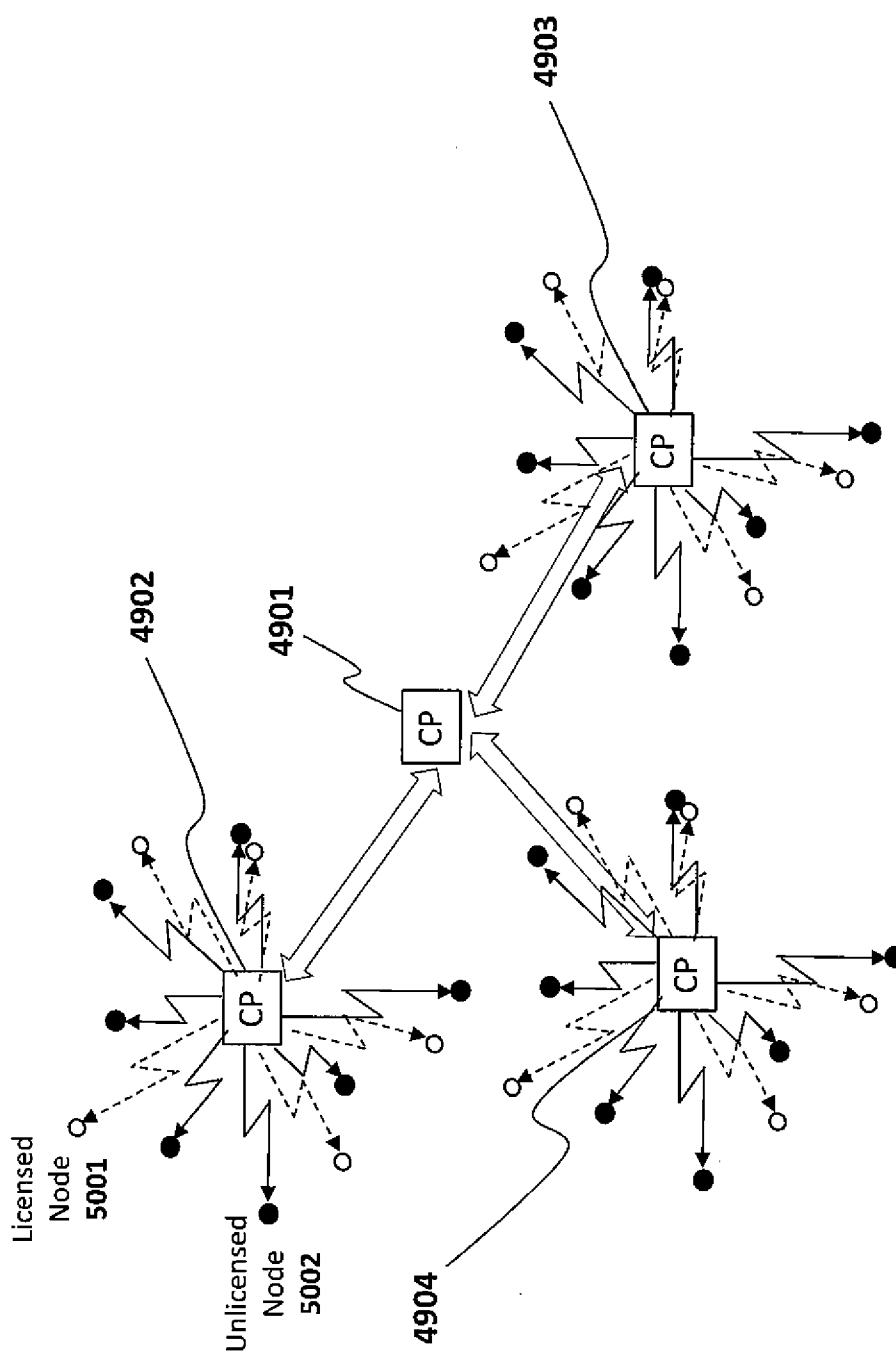
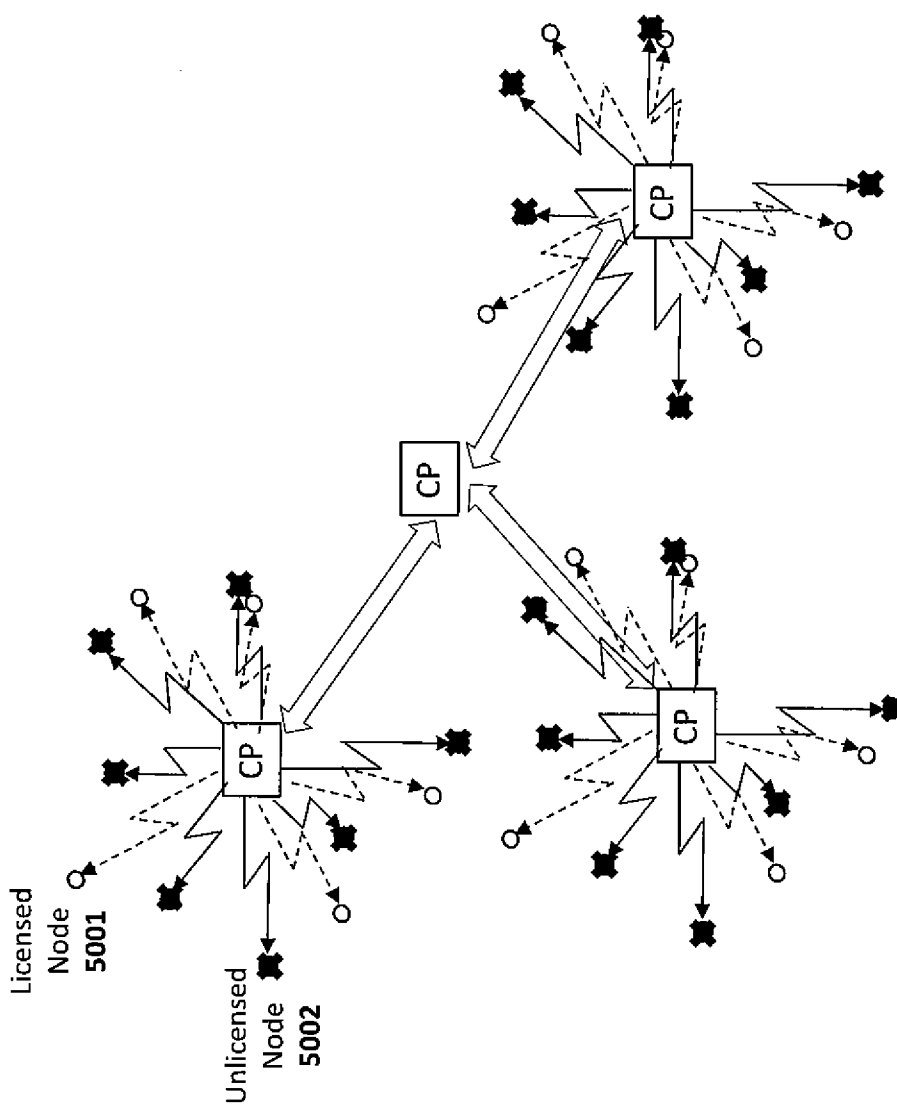


Fig. 49



*Fig. 50*



*Fig. 51*

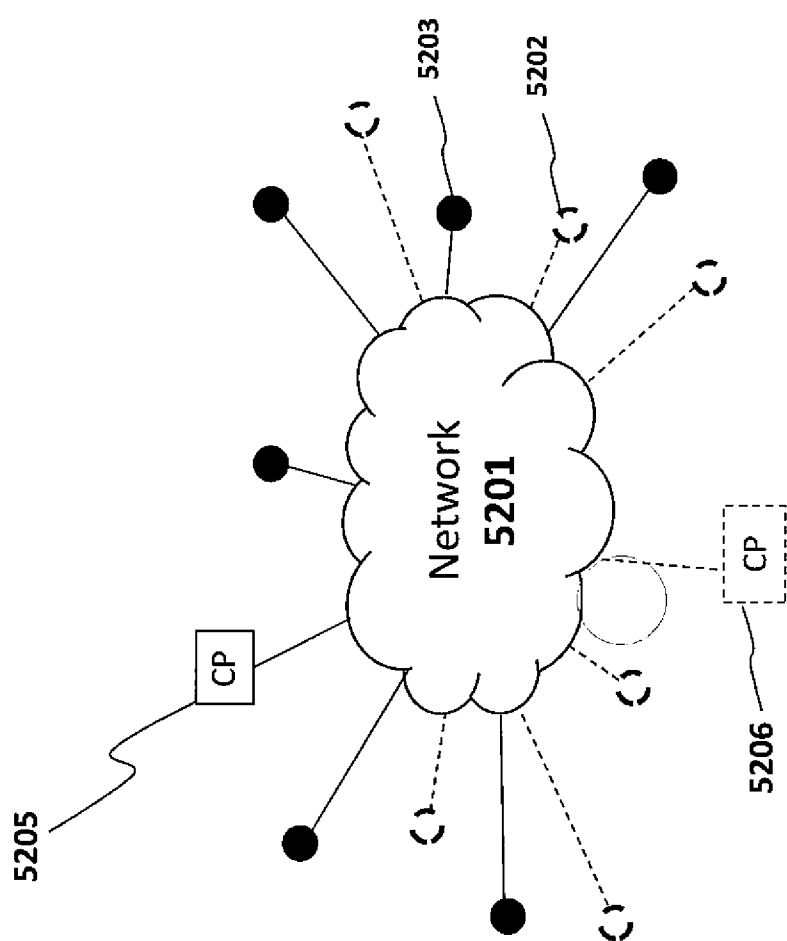


**Fig. 52**

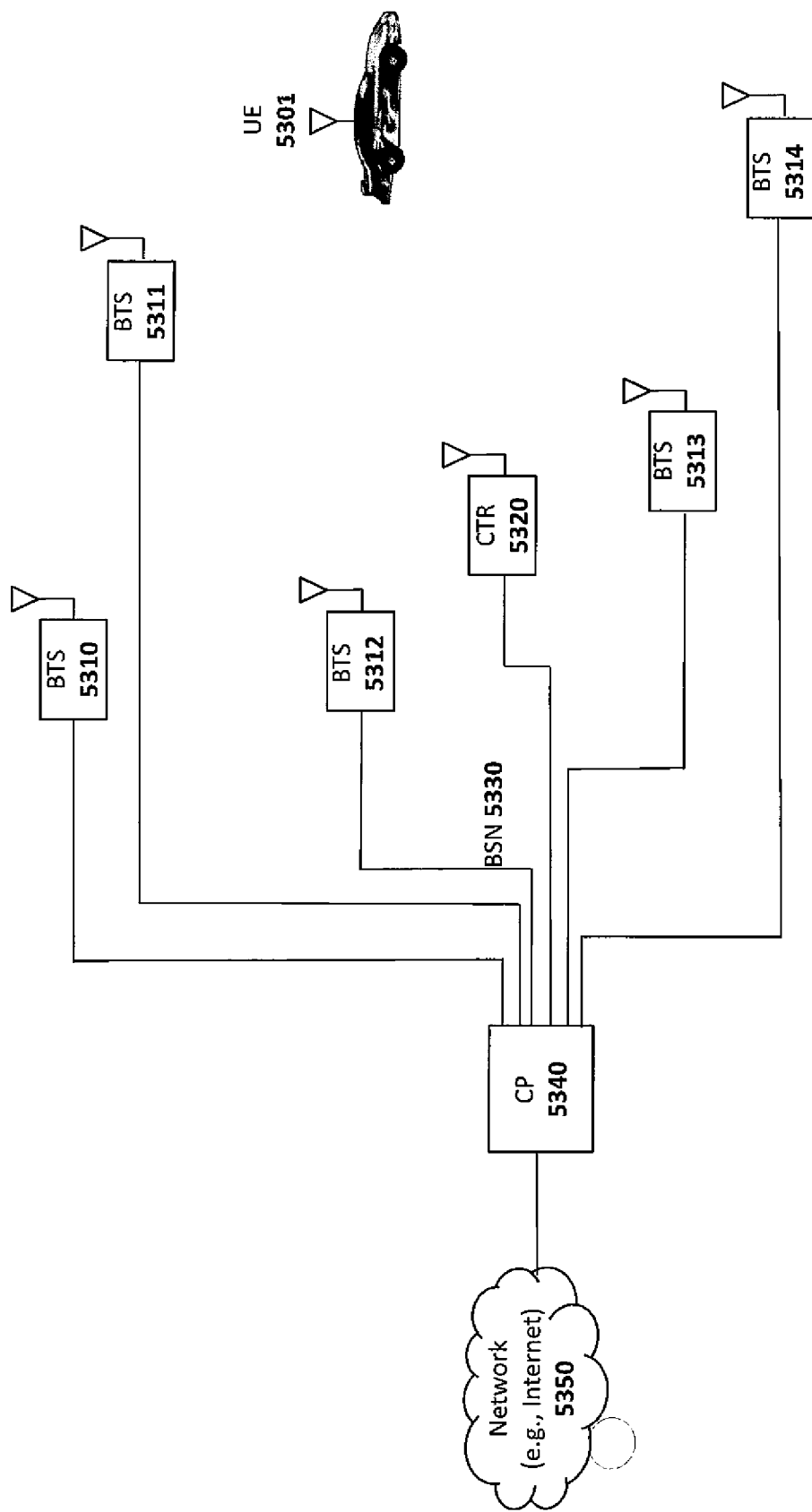
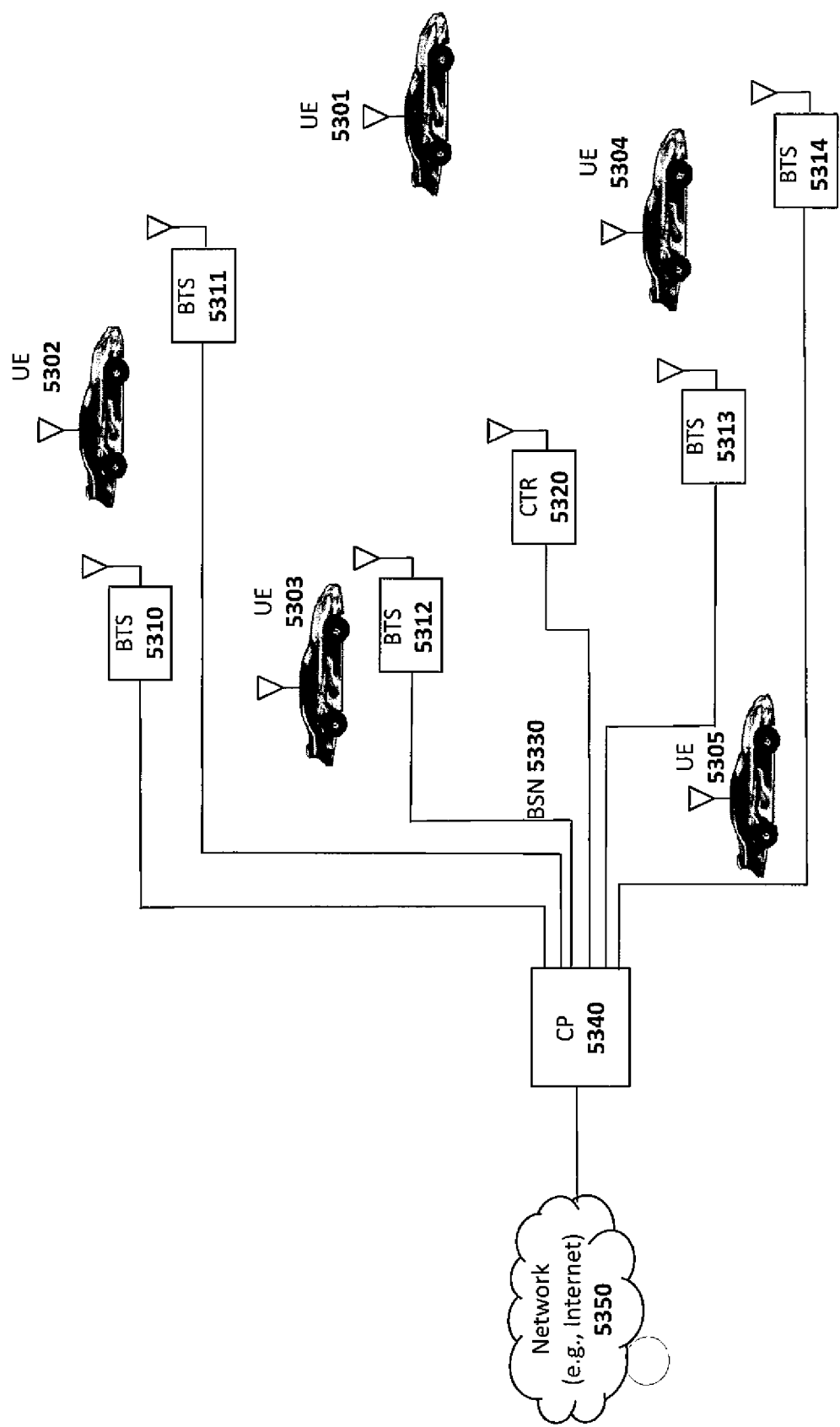
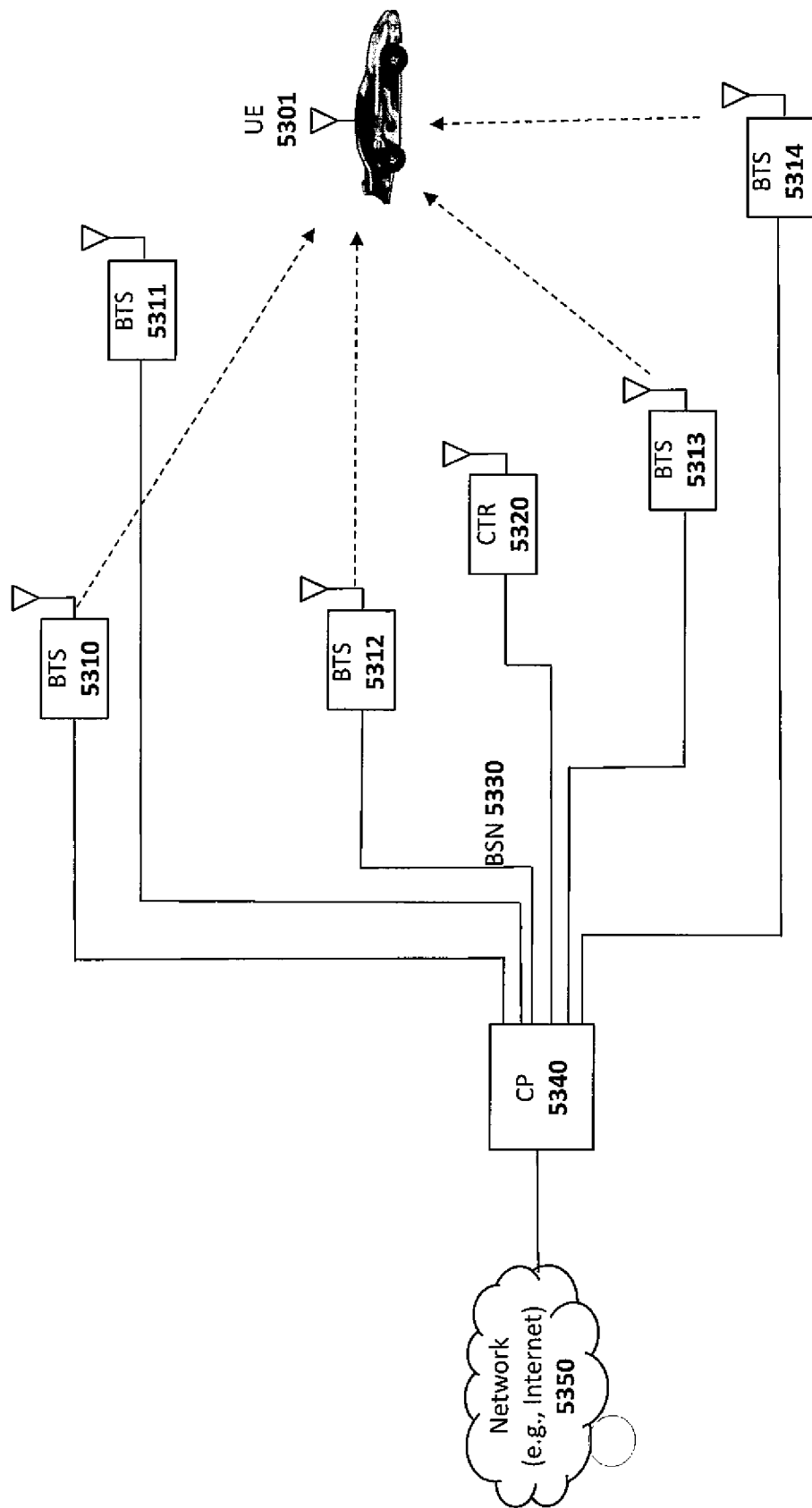


Fig. 53



**Fig. 54**



*Fig. 55*

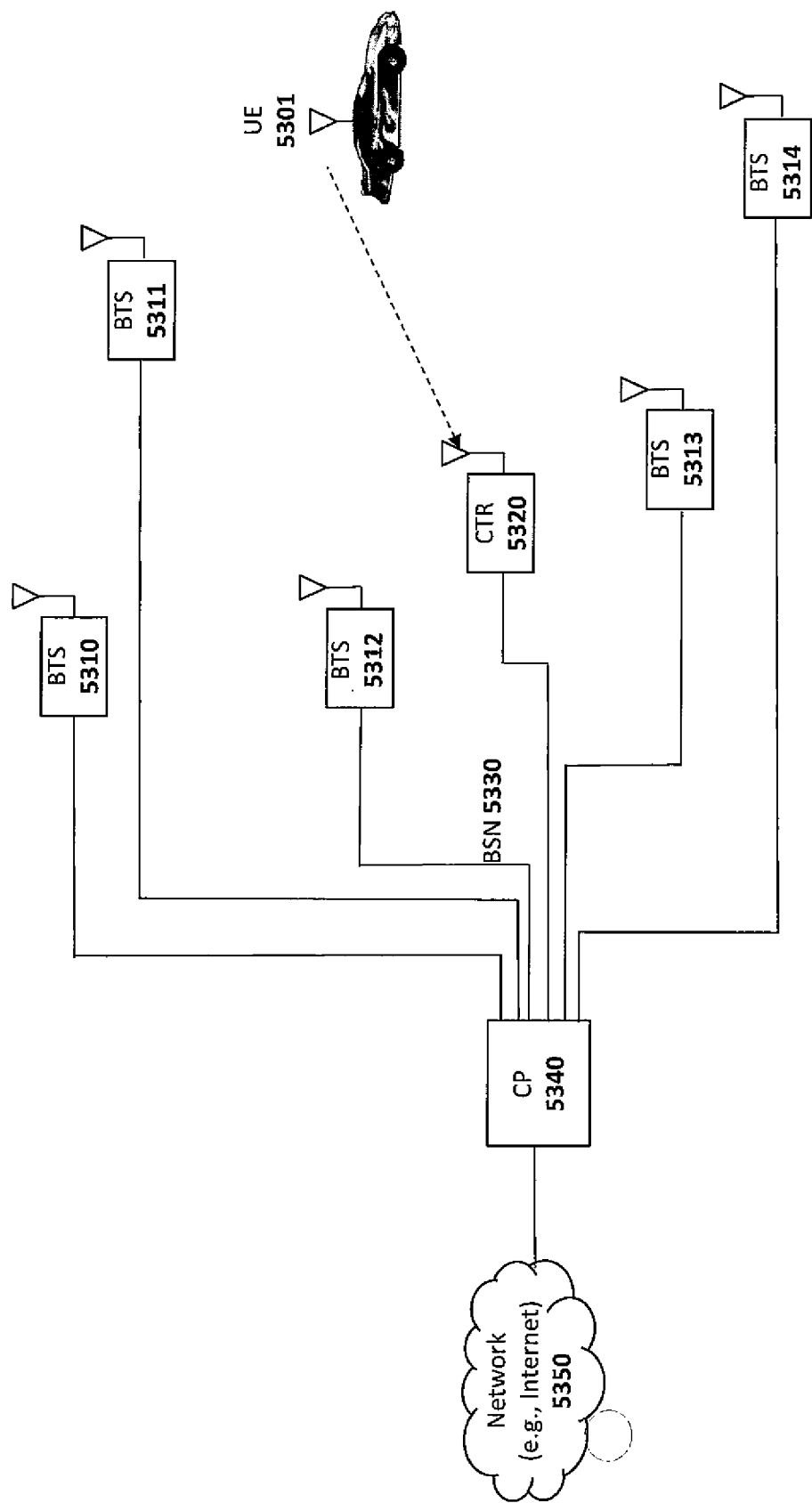


Fig. 56

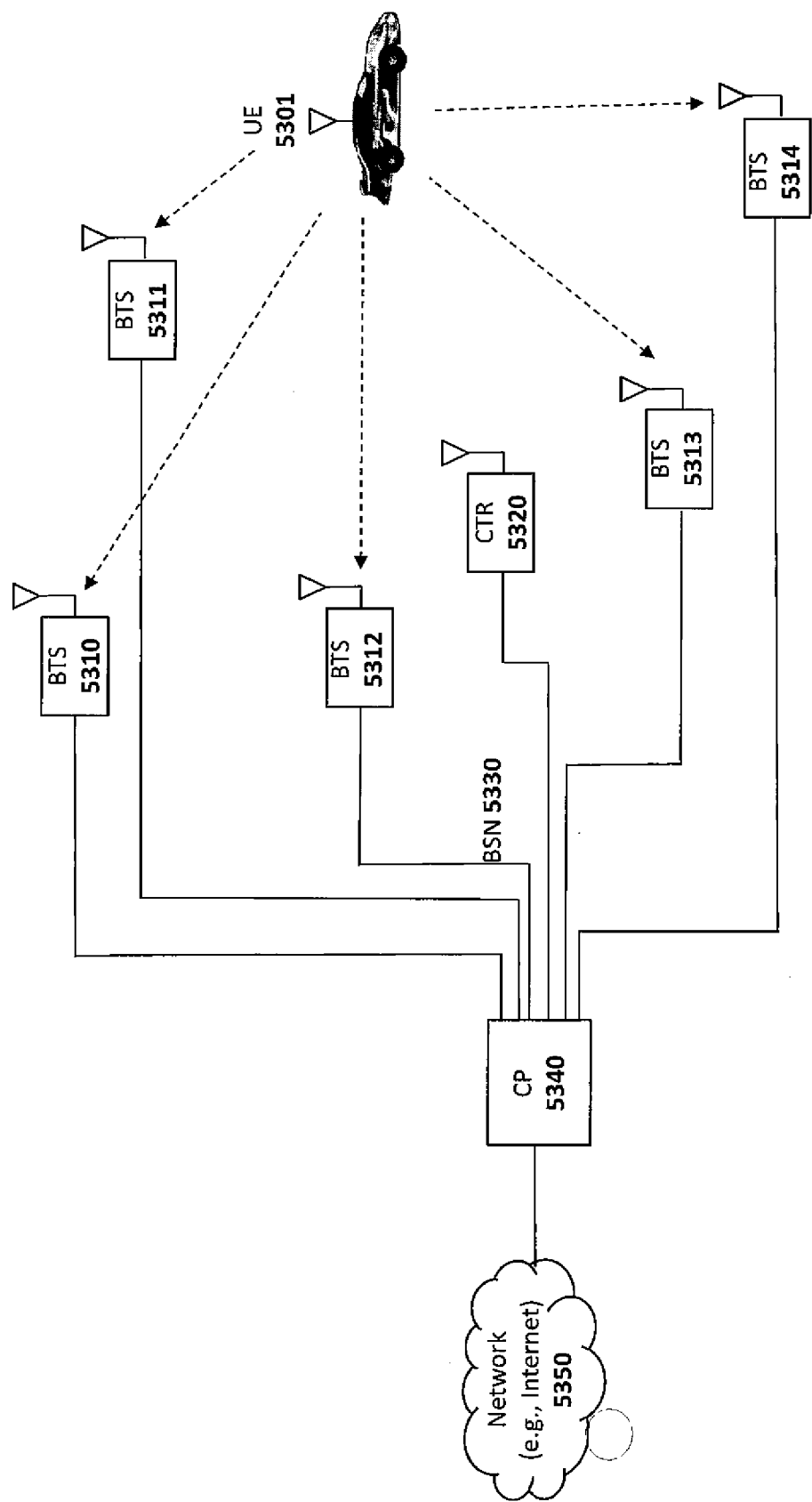


Fig. 57

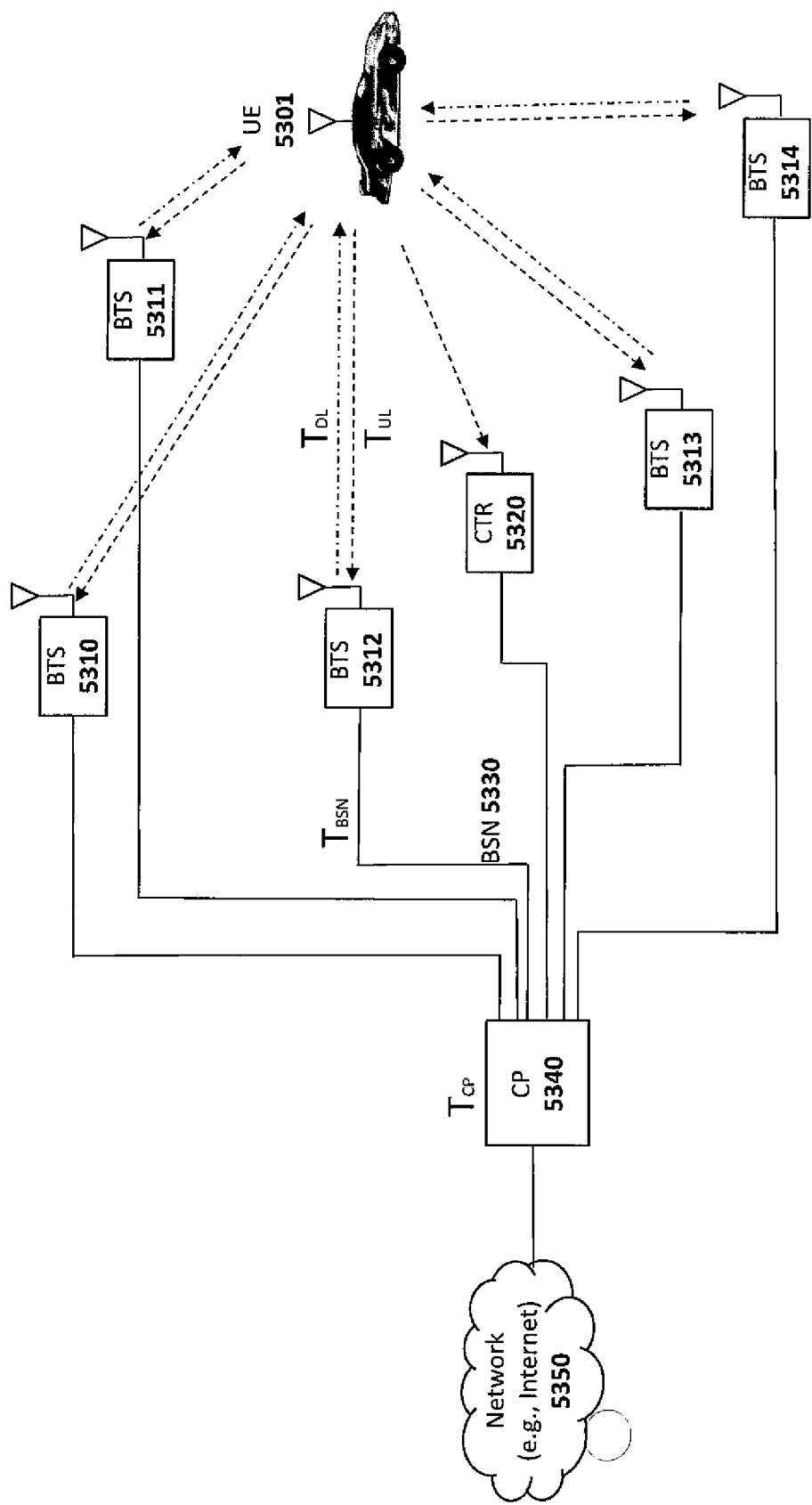


Fig. 58

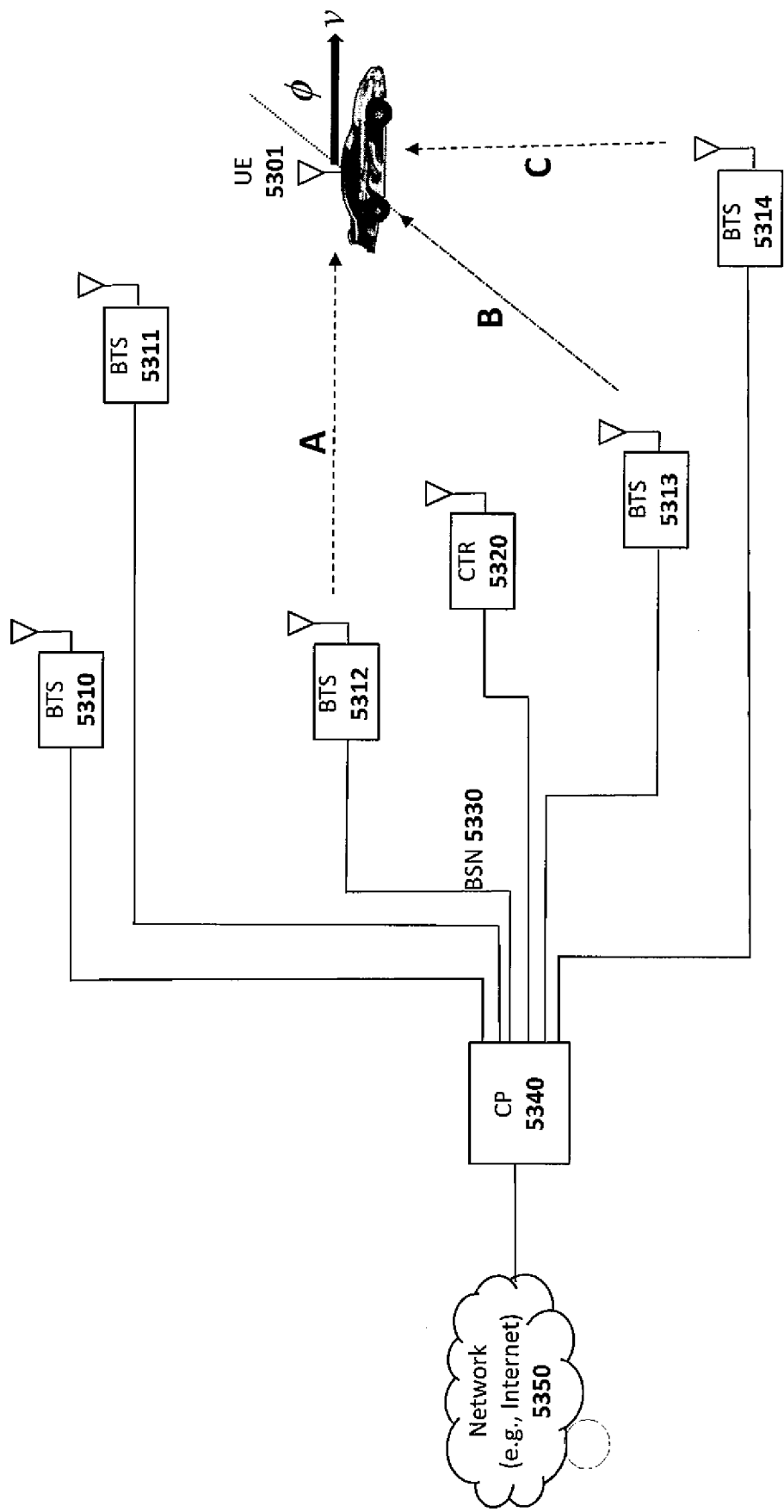


Fig. 59

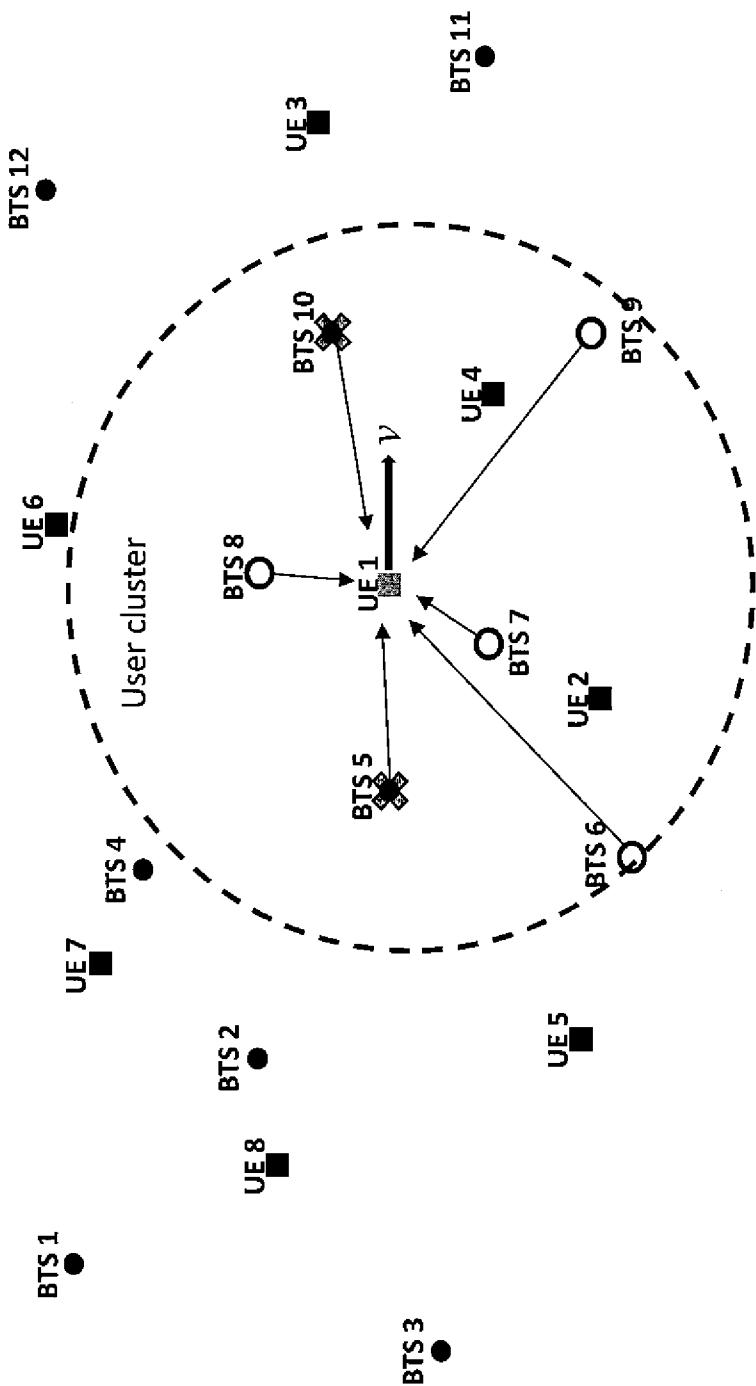


Fig. 60

	8751	8752	8753	8754	8755	8756	8757	8758	8759	875A	875B	875C	875D	875E	875F	875G	875H	875I	875J	875K	875L	875M	875N	875O	875P	875Q	875R	875S	875T	875U	875V	875W	875X	875Y	875Z
U61	0	0	0	0	0	0	0	0	0	0	0	0	0	0	0	0	0	0	0	0	0	0	0	0	0	0	0	0	0	0	0	0	0		
U62	0	0	0	0	0	0	0	0	0	0	0	0	0	0	0	0	0	0	0	0	0	0	0	0	0	0	0	0	0	0	0	0	0		
U63	0	0	0	0	0	0	0	0	0	0	0	0	0	0	0	0	0	0	0	0	0	0	0	0	0	0	0	0	0	0	0	0	0		
U64	0	0	0	0	0	0	0	0	0	0	0	0	0	0	0	0	0	0	0	0	0	0	0	0	0	0	0	0	0	0	0	0	0		
U65	0	0	0	0	0	0	0	0	0	0	0	0	0	0	0	0	0	0	0	0	0	0	0	0	0	0	0	0	0	0	0	0	0		
U66	0	0	0	0	0	0	0	0	0	0	0	0	0	0	0	0	0	0	0	0	0	0	0	0	0	0	0	0	0	0	0	0	0		
U67	0	0	0	0	0	0	0	0	0	0	0	0	0	0	0	0	0	0	0	0	0	0	0	0	0	0	0	0	0	0	0	0	0		
U68	0	0	0	0	0	0	0	0	0	0	0	0	0	0	0	0	0	0	0	0	0	0	0	0	0	0	0	0	0	0	0	0	0		

Fig. 61

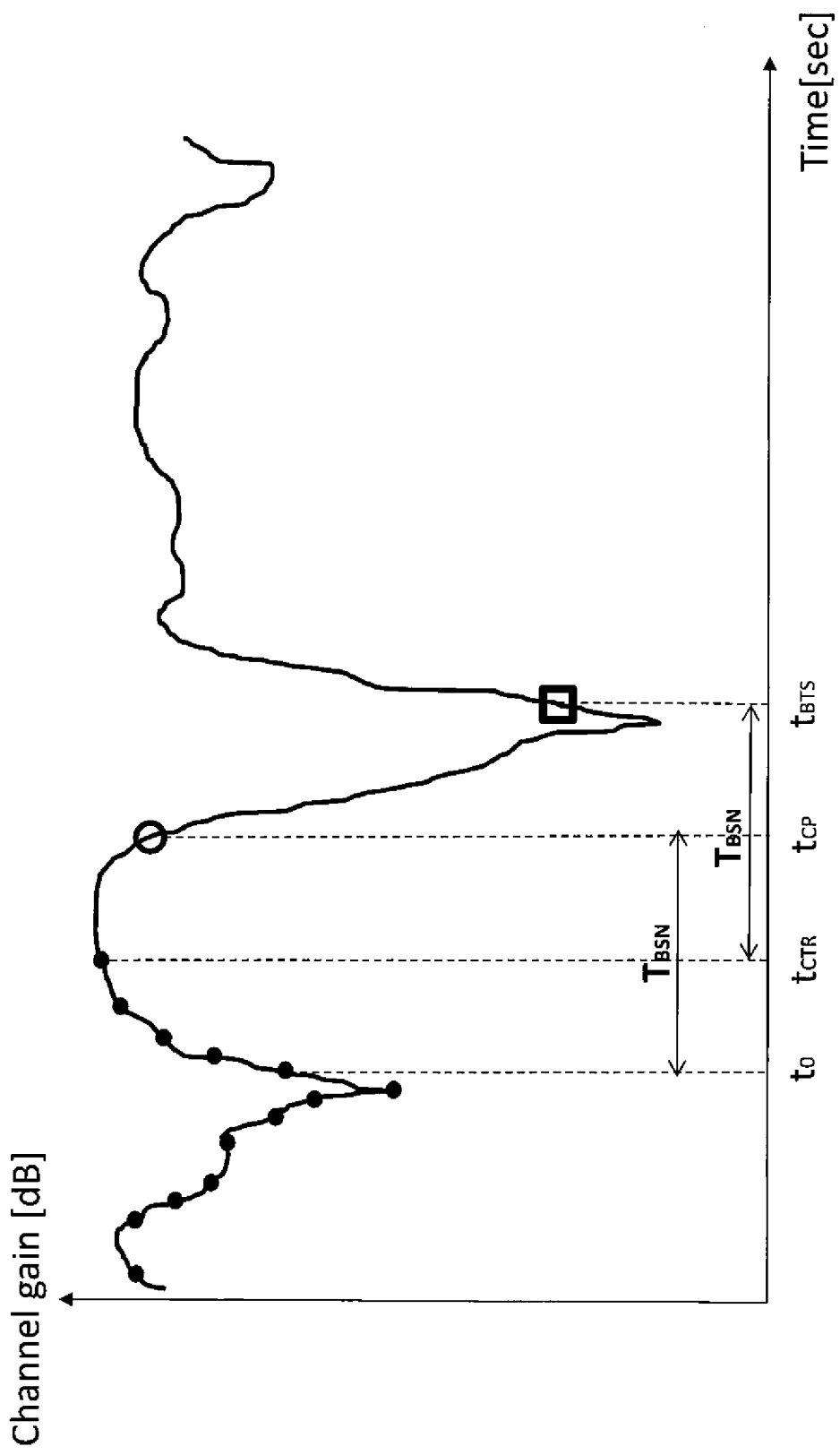


Fig. 62